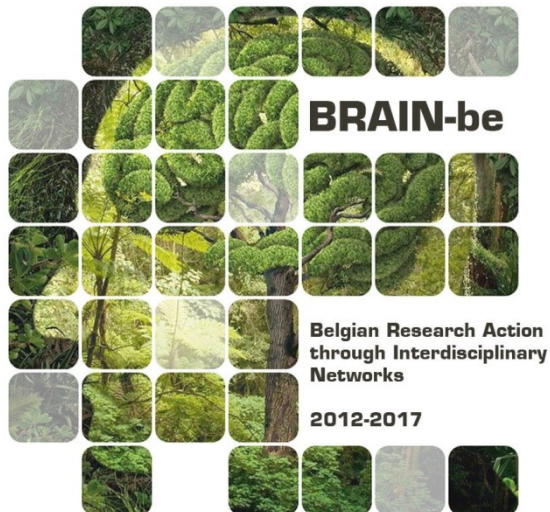


## CORDEX.be

### Combining regional downscaling expertise in Belgium: CORDEX and beyond

Piet Termonia (RMI), Bert Van Schaeybroeck (RMI), Lesley De Cruz (RMI), Rozemien De Troch (RMI), Olivier Giot (RMI), Rafiq Hamdi (RMI), Stéphane Vannitsem (RMI), François Duchêne (RMI), Patrick Willems (KU Leuven), Hossein Tabari (KU Leuven), Els Van Uytven (KU Leuven), Parisa Hosseinzadehtalaei (KU Leuven), Nicole Van Lipzig (KU Leuven), Hendrik Wouters (KU Leuven), Sam Vanden Broucke (KU Leuven), Matthias Demuzere (KU Leuven), Jean-Pascal van Ypersele (UCL), Philippe Marbaix (UCL), Cecille Villanueva-Birriel (UCL), Xavier Fettweis (ULg), Coraline Wyard (ULg), Chloé Scholzen (ULg), Sébastien Doutreloup (ULg), Koen De Ridder (VITO), Anne Gobin (VITO), Dirk Lauwaet (VITO), Trissevgeni Stavrakou (BIRA), Maite Bauwens (BIRA), Jean-François Müller (BIRA), Patrick Luyten (KBIN), Stéphanie Ponsar (KBIN), Dries Van den Eynde (KBIN), Eric Pottiaux (ROB)

Axis 2: Geosystems, universe and climate



NETWORK PROJECT

## CORDEX.be

### Combining regional downscaling expertise in Belgium: CORDEX and beyond

Contract - BR/143/A2/CORDEX.be

#### FINAL REPORT

**PROMOTORS:** Piet Termonia (RMI), Patrick Willems (KU Leuven), Nicole Van Lipzig (KU Leuven), Jean-Pascal van Ypersele (UCL), Xavier Fettweis (ULg), Koen De Ridder (VITO), Anne Gobin (VITO), Trissevgeni Stavrakou (BIRA), Patrick Luyten (KBIN), Stéphanie Ponsar (KBIN), Eric Pottiaux (ROB)

**AUTHORS:** Bert Van Schaeybroeck (RMI), Lesley De Cruz (RMI), Rozemien De Troch (RMI), Olivier Giot (RMI), Rafiq Hamdi (RMI), Stéphane Vannitsem (RMI), François Duchêne (RMI), Cédric Bertrand (RMI), Hossein Tabari (KU Leuven), Els Van Uytven (KU Leuven), Parisa Hosseinzadehtalaei (KU Leuven), Hendrik Wouters (KU Leuven), Sam Vanden Broucke (KU Leuven), Matthias Demuzere (KU Leuven), Philippe Marbaix (UCL), Cecille Villanueva-Birriel (UCL), Coraline Wyard (ULg), Chloé Scholzen (ULg), Sébastien Doutreloup (ULg), Dirk Lauwaet (VITO), Maite Bauwens (BIRA), Jean-François Müller (BIRA), Stéphanie Ponsar (KBIN), Dries Van den Eynde (KBIN).

[www.euro-cordex.be](http://www.euro-cordex.be)





Avenue Louise 231  
Louizalaan 231  
B-1050 Brussels  
Belgium  
Tel: +32 (0)2 238 34 11 - Fax: +32 (0)2 230 59 12  
<http://www.belspo.be>  
<http://www.belspo.be/brain-be>

Contact person: Martine Vanderstraeten  
Tel: +32 (0)2 238 36 10

Neither the Belgian Science Policy nor any person acting on behalf of the Belgian Science Policy is responsible for the use which might be made of the following information. The authors are responsible for the content.

No part of this publication may be reproduced, stored in a retrieval system, or transmitted in any form or by any means, electronic, mechanical, photocopying, recording, or otherwise, without indicating the reference:

**AUTHORS:** Piet Termonia (RMI), Patrick Willems (KU Leuven), Nicole Van Lipzig (KU Leuven), Jean-Pascal van Ypersele (UCL), Xavier Fettweis (ULg), Koen De Ridder (VITO), Anne Gobin (VITO), Trissevgeni Stavrakou (BISA), Patrick Luyten (KBIN), Stéphanie Ponsar (KBIN), Eric Pottiaux (ROB), Bert Van Schaeybroeck (RMI), Lesley De Cruz (RMI), Rozemien De Troch (RMI), Olivier Giot (RMI), Rafiq Hamdi (RMI), Stéphane Vannitsem (RMI), François Duchêne (RMI), Cédric Bertrand (RMI), Hossein Tabari (KU Leuven), Els Van Uytven (KU Leuven), Parisa Hosseinzadehtalaei (KU Leuven), Hendrik Wouters (KU Leuven), Sam Vanden Broucke (KU Leuven), Matthias Demuzere (KU Leuven), Philippe Marbaix (UCL), Cecille Villanueva-Birriel (UCL), Coraline Wyard (ULg), Chloé Scholzen (ULg), Sébastien Doutreloup (ULg), Dirk Lauwaet (VITO), Trissevgeni Stavrakou (BISA), Maite Bauwens (BISA), Jean-François Müller (BISA), Stéphanie Ponsar (RBINS), Dries Van den Eynde (RBINS). **Combining regional downscaling expertise in Belgium: CORDEX and beyond.** Final Report. Brussels: Belgian Science Policy 2018 – 119 p. (BRAIN-be - (Belgian Research Action through Interdisciplinary Networks)

## TABLE OF CONTENTS

table of contents.....	4
ABSTRACT.....	7
Context.....	7
Objectives & their results.....	7
Conclusions and recommendations.....	8
Keywords.....	9
1 INTRODUCTION.....	10
1.1 International context .....	10
1.2 National context: Climate services for Belgium.....	11
1.3 National context: Downscaling approach over Belgium.....	12
1.4 Climate change impact studies for Belgium .....	12
2 The core CORDEX.be OBJECTIVES.....	17
3 METHODOLOGY .....	18
3.1 General methodology underlying CORDEX.be.....	18
3.2 Methodology of the regional climate models .....	19
3.3 Methodology of regional climate simulations using the ALARO-0 model.....	21
3.4 Methodology of regional climate simulations using COSMO-CLM.....	23
3.5 Methodology of regional climate simulations using the MAR model .....	27
3.6 Methodology of RCM model validation using GNSS products .....	29
3.7 Methodology of impact study on biogenic emissions .....	30
3.8 Methodology of impact study on agricultural crop performance and yield .....	31
3.9 Methodology of the impact study on urban impacts .....	31
3.10 Methodology of impact study on waves and storm surges.....	32
3.11 Methodology of statistical and uncertainty estimation .....	34
4 SCIENTIFIC RESULTS .....	35
4.1 The performed regional climate simulations.....	35
4.2 Evaluation and climate projection of all H-Res simulations .....	36
4.3 Evaluation of the regional climate simulations using ALARO-0.....	40
4.4 Evaluation of the regional climate simulations with COSMO-CLM .....	42
4.5 Evaluation of regional climate simulations using MAR.....	51
4.6 Validation of climate simulations using GNSS-derived products.....	55

4.7	Climate change impact on extreme precipitation .....	57
4.8	Climate change impact on snow cover .....	59
4.9	Climate change impact on hail.....	61
4.10	Climate-change impact on urban heat stress .....	63
4.11	Climate change impact on the heat waves.....	64
4.12	Climate change impact on urban environment .....	66
4.13	Climate change impact on agricultural crop performance and yield .....	70
4.14	Climate change impact on isoprene emissions over Europe .....	72
4.15	Climate change impact on storm surges and waves.....	76
4.16	Statistical interpretation and uncertainty estimation .....	78
5	CONCLUSIONS and Recommendations.....	86
5.1	General CORDEX.be conclusions & Stakeholders meeting.....	86
5.2	Climate change impact on extreme precipitation .....	88
5.3	Climate change impact on snow cover .....	89
5.4	Climate change impact on urban environment: heat waves, urban heat stress and thermal comfort parameters.....	89
5.5	Climate change impact on biogenic emissions .....	89
5.6	Climate change impact on agricultural crop performance and yield .....	90
5.7	Climate change impact on waves and storm surges.....	90
5.8	GNSS-based model validation of the high-res climate model runs .....	90
6	DISSEMINATION AND VALORISATION .....	93
6.1	Stakeholder meetings during the project .....	93
6.2	Final CORDEX.be stakeholders meeting 26-09-2017 .....	93
6.3	Follow-up meeting .....	94
6.4	Scientific publications in international journals.....	94
6.5	Contributions to conference proceedings & national publications.....	96
6.6	Outreach to the scientific community .....	97
6.7	Outreach articles for the general public.....	97
6.8	Posters & Presentations.....	98
7	References .....	101
	ACKNOWLEDGEMENTS.....	109
	Data AVAILABILITY .....	109
	ANNEXES .....	110



## ABSTRACT

### Context

In the context of the Paris Agreement, there exists a clear demand from different stakeholders for Climate services in Belgium. Until recently, however, Belgium lacked the foundation for enabling such services.

The CORDEX.be project brought together the Belgian climate and impact modeling research groups into one network as the first step towards the realization of climate services. It is based on the international CORDEX (“COordinated Regional Climate Downscaling Experiment”) project but the “.be” indicates it goes beyond for Belgium.

The key to the foundation of national climate services is a combination of the existing expertise on high-resolution downscaling, local-impact models, ensemble dynamical and statistical downscaling, combined with links to international initiatives and stakeholder dialogue. This allows to address the propagation of climate change and uncertainty from the global to the local scale combined with a better representation of climate extremes.

The CORDEX.be climate network consists of nine partners using three upper-air Regional Climate Models and seven Local Impact Models. The CORDEX.be framework and guidelines are based on a user-oriented bottom-up approach.

The CORDEX.be framework provides the first building block for a research network which could be extended, both nationally and internationally, with the objective of providing climate services.

### Objectives & their results

The main objectives of the CORDEX.be project were:

1. Contribute to the international climate community by participating to EURO-CORDEX by performing regional climate simulations over Europe.
2. Provide an ensemble of High-Resolution (H-Res) climate simulations over Belgium i.e. to create a small ensemble of high-resolution future projections over Belgium at convection-permitting resolutions.
3. Couple these model simulations to seven local-impact models for impact studies.
4. Present an overview of the ongoing climate modeling activities in Belgium.
5. Provide coherent climate information for Belgium targeted to end-users, backed by: (i) a unified framework for the H-Res climate runs and (ii) uncertainty estimations on the climate change signal;
6. Provide and present a climate-impact report for stakeholders and the general public that highlight the most important results of the project.

Target 1 resulted in contributions to the EURO-CORDEX project with three climate models and data submitted to the international data hub of the Earth System Grid Federation ([ESGF](#)) which is publicly available for research purposes.

The RCM groups have performed simulations in the past and different climate projections and have thoroughly validated the climate model results against observations from the past (see Section 4). A wide range of climate-change impact studies were performed. Moreover, a centralized Belgian data hub was established containing H-Res model output for further impact studies.

End users can use the CORDEX.be ensemble to address questions related to climate change in Belgium without having to ask whether the information is consistent with other Belgian and European climate information. The most important results are highlighted in a climate-impact leaflet for stakeholders and the general public.

## Conclusions and recommendations

While Belgium does not formally have a national climate center (Fonteyn, 2013), the CORDEX.be project provides a platform for data exchange and communication among the Belgian climate-modeling groups. This is coordinated through the website [euro-cordex.be](http://euro-cordex.be). This website will be maintained and updated with new results and serves as a link between the Belgian activities and the international ones of the CORDEX project.

Different climate impact studies have been performed in the context of CORDEX.be and are presented here. These include the impact of climate change on

- extreme precipitation for Belgium;
- maximum snow height for Belgium;
- urban parameters for Brussels; including outdoor labor productivity, excess energy consumption and heat stress due to heat waves;
- agricultural crop performance and yield for Belgium;
- and biogenic emissions for Europe and Belgium.

Focusing on the future period 2070-2100 for the scenario with the largest greenhouse gas emissions (RCP8.5), the most prominent impacts of climate change for Belgium include:

- A strong increase in tropical days and heat wave days.
- An increase in winter precipitation and long extremely wet periods.
- Intensification of summer precipitation extremes, especially in urbanized areas. The precipitation intensity with hourly time scale and 10-year return period may increase up to 100%.
- For the Brussels urban environment:
  - An increase of a factor 3 to 4 in the number of heat waves.
  - Significant increase of heat stress for people living in the city of Brussels, up to twice as large as in the surrounding rural areas.
  - Significant impact on the outdoor productivity due to thermal discomfort. More specifically, a doubling of lost working days may be expected.
  - A doubling of days when air-conditioning is intensively used, impacting the urban energy consumption.
- An increased variability for biomass production and yields. Average yields for fodder maize and late potatoes will also decline.

- Severely reduced winter snow height maxima (above 500m altitude).
- An increase of 51% of biogenic emissions from isoprene with the highest emissions in the Ardennes and Campine forests (disregarding the CO<sub>2</sub> inhibition effect).
- Indications exist that there will be less hail events but increase of mean hail size.

A table including the climate change numbers and their uncertainty estimates for Belgium is provided (see Termonia et al, 2018). Based on interactions and feedback with stakeholders, different applications are ongoing that demonstrate the use of the climate data (e.g. Vanderhoeven et al., 2017).

## Keywords

Climate Services, Regional Climate Modeling, Climate Impact Modeling, Statistical Downscaling, Dynamical Downscaling, Local Impact Models, Climate Change, CORDEX, Belgium, Water Vapor Observations

## 1 INTRODUCTION

### 1.1 International context

As described in the latest assessment report of the Intergovernmental Panel for Climate Change (IPCC) the warming of the global climate system, caused by increased greenhouse gas concentrations, is unequivocal. For most people, however, climate change remains an elusive concept. For instance much debate concerns the questions when global warming will reach the 2°C level but the impact on everyday life may not be clear. In fact, climate change is and will be felt mostly through the occurrence of extreme weather events (e.g. extreme storms, flooding, heat waves, and droughts) which critically depend on the type of environment people live in. For instance near rivers and coasts people frequent flooding may occur while heat waves are mostly felt within urbanized areas. The assessment of such local risks is a complex and scientifically multidisciplinary challenge. Although dispersed over different universities and research institutes there is a strong Belgian expertise in this context. The aim of CORDEX.be is to build a research network based on coherent modeling efforts as a basis for answering questions concerning climate change impact for Belgium.

IPCC results are mostly based on results from model simulations using so-called Global Circulation Models (GCMs) that describe the atmosphere and the ocean using variables such as temperature and precipitation on a grid. Typically the distance between the points on such a grid is of the order of 50-100 kilometer for the “low-resolution” GCMs. Therefore, although reliable for estimating global warming they fail to capture the important local environmental details and extremes. These, on the other hand, can be reliably represented by “downscaling”, that is, by running “high-resolution” Regional Circulation Models (RCMs) models with small grid distances but on a limited geographical area. Within CORDEX.be, four RCM models have been run over Europe and Belgium. Although RCMs over Belgium with resolutions of 5-km represent well phenomena such as extreme precipitation events, different models with even higher resolutions are required to study specific impacts or for even more details, for instance temperature differences between rural and urban areas or water levels in river basins. Therefore RCMs are coupled with models of very high-resolutions, called Local Impact Models. Within the CORDEX.be project six LIMs were used for impact assessment studies

Climate change is a global phenomenon and is of strong international interest so the national initiative is bi-directionally linked to existing international frameworks. The IPCC describes in their Fifth Assessment Report (AR5, Stocker et al. 2014) the so-called Representative Concentration Pathways (RCPs) for atmospheric greenhouse gases, based on which a set of GCMs are run and collected in the 5th Coupled Model Inter-comparison Project (CMIP5, Taylor et al. 2012). CORDEX is an international project for modeling the regional climate (Giorgi et al. 2009, Jacob et al. 2014) and provides detailed prescriptions for RCMs and their data exchange. The initiatives deliver data for climate change projections and their uncertainties. Analogue to CMIP5 and CORDEX, and based on the existing Belgian expertise, CORDEX.be provides a prototype framework to go beyond CORDEX to close the gap between regional climate runs and “local”-impact assessment for climate services.

According to the Global Framework for Climate Services (GFCS) there are four pillars required to build climate services (Hewitt et al. 2012): i) observations and monitoring, ii) research modeling and projection, iii) climate services information system and, iv) a user interface platform. CORDEX.be focuses on point (ii) by data-driven capacity development and community building in Belgium based on interactions with users. The overall and long-term target is to provide standardized information to the stakeholder community concerning climate-change information for Belgium. The GFCS also distinguishes the global, regional and national levels of climate services and emphasizes the interactions among the different levels. CORDEX.be is a national initiative that contributes to the international climate community through the production of climate simulations over Europe. Based on these simulations and H-Res simulations over Belgium, the impact of climate change on urban environment, storm surges and waves, impact on crop production and changes in emissions from vegetation, has been investigated.

## 1.2 National context: Climate services for Belgium

Several reasons exist why Belgian climate change is important and climate services must be established. Belgium has an Atlantic climate, is partly low-lying, densely populated, urbanized, and industrialized. Therefore it is strongly susceptible to different types of extreme weather events including urban heat stress, droughts, thunderstorms and different types of floods (van Ypersele and Marbaix, 2004). A proper assessment of these events under climate change is highly relevant. Moreover climate services are necessary to help inform the general public and to enable decision support based on stakeholders dialogue and impact assessment studies.

CORDEX.be is a platform for interaction between the Belgian modeling groups. This platform is used to inter-compare the Belgian simulations and to situate them with respect to the CORDEX ensemble. This extra information is now provided to the stakeholders to show that the data from any of the Belgian simulations is consistent with the other Belgian CORDEX.be simulations and with the CORDEX ensemble.

It was explained by Dilling and Lemos (2011) in the context of climate services that, for the successful production of actionable science and user-oriented services, the interaction between knowledge producers and users is of critical importance. CORDEX.be established the foundation for climate services within Belgium and while there were many interactions with users in different stakeholders meetings no co-production was established due to limited resources. However, given the existing fundament, different applications are currently being worked out that demonstrate the use of the climate data (e.g. Vanderhoeven et al., 2017). A two-way interaction, as described by Dilling and Lemos was, already present at the level of modelers. While downscaling is by definition top-down by nature, specific bottom-up guidelines were necessary as explained in detail in Section 3.2. These specifications came about due to the lengthy climatological integration time that sets a limit to the data that can possibly be stored but that is necessary as input for impact models.

### 1.3 National context: Downscaling approach over Belgium

There are a number of reasons for which impact assessment must be provided at the local scale for Belgium, justifying the model simulations at high resolution as done in CORDEX.be. While the proximity to the sea and the presence of orography are known to affect the current local climate averages (Journée et al, 2015) and extremes (Brisson, 2011; Sneyers, 1989; Van Meijgaard, 1995; Van de Vyver, 2012; Wyard et al., 2017a; Zamani, 2016), they also affect the climate change signal. For example, projected changes of precipitation are generally different over mountainous areas while coastal precipitation responds differently to changing ocean temperatures than more inland precipitation. Additionally, it is important to correctly capture the correct land-use features in the climate models since Belgium is one of the most densely urbanized areas in Europe and large areas are strongly sensitive to the urban heat island effect (Wouters, 2016; Hamdi, 2015; Lauwaet, 2015).

The CORDEX.be H-Res ensemble allows studying the local response of temperature and precipitation to climate change by taking into account fine-scale processes and land-use details that are not captured by coarser-scale models. The differences in the model results from the CORDEX.be, CORDEX and CMIP ensemble results are considered as uncertainties and put against each other in a table (see Termonia et al., 2018).

### 1.4 Climate change impact studies for Belgium

CORDEX.be established a large set of climate model data sets. Additionally, different climate-change impacts studies for Belgium have been performed and are presented in this report. A climate impact report for Belgium was already established in 2004 (van Ypersele and Marbaix, 2004) and more recent reports focus on the hydrological impact (Willems et al., 2010) and on the Flanders region (Brouwers et al., 2015) based on coarse-resolution climate projections. This report updates and goes beyond these previous efforts based on the high-resolution model results and a range of supplementary impact assessments.

#### 1.4.1 Introduction on extreme precipitation over Belgium

Due to increased and continued greenhouse gas emissions, significant future impacts are expected on both: total seasonal precipitation and the frequency and intensity of extreme short-duration precipitation events. Both are important from a societal perspective, as they can potentially lead to changes in the frequency of droughts, river floods, or high impact flash flood events. Current projections for Belgium, derived from global and regional climate modeling simulations, predict that total precipitation will decrease in summer and increase in winter, while the frequency of extreme short-duration precipitation events will increase in winter but remains at present levels in summer.

These projections are largely based on global and regional climate modeling experiments with coarse grid resolutions. Recent studies have shown that higher resolution climate simulations are vastly superior in simulating precipitation on the daily and sub-daily timescales, especially in summer, and for the more extreme tail of the precipitation distribution (Kendon et al. 2012, Ban et al. 2014, Chan et al. 2014b, Fosser et al. 2014, Brisson et al. 2016). Consequently, numerous recent studies have performed future precipitation projections using high resolution RCMs, with a

particular focus on extreme precipitation on the daily and sub-daily timescale. When compared to low resolution models, these high resolution simulations appear to lead to an increased future extreme precipitation in experiments over some regions (Chan et al. 2014a, Kendon et al. 2014), but not in others (Fosser et al. 2017, Ban et al. 2015). Therefore, the goal of the impact study presented in this report is to compare the simulated future increase in extreme precipitation of low and high resolution RCM simulations with a focus on Belgium.

#### **1.4.2 Introduction on snow cover for Belgium**

Over the last decades, a significant general trend toward decreasing snow depth, snow duration and snowfall amount with interdecadal variability has been identified in various European regions such as the Alps (e.g. Beniston, 2012), Britain (e.g. Kay, 2016), Norway (e.g. Dyrødal et al., 2013), or Eastern Europe (e.g. Birsan and Dumitrescu, 2014).

In Belgium, snow can cover the summits of the Ardennes massif from 1 to 2 months per year on average, and can reach up to 70-80 cm for the most snowy winters with consequences on water management, biodiversity and tourism. In fact, when combined with heavy rainfall events, the abrupt melting of the snowpack covering the Ardennes is responsible for major floods in the Meuse River catchment, located in the south-east of Belgium (Pauquet and Petit, 1993; de Wit et al., 2007). In addition, the peculiar climate which characterizes the summits of Belgium allows the existence of alpine and even subarctic species of animals and plants. Most of these plant species can survive extreme cold temperatures in the winter months thanks to the protective snow cover that acts as a thermal insulator. Both the peculiar climate and ecosystem of the Belgian high plateaus also generate tourism especially in winter (skiing, hiking, educative walks).

Despite the aforementioned implications, very few studies about the recent and future evolution of seasonal snow cover have been carried out in Belgium. Therefore, our research assessed whether seasonal snow cover has changed over the last 50 years in Belgium and how this seasonal snow cover could evolve by the end of the 21st century. For this purpose, the regional climate model (RCM) MAR (or *Modèle Atmosphérique Régional*) was used. As snow cover records over the Belgian territory are patchy, discontinuous or made with techniques that change over time, a RCM like MAR, which was specially designed to model snow (Gallée et al., 2001; Fettweis et al., 2013), is a highly valuable tool for studying the recent and future changes in snow cover at a high-spatial resolution.

#### **1.4.3 Introduction on Belgian urban environment: heat waves, urban heat stress and thermal comfort parameters**

Urban areas are usually warmer than their surrounding natural areas, an effect known as the urban heat island (UHI) effect. As such, these areas are particularly vulnerable to global warming and associated increases in extreme temperatures. Yet, ensemble climate-model projections are generally performed on a scale that is too coarse to represent the evolution of temperatures in cities. Especially greenhouse gas emissions and land-use changes both lead to incessant temperature increases and shifts in weather extremes, in particular more intense, more frequent and longer lasting heatwaves. In turn, they have an adverse impact on human health, the economy and eco-

systems. Heat waves generally result in excessive mortality, higher hospital admissions, preterm delivery, economic and labour productivity, damage to infrastructure and higher energy usage.

The cities - housing already more than 50% of the global population [United Nations, 2014] - experience an excessive death toll during heatwaves compared to the natural surroundings because of the UHI effect and also an excessive economic loss.

Recent studies have been using ensemble GCMs and RCMs to address the future (heatwave-related) risks of climate change around the globe including the role of urbanization. However, all of these studies use climate information on a scale of 50 km or beyond that is too coarse to resolve the inter-urban variability of the cities.

In order to capture the associated heterogeneity in urban-atmospheric feedbacks, the local circulations and weather conditions, one requires to resolve at least the scale of the cities themselves i.e. at a scale below 10 km. The latter is particularly a prerequisite to distinguish between the different urban characteristics, including the imperviousness (abundance of buildings, streets, parking lots and other man-made water-impermeable pavements) and other local environmental aspects (distance from the coastline, soil texture, orography, vegetation...). It is also indispensable for taking the local land-use change such as urban expansion into account. Convection-permitting climate models in CORDEX.be offer more than 100 times more grid cells per unit area than those previous assessments, hence are able to explicitly resolve the local heterogeneous weather conditions and especially the urban heat island effect. As such, they allow identifying the local hot spots and the associated urban climate-change risks. More information and references can be found in Wouters et al. (2017).

#### **1.4.4 Introduction on biogenic emissions over Belgium**

Vegetation is the dominant source of volatile organic compounds (VOCs) in the atmosphere, accounting for about 1000 Tg globally on a yearly basis (Guenther et al. 2012), and representing about 90% of the estimated total VOC emission. Isoprene accounts for almost half of the total biogenic VOC emission (400-600 Tg, Guenther et al. 2006) and plays a key role in the atmospheric composition because of its influence on tropospheric ozone formation in polluted environments and its contribution to particulate matter. Isoprene emissions depend on the type and abundance of plants, and are modulated by meteorological parameters, in particular temperature and solar radiation. Climate changes therefore affect the spatiotemporal and inter-annual variation of these emissions. Increases in surface temperature and/or solar radiation are expected to lead to enhanced biogenic emissions, and thereby to higher ozone concentrations.

The question of how biogenic emissions will evolve in future warming climate has been addressed in several studies. The most recent studies conclude that global warming will lead to stronger global isoprene emissions (Meleux et al., 2007; Wiedinmyer et al., 2006), but that the inhibitory effect of CO<sub>2</sub> on isoprene production is likely to counteract this effect (Arneth et al., 2007; Young et al., 2009). Moreover, rising CO<sub>2</sub> levels are likely to induce an increase in biomass, which will also lead to stronger biogenic emissions (Arneth et al., 2007), even though human-induced land use changes such as deforestation and urbanization could counteract this effect (Heald et al., 2009; Wu et al., 2012). Overall, the uncertainties on future isoprene emission are quite large, with isoprene

emissions over Europe estimated to decrease by 30% (Arneth et al., 2007) or to increase by 100% (Katragkou et al., 2011) by the end of the century. Our objective is to estimate the evolution of isoprene emissions over the EURO-CORDEX domain (with a focus on Belgium) at high resolution (12-km) for past and future climate conditions. To this purpose, we use the MEGAN-MOHYCAN coupled emission-canopy environment model (Müller et al., 2008, Stavrou et al. 2014) driven by meteorological fields provided by CORDEX.be simulations.

#### **1.4.5 Introduction on agricultural crop performance and yield for Belgium**

Meteorological patterns of evapotranspiration, rainfall and temperature during the growing season strongly determine agricultural crop growth and production. These patterns are projected to change under future climatic conditions and hence influence agricultural crops. The impacts, however, will vary per crop and region.

The temporal overlap between meteorological conditions and crop stages in arable crops requires a modeling framework that couples phenology to the soil water balance and crop growth (Gobin, 2010, 2012). A shift in both crop phenology and meteorological conditions is already observed under current conditions (Gobin, 2017), and is expected to continue under climate change. The positive effects of climate change on agriculture in temperate regions are concerned with the longer crop growth periods due to warmer temperatures (e.g. Myeni et al., 1997) and increased biomass production due to elevated CO<sub>2</sub> concentrations (e.g. Ainsworth and Long, 2005). The early reported positive effects were followed by research on the negative effects owing to adverse weather conditions and extreme meteorological events (e.g. Lesk et al., 2016). Both positive and negative effects are difficult to disentangle since crop performance is usually measured by yield records, which in turn is the harvestable fraction of total biomass production accumulated during the growing season.

We hypothesised that the regional dynamic agro-meteorological model (REGCROP; Gobin, 2010, 2012) could be employed to simulate climate impacts on biomass production of arable crops. The objectives were to run experiments such that observed and modeled meteorological records could be compared in terms of crop performance and production; and, that projections could be made for a future climate.

#### **1.4.6 Introduction on waves and storm surges for Belgium**

The marine component of the CORDEX.be project focuses on the hydrodynamic impacts of climate change at the regional level. In that context, the most important societal risks come from higher storm surges as well as from an increased damaging power of waves. Storm surges result from the combined effect of wind and tides. The wind can hold back a tide or push it along. At the Belgian coast, the highest storm surges occur when a spring tide combines with wind blowing from the northwest. Moreover, during storms, changes in atmospheric pressure affect the actual water level.

Waves are created by the action of the wind blowing over the sea. Their size in coastal areas varies widely depending on the wind speed but also on the water depth. The changes in the local

meteorological conditions (e.g. changes in wind patterns) that may be associated with global climate change can thus have an impact on the height of waves.

Within CORDEX.be an impact assessment of climate change on storm surges and waves for the Belgian coastal zone was done, based on the comparison between past and future climate conditions performed with high-resolution models. To this aim, the hydrodynamic model of RBINS, COHERENS, was used to study the impact of climate change on storm surge. The impact of climate change on waves is estimated using the WAM wave model. Both models are run with a resolution of about 4km and are forced using the ALARO-0 meteorological conditions.

## 2 THE CORE CORDEX.BE OBJECTIVES

The initiative “CORDEX and beyond” creates a framework to address the following four targets.

- *Target 1:* To contribute to the EURO-CORDEX project with three regional climate models.
- *Target 2:* Perform H-Res climate simulations at convection-permitting resolutions over Belgium supplemented by verification based on Global Navigation Satellite Systems (GNSS).
- *Target 3:* Output of Targets 1 and 2 is used to drive the following LIMs: three urban-climate models, a crop model, a model for tides and storms, a wave-height model and a model for biogenic emissions. Their output is used for case studies over Belgium.
- *Target 4:* Uncertainties of the different H-Res results are inferred.

### 3 METHODOLOGY

#### 3.1 General methodology underlying CORDEX.be

Methodologically CORDEX.be has two cornerstones: downscaling and the multi-model approach. Dynamic downscaling will be explained further in Section 3.2 and it determines the data stream and interactions within the project as shown in Figure 1. Analogous to CMIP5 and CORDEX, the multi-model approach is necessary for uncertainty estimation and therefore crucial for policy-making purposes.

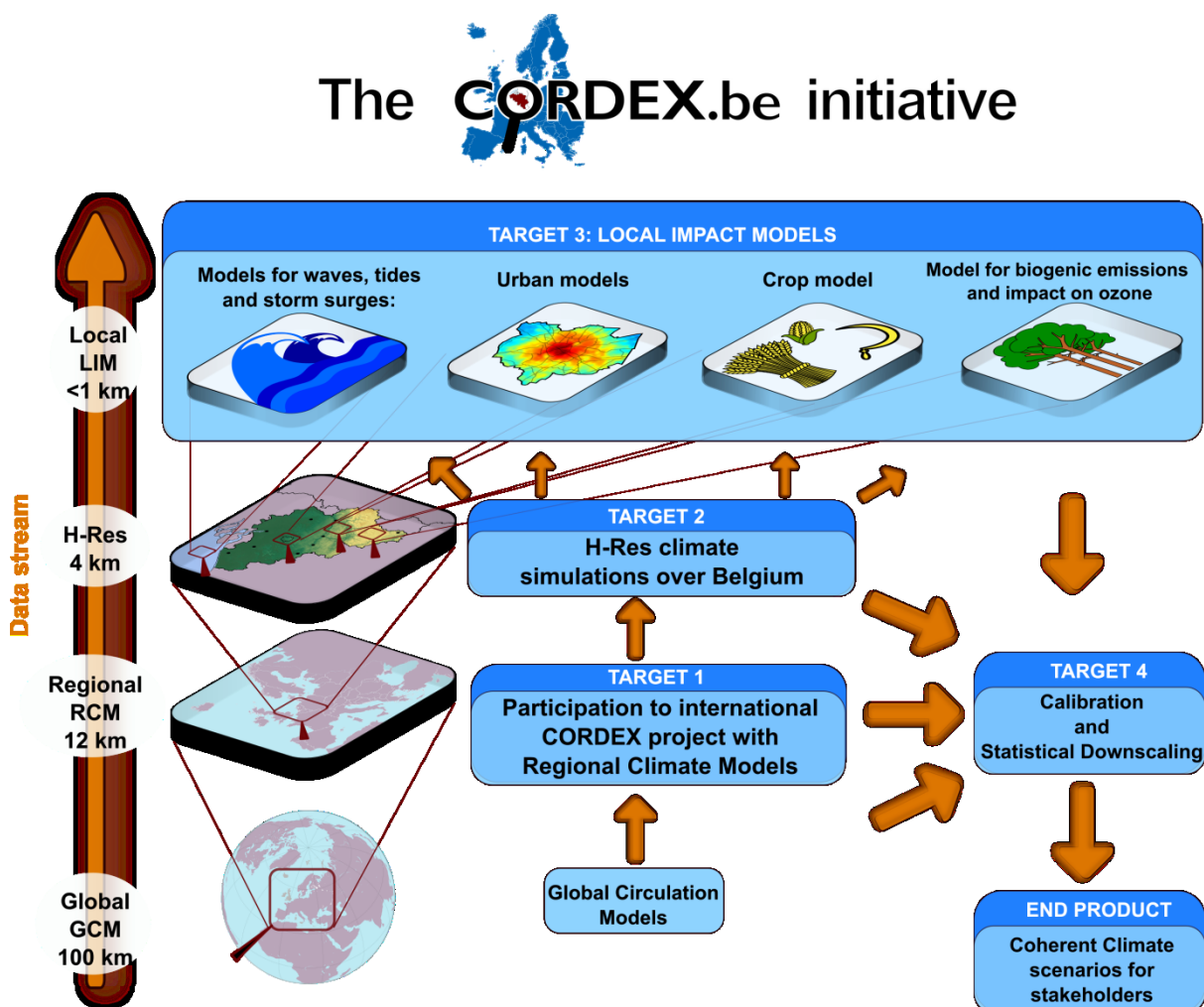


Figure 1: The CORDEX.be framework is naturally structured by the concept of dynamical downscaling. Low-resolution model runs over large domains are nested successively to H-Res runs over small domains. This approach determines the data stream, the timing and the network structure of the Belgian research activities.

The CORDEX.be concept, methodology and data will be used, after the finalization of the project through the existing website ([euro-cordex.be](http://euro-cordex.be)) for the coordination between the Belgian climate-modeling groups and as a contact point for the Belgian activities related to the international CORDEX project. This work provides a reference framework for other collaborative climate initiatives aiming at the development of climate services.

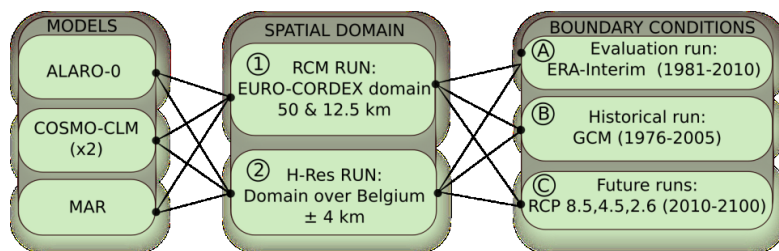


Figure 2: Illustration of the different combinations of climate runs for CORDEX.be. A combination among each column item will be performed.

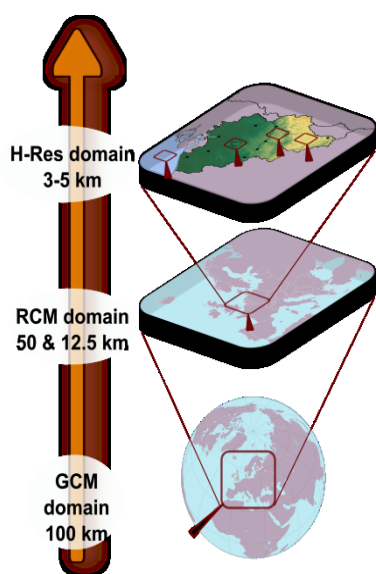
At the start of the project, the following decisions were made concerning the data format and flow that will be used throughout the entire project:

1. The CORDEX prescriptions are adopted as a minimal framework (see Christensen et al. 2012)
2. The mandatory climate data of the RCM runs will be transferred to the CORDEX Archive.
3. High-resolution temporal and spatial prescriptions were decided, that go beyond the CORDEX prescriptions (see Annex F).
4. Among the CORDEX.be runs a sequence of the prioritized climate run was determined (see Figure 2).

Note that the methodology of the CORDEX.be project is outlined on the website [euro-cordex.be](http://euro-cordex.be), and described in Termonia et al (2017, under review in Climate Services).

## 3.2 Methodology of the regional climate models

### 3.2.1 Dynamic Downscaling



Here the methodology is explained to obtain the RCM results that are detailed in Section 4.1. In order for the RCM model results to be compared and combined for uncertainty estimation, a coherent framework was established prior the start of the computer simulations. Therefore, analogous to the international CMIP5 and the CORDEX projects, CORDEX.be imposed coherent climate run prescriptions.

As described in the flowchart Figure 1, the basis for climate impact studies within CORDEX.be are the regional climate runs over Europe with horizontal model resolutions of 50 km or 12.5 km. These are indicated further as the “RCM runs” (see Figure aside). The “H-Res runs”, on the other hand, are done using a small domain over Belgium and have resolutions in the range of 3 to 5 km.

### 3.2.2 Description of the climate simulations

Figure 2 shows a diagram with all possible model simulations, obtained by a combination of all 4 models with all spatial domains and all forcing data. The models used are ALARO-0 at RMI, MAR at ULg and COSMO-CLM at KU Leuven and UCL. The model specifics are explained further and in Annex A.

The RCM and H-Res runs are performed on a limited geographical domain using a top-down approach i.e. by imposing meteorological conditions at the boundaries from model simulations at lower resolution. Three types of model runs can be distinguished as described by the CMIP5 project (Taylor et al. 2012):

- **The evaluation run:** At the European boundaries the lateral boundary conditions from reanalysis. These are the most “realistic” data available in the sense that they approximate the available observations in a coherent way. The most common reanalysis dataset is ERA-Interim from ECMWF, used here for period 1979-2010 (Dee et al., 2011). For the period 1950-1979 the previous-generation ERA-40 dataset is used (Uppala et al., 2005)<sup>1</sup>.
- **Control run:** At the European boundaries these runs are forced by GCM runs that were initialized in 1850 and afterwards forced using realistic greenhouse gas and aerosol concentrations, volcanic eruptions and land uses (Taylor et al., 2011). These runs over Europe have been performed here covering the period 1976-2006. The Table in Annex A specifies the GCM model used as boundary forcing.
- **Future or projected runs:** Taking the control run for the year 2006 as initial state, these runs are forced at the European boundaries by GCM simulations from CMIP5 that follow the so-called Representative Concentration Pathways (RCPs) for atmospheric greenhouse gases. The three scenarios used here are RCP2.6, RCP4.5 and RCP8.5 (Van Vuuren et al., 2014), which are consistent with a range of possible changes in future anthropogenic emissions. The equivalent CO<sub>2</sub> evolution from 1951-2100, as described by the three RCPs is illustrated in Figure 3. Besides the “high” scenarios such as RCP4.5 and RCP8.5, which are very relevant for adaptation planning, there is also the “low” RCP2.6 scenario. This scenario is relevant in the context of the Paris Agreement, to distinguish the differences in terms of impact between the 1.5°C and 2°C global warming case. Note that, for the period 2006 until 2017 the observations follow most closely the “highest” scenario RCP8.5.

Due to the realistic boundary conditions of the evaluation runs, these are used to validate the models. Such validation step is indispensable as it should give confidence in the use of the models for climate change purposes. In Section 4 different model validations are provided.

<sup>1</sup> Note that the H-Res evaluation model runs with the model MAR are performed with four sets of reanalysis datasets: ERA-Interim, ERA-40, ERA20C and NCEP-NCAR-v1. The RCM and H-Res evaluation run with COSMO-CLM at KU Leuven were all forced using ERA-Interim but used three land-use schemes: using urbanization of the year 2000, a vegetation land-use scenario and using the projected urbanization of the year 2060.

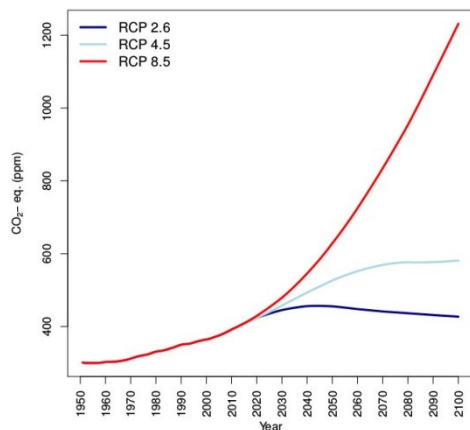


Figure 3 The equivalent  $\text{CO}_2$  evolution as described by the three RCPs (RCP 2.6, RCP 4.5, RCP 8.5) used in the CORDEX.be project.

In climate-change studies, the climate projections are always contrasted with the control runs in order to estimate the climate sensitivity with respect to changing greenhouse gases. In most cases what is called the “climate change” is then the difference between averages over two 30-year periods. For instance, often in this report the climate change signal shown is the difference between the average from the period 2070-2100 (following RCP8.5) with the average from the period 1976-2006.

As boundary conditions for the H-Res runs, the RCM runs over Europe are used from the same model<sup>2</sup>. Therefore the finalization of the RCM runs was a necessary condition to start the H-Res runs.

### 3.2.3 Additional CORDEX.be model prescriptions

For data exchange among the project partners, a standardized data format (NetCDF v. 4) was adopted and this implied data format conversion for most model groups. For the RCM model runs on the European domain detailed prescriptions exist (Christensen et al., 2012, Kotlarski et al., 2014) from the CORDEX consortium and are adopted for our purposes. Furthermore for the H-Res simulations over Belgium all CORDEX prescriptions (except for the domain) were adopted as a minimal framework. Additionally, for all runs, data is stored at temporal and spatial resolutions exceeding the CORDEX (See Annex F for a list of exchanged variables). This was necessary since the LIMs require such high resolutions. For instance, CORDEX minimally prescribes daily-averaged quantities while different variables are stored at hourly or sub-hourly frequency. The RCM and H-Res climate runs that were done in the context of CORDEX.be are outlined in Table 1 (see Section 4.1) and are stored in a local data hub at RMI. Note that the redundancy in model runs (see Figure 2) was necessary to anticipate potential technical difficulties and computational limitations.

## 3.3 Methodology of regional climate simulations using the ALARO-0 model

### 3.3.1 Model description

Here the methodology is explained to obtain the RCM results with ALARO-0 that are detailed in Section 4.3. The ALARO-0 model used at RMI and was established within the ALADIN consortium (Aire Limitée Adaptation Dynamique Développement International). This international consortium has over the past two decades developed a Local Area Model (LAM) to serve the specific NWP needs of its participating partners (ALADIN international team, 1997). Currently this consortium consists of 16 partners, covering Europe and the Mediterranean region and including some North African countries. The code of the ALADIN model (Bubnova et al., 1995) is mostly shared with the code of

<sup>2</sup> Note that this approach was not used by the MAR model. Simulations over the H-Res domain were directly coupled to GCM or reanalysis.

the French global ARPEGE (Action de Recherche Petite Echelle Grande Echelle) model and the Integrated Forecast System (IFS) of the ECMWF. The ALADIN model runs operationally in the countries of the ALADIN and HIRLAM consortia for national NWP applications (Termonia et al., 2009, 2012, 2017).

ALADIN has been further developed with a physics parameterization package called ALARO, which has been designed specifically to be run at “convection-permitting” resolutions, i.e. below 10 km when convection is partly parameterized and partly resolved explicitly. The key concept behind this package lies in the precipitation and cloud scheme called Modular Multi-scale Microphysics and Transport (3MT) and is developed in Gerard et al. (2005, 2007, 2009). The multi-scale behavior of 3MT has been validated in a NWP context up to a spatial resolution of 4 km (see Gerard et al. 2009). The ALARO model version ALARO-0, which has been used for the present study, utilizes a semi-Lagrangian horizontal diffusion scheme called SLHD (Vana et al. 2008), some pseudo-prognostic Turbulent Kinetic Energy scheme and a statistical sedimentation scheme for precipitation within a prognostic-type scheme for microphysics (Geleyn et al 2008). The ALARO physics package is coupled to the dynamics of the ALADIN model via a physics-dynamics interface based on a flux-conservative formulation of the equations proposed by Catry et al. (2007). Note that this model version is also used operationally.

The ALARO-0 model has been used twice to downscale ERA-Interim (De Troch et al. 2013, Giot et al. 2016) and a significant improvement was found in the statistics of extreme precipitation. These tests show good multi-scale behaviour, i.e. the results at of 4-km runs are coherent with 10-km and 40-km runs (De Troch et al. 2013). This gives this model a unique place among the regional models worldwide.

### 3.3.2 Model setup of ALARO-0 for EURO-CORDEX and H-Res simulations

The ALARO-0 group has performed all the RCM climate experiments as described by the EURO-CORDEX Project and the H-Res simulations as specified in Section 3.2. The model elevation over Belgium of the H-Res run is shown in Figure 67 in Annex C. The data is also transferred to the [ESGF data hub](#). For these runs cycle 36t1 of ALARO-0 has been used while boundary conditions are taken from ERA-40 (period 1950-1979), ERA-Interim (evaluation period, 1979-2014) and the GCM model data of the CNRM-CM5 model as present in the CMIP5 database (control and future simulations). Continuous climate simulations are done for 31-year periods. A data extraction program (CORDEXtractR) was written in R to convert the standard output to CORDEX-compliant NetCDF format.

ALARO-0 is coupled by the classical Davies procedure with a relaxation zone of 8 grid points and new boundary conditions are provided every six hours. No further nudging or relaxation towards the boundary conditions was done inside of the domain. Some fields in ALARO-0 are constant during run-time, most notably Sea Surface Temperatures (SSTs). Simulations are however interrupted and restarted monthly to allow for SSTs to be updated. Other fields that have monthly updates, but are constant during any given month are surface roughness length, surface emissivity, surface albedo and vegetation parameters. Following the EURO-CORDEX guidelines, two new grids with a 12.5 and 50 km resolution were defined for the ALARO-0 simulations. The grids were chosen such that the common EURO-CORDEX analysis domain is completely included in the non-coupling zone. The low-

resolution Lambert 5 domain consists of 139-by-139 grid points, while the high resolution domain consists of 501-by-501 grid points. In both simulations the number of vertical levels was 46. Further setup details can be found in Giot et al. (2016).

## 3.4 Methodology of regional climate simulations using COSMO-CLM

### 3.4.1 Model description

Here the methodology is presented to obtain the RCM results with COSMO-CLM that are detailed in Section 4.4. Within the CORDEX.be project the COSMO-CLM models was used by two partners, UCL and KU Leuven, using separate setups. The differences will be detailed further.

The COSMO model (Consortium for Small-scale Modeling) is a non-hydrostatic limited area model, designed for both operational numerical weather forecasting (NWP) and climate simulations. It is used and further developed for climate-related applications by the CLM-Community, [an open international network of scientists](#), and is referred to as the COSMO-CLM model. There is an active collaboration between the NWP and climate communities.

Since 2005, the COSMO-CLM model has been taking part in international coordinated regional climate modeling projects like PRUDENCE (Déqué et al., 2005). COSMO-CLM was present in the ENSEMBLES project and more recently CORDEX simulations have been performed with the COSMO-CLM model both at 12 km and 50 km resolution. A joint standard evaluation of the EURO-CORDEX RCM ensemble (Kotlarski et al., 2014) highlights the general ability of COSMO-CLM to represent the basic spatio-temporal patterns of the European climate and the good performance of the COSMO-CLM model compared to other ensemble members.

Even with a mesh size of 12 km, as used in EURO-CORDEX, several processes are not resolved and have to be parameterized. This introduces model deficiencies and large uncertainties in the projections of future climate (e.g., Déqué et al. 2007). An important benefit of increasing the mesh size to the scale is that deep convection is (at least) partly resolved. Such convection permitting model simulations with COSMO-CLM have shown added value in the diurnal cycle and timing of summer convective precipitation, the intensity of most extreme precipitation, and the size and shape of precipitation objects (Prein et al., 2013). Recent simulations over the Belgian region have confirmed this added value (Brisson et al., 2016a,b; Saeed et al., 2017). Experiments with COSMO-CLM also suggest that a more detailed representation of cloud physics (2-moment schemes) do not substantially improve most results at present, due to insufficient knowledge of the relevant parameters (van Weverberg et al., 2014), but appears valuable for the simulation of hail reaching the surface. In addition, -scale model integrations allow taking into account land-use changes such as urbanization into the climate projections for the future. The model elevation over Belgium of the H-Res COSMO-CLM runs is shown in Figure 67 in Annex C.

### 3.4.2 Extension 1 of COSMO-CLM: The Urban land-surface scheme TERRA\_URB

A computationally efficient urban parameterization was recently implemented in COSMO-CLM by the group of KU Leuven (Wouters et al., 2012; 2015; 2016; Demuzere et al., 2017).

In order to capture the urban physics and associated atmospheric features including urban heat islands, the urban land-surface scheme TERRA\_URB (Wouters et al., 2015, 2016) was introduced in the COSMO(-CLM) model. It provides an urban upgrade of its soil module TERRA ML, the land-atmosphere interactions, and the land-surface parameters. As such, it represents the variability of ground heat and moisture transport, the turbulent transfer of momentum, heat and moisture, and the surface-atmosphere radiative exchanges in urban areas. The initial release of TERRA\_URB features the non-iterative calculation of surface-layer stability functions accounting for the roughness sub-layer and the impervious water-storage parametrization based on a probability density function of water reservoirs, see Wouters et al., 2015. Anthropogenic heat emissions are included as an additional heat source to the first above-ground model layer. Hereby, the magnitude takes into account latitude-dependent seasonal and diurnal distribution functions that are superimposed on the annual-mean anthropogenic heat flux. The latest version of TERRA also implements the Semi-empirical Urban canopY dependency parametrization (SURY) and the coupling with the turbulence kinetic energy based surface-layer transfer module of the COSMO(-CLM) model, see Wouters et al. (2016).

TERRA\_URB has been extensively evaluated in several recent studies, in which it reproduces very well the different components of the urban surface energy balance (Wouters et al., 2015; Demuzere et al., 2017) and the different urban heat islands from satellite imagery, in-situ measurements and tower vertical profiles (Trusilova et al., 2015; Wouters et al., 2016; Wouters et al., 2017).

A way to quantify heat stress for Belgium under climate change is by considering the frequency, length and intensity of heatwaves. Therefore, the indicator from the [Flanders Environment Agency](#) is applied. It has been developed in cooperation with several research institutes and governmental agencies regarding climate, care and health in Belgium. It is used to monitor the potential effect of heat stress episodes on a yearly basis, as a part of the state of the environment reporting in Flanders. The heat-stress indicator is obtained by the following expression:

$$\sum_i \left[ (T_{\min,i} - 18.2^\circ\text{C})^+ + (T_{\max,i} - 29.6^\circ\text{C})^+ \right] h_i$$

On the one hand, the frequency and length of heatwaves are considered by means of  $h_i$ , which indicates the occurrence of a heatwave day when heat wave alarm levels for temperature are exceeded: It equals to one in case the daily minimum ( $T_{\min,i}$ ) and maximum ( $T_{\max,i}$ ) temperature simultaneously exceed their respective thresholds 18.2°C and 29.6°C during three consecutive days, whereas it equals to zero for the other days. On the other hand, the intensity of the heatwaves is taken into account with the level of exceedance of those temperature thresholds. Therefore, the terms in the inner brackets  $(...)^+$  represent the exceedance of  $T_{\min,i}$  and  $T_{\max,i}$  above their respective threshold values 18.2°C and 29.6°C. More details and references of the heat-stress indicator can be

found in Wouters et al. (2017) and Brouwers et al. (2015). The results following this methodology are detailed in Section 4.10.

### 3.4.3 Extension 2 of COSMO-CML: hail with the 2-moment scheme

An important aspect, addressed by the COSMO-CLM group at UCL, for accurate deep convective storm simulations is in the parameterization of hail within models, which can substantially impact precipitation and dynamical features within the cloud. Generally, hail formation depends on strong thunderstorms with high upward speeds and great vertical extent. Additionally, hailstorms require the presence of hail embryos such as frozen raindrops and regions of high liquid water content where the hailstone will increase in size by either dry or wet growth mechanisms. Furthermore, the right conditions need to be present such that melting is minimized and the falling hailstones are able to reach the surface (i.e. large hail sizes, decreased height of the melting layer).

One of the most important outcomes found by tests done within the previous MACCBET project using this specific model configuration over the Belgian territory at this resolution is the improved simulated hail at the surface when using a 2-moment microphysical scheme, with potential implications for climate and extreme weather events. Hence, demonstrating its added value of utilizing a more computationally expensive and complex scheme. CORDEX.be gave the opportunity to directly study possible future trends of hail formation within deep convective storms potentially affecting flooding events in the regions. This information is crucial for local impact models.

In order to represent hail, the 2-moment microphysical scheme from Seifert and Beheng (2006)

microphysical scheme is used, which originally includes 5 hydrometeor species (cloud water, rain, ice, snow, graupel (soft hail or snow pellets)). A new hail category added by Blahak (2011) was added and tested by Van Weverberg et al. (2014). This scheme calculates prognostically the mass-mixing ratio and number concentration of these six hydrometeor species. This enables a direct estimation of hail size in the simulations. A gamma function is used for the size distribution of all hydrometeor species to alleviate the excessive size sorting occurring in 2-moment schemes that occurs when using an exponential functional form instead. Another important aspect of this scheme is the inclusion of a look-up table by Segal and Khain (2006) that contains a solubility parameter of the aerosol spectrum and also depends on environmental conditions such as updraft speed, bridging microphysical and dynamic aspects of hail formation within the model. The results for COSMO-CLM following this methodology are detailed in Sections 4.4.4, 4.4.3 and 4.9.

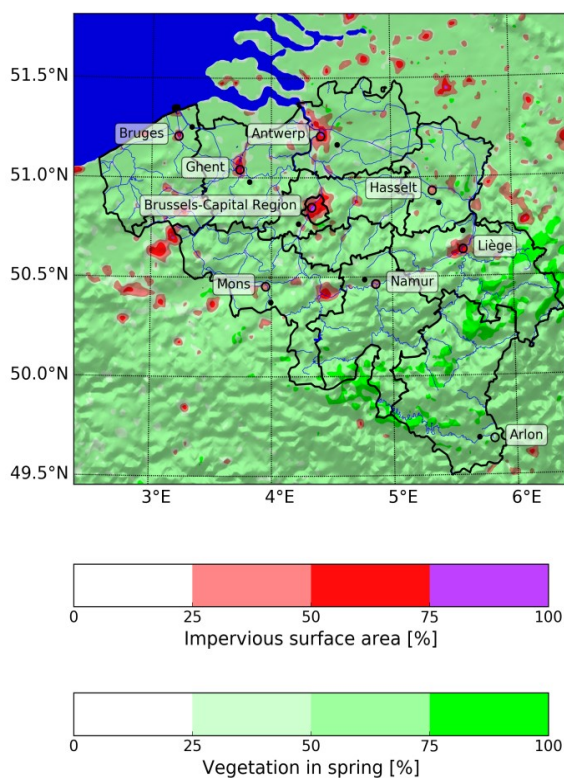


Figure 4: Land-surface parameters and orography (shadow mask) for the H-Res Belgian domain used for the convection-permitting downscaling with the COSMO-CLM model at KU Leuven

#### 3.4.4 The COSMO-CLM setup for the simulations

The COSMO-CLM groups have followed the EURO-CORDEX Project prescriptions for the runs over Europe and the H-Res simulations as specified in Section 3.2.

Evaluation runs have been performed using the COSMO-CLM model. First, the evaluation simulations are done at 12.5km resolution by forcing the domain boundaries over Europe with realistic meteorological conditions from ERA-Interim reanalysis (Dee et al., 2011). The output of this EURO-CORDEX simulation is used as boundary conditions for a second nesting that employs the H-Res simulations over Belgium at 2.8 km resolution as specified in Section 3.2. This H-Res setup is based on the Convection-Resolving Climate Setup (CRCS) developed by the CLM-community and adapted for the Belgian territory (Brisson et al., 2016a,b; Saeed et al., 2017) in the BELSPO-funded MACCBET project. The H-Res domain covers 192 by 175 grid cells centered over Brussels with a horizontal grid spacing of 2.8 km and 40 vertical layers. Additional technical features are outlined in the Annex A, while the land-surface parameters and orography of the H-Res runs are shown in Figure 67.

Two sets of simulations are performed on the CORDEX.be domain. The first one uses extension 1 consisting of the TERRA\_URB urban land-surface scheme (see section 3.4.2) and is performed by the KU Leuven. The second one uses extension 2 consisting of the two-moment scheme with hail parameterization (see section 3.4.3) and is performed by UCL. Each series of nesting (either with extension 1 or 2) are used as a basis for additional climate scenarios provided in the next sections.

#### 3.4.5 The COSMO-CLM downscaling methodology using EC-EARTH

In addition to contributing to the evaluation runs on the EURO-CORDEX and H-Res grids, the KU Leuven is assigned to downscale one of the 16 members of the EC-EARTH RCP8.5 ensemble used by the KNMI 14 report (KNMI, 2014). Except for the boundary conditions, it follows the nesting strategy of Section 3.4.4 and uses extension 1 consisting of the TERRA\_URB urban land-surface scheme.

Owing to the internal climate variability of the Earth's climate system, the climate-change signal varies with the GCM member being downscaled. In principle, the downscaling needs to be done for every member of a GCM ensemble in order to obtain the probability distribution of any climate-change signal. For example, the ensemble median climate change of any climatological variable can be obtained by calculating the median over the different members. Unfortunately, it is impossible to downscale every member with the today's computing infrastructure. A way out of this impasse is the selection and the downscaling of the member with the median climate-change signal developed in Vanden Broucke et al. (2017). As such, the first of the 16 members from the KNMI'14 ensemble was selected. The resulting climate projection runs are detailed in Section 4.7

### 3.4.6 The COSMO-CLM downscaling methodology using MPI-ESM-LR

The UCL was assigned to downscale, in addition to the evaluation runs on the EURO-CORDEX and H-Res grids (section 3.4.4), the first realization from the Max Planck Institute Earth System Model GCM (first realization, MPI-ESM-LR r1) at base resolution (Giorgetta et al. 2013) with the latter composed of control runs and climate scenario RCP8.5. Except for the boundary conditions, it follows the nesting strategy of Section 3.4.4 using extension 2 consisting of the two-moment scheme with hail parameterization.

An overview of all UCL downscaling simulations can be found in Figure 5: the ERA-Interim and GCM output data is first downscaled to a European domain with 12 km grid spacing. The output from these initial runs is further downscaled to an H-Res (2.8 km) domain centered on Belgium with 192 and 175 grid points in the East-West and North-South direction, respectively and 40 vertical levels. These final H-Res simulations will be further analyzed. An analogous procedure (using EC-EARTH instead of MPI-ESM-LR; using extension 1 instead of extension 2) is followed by the KU Leuven.

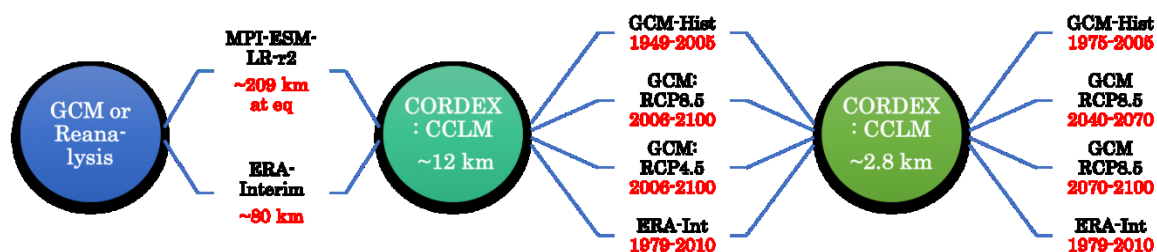


Figure 5: Flowchart showing the downscaling of the ERA-Interim and GCM MPI-ESM-LR r1 to the COSMO-CLM (COSMO-CLM) model at UCL at 12 km grid spacing. This step generates 3 sets of output data for further downscaling using COSMO-CLM at 2.8 km grid-spacing generating again 3 sets of output data.

### 3.4.7 The COSMO-CLM urbanization scenarios

The implementation of the TERRA\_URB scheme enables to address the role of urbanization on the climate system and statistics of Belgium. Therefore, KU Leuven has performed two additional H-Res climate simulations on top of the ERA-INTERIM-driven hindcast simulation with the present-day urbanization (using extension 1). They include a future business-as-usual urbanization scenario towards the year 2060 and a vegetation (no-urbanization) scenario. The urbanization scenarios are obtained from the BELSPO MULTIMODE project (Acosta-Michlik, 2011).

## 3.5 Methodology of regional climate simulations using the MAR model

### 3.5.1 Model Description

Here the methodology is presented to obtain the RCM results with the model MAR that are detailed in Sections 4.5 and 4.8. The University of Liège (ULg) contributed to the CORDEX.be project by performing high-resolution (5 km) simulations over Belgium with its regional climate model MAR ("Modèle Atmosphérique Régional"). MAR is a hydrostatic primitive equation model in which

convection is parametrized according to Bechtold et al. (2001). The atmospheric part of MAR is completely described in Gallée and Schayes (1994) and Gallée (1995). Furthermore, MAR is coupled to the 1-D surface vegetation atmosphere transfer scheme SISVAT (Soil Ice Snow Vegetation Atmosphere Transfer) which is detailed in De Ridder and Gallée (1998). The snow-ice part of SISVAT is the snow model CROCUS from the CEN (Centre d'Etudes de la Neige) described in Brun et al. (1992). The MAR-SISVAT coupling allows the consideration of three sub-pixel surface characteristics for a same MAR pixel. The coupling also allows interaction between surface and atmosphere (energy and moisture transfers), snow accumulation and snow melting on the surface, water percolation into the soil/snow, and run-off of exceeding water.

Although being initially designed for polar regions (Fettweis et al., 2013 ; Gallée et al., 2001), MAR was successfully calibrated to the climate of Tropical Africa in Gallée et al. (2004) and Doutreloup et al. (2017) and to Belgium in Wyard et al. (2017a). The most recent MAR version is the version 3.7 which is described and applied in Belgium in Fettweis et al. (2017) and Wyard et al. (2017b, submitted).

### 3.5.2 Simulations performed using MAR over Belgium

All MAR simulations were performed using the version 3.6 of MAR as Wyard et al. (2017a). Simulations were performed at a resolution of 5 km over a domain of 120 by 110 points centered on (4.3° W; 50.4° N) as shown in Figure 6 (left). Boundary conditions (i.e. temperature, wind, humidity and pressure at each pressure level of MAR, sea surface temperature and sea ice cover) were provided every 6 hours by forcing reanalyses or GCM outputs. Land cover was derived from the CORINE (Coordination of the information on the Environment) land cover database from the EEA (European Environment Agency). Regarding the other surface characteristics prescribed in SISVAT, such as vegetation seasonality (provided by the monthly normalized difference vegetation Index (NDVI)), vegetation cover fraction (derived from the leaf area index (LAI)) or soil type, we used the same datasets as Gallée et al. (2004).

The evaluation runs used three sets of reanalysis as boundary conditions: the ECMWF ERA-Interim (Dee et al., 2011) (1979-2014) completed by ERA40 (Uppala et al., 2005) (1958-1978), the NCEP-NCAR-v1 (Kalnay et al., 1996) (1948-2014), and the ERA-20C (Poli et al., 2013) (1900-2010). Wyard et al. (2017a) present a full validation of MAR comparing the results of these three simulations to synoptic observations from 20 land-based weather stations.

Regarding future projections over Belgium, all CMIP5-GCMs were compared with ERA-Interim in order to check their ability to represent the current mean climate over Europe with the help of a statistical classification based on the calculation of skill-scores evaluating notably the winter/summer temperature at 850 hPa and the geopotential height at 500 hPa. Two GCMs were selected from the CMIP5 database to force MAR at its boundaries: NorESM1 and CanESM2 also used by Fettweis et al. (2013) for forcing MAR over Greenland.

### 3.5.3 Simulations performed using MAR over Europe

The EURO-CORDEX simulations with MAR were also performed using the version 3.6 of MAR as described in Wyard et al. (2017a). Simulations were done at a resolution of 50 km over a domain of 106 by 106 points centered on (10° E; 49,5° N) as shown in Figure 6. These runs use the same configuration as the simulations over Belgium.

The evaluation run is forced by ERA-Interim, while the control and RCP8.5 scenario runs are forced by Nor-ESM1 respectively which came from the CMIP5 database.

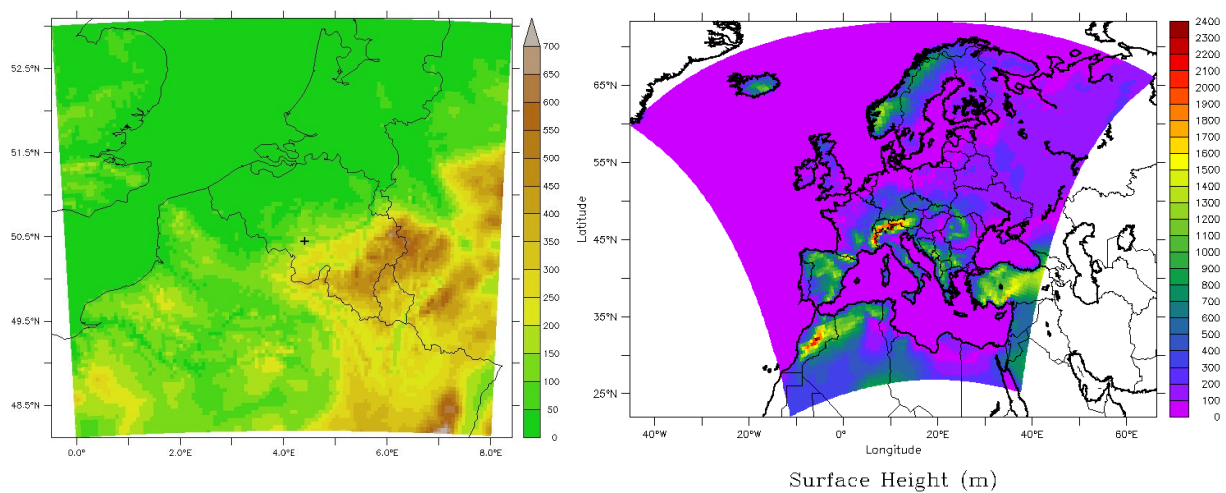


Figure 6: MAR domain and orography for the H-Res simulations over Belgium (left) and the EURO-CORDEX simulations over Europe (right).

### 3.6 Methodology of RCM model validation using GNSS products

The main objective of the use of GNSS products is to go beyond the standard verification procedure of climate simulations. The traditional manner is to compare the results from climate runs with long-term ground-based observations. Additional to that, CORDEX.be implements a verification based on products estimated from continuously observing GNSS (Global Navigation Satellite Systems, such as the American Global Positioning System, GPS) stations.

Validating climate model based on GNSS products is a pioneering task. As such, at the beginning of the project, a dedicated Working Group (WG) was set up to work out the model validation procedure based on GNSS-derived products. This WG met at several occasions to structure and plan in details the work to be carried out throughout the project. The main lines of the work plan was defined as

1. Defining the specific requirements to be imposed to the GNSS re-processing activity done for this project, taking into account the different high-resolution climate model specifications,
2. Developing the proper GNSS re-analysis methodology to satisfy all project requirements,
3. Producing the climate-quality GNSS-based tropospheric delay dataset (done by ROB),

4. Defining the optimal procedure (including the algorithmic and the mandatory meteorological data) for the conversion from the GNSS-based tropospheric products (ZTD) to IWV (Integrated Water Vapor),
5. Defining and developing the best method to achieve the validation between the various climate model run output and the GNSS-based products (including the selection of the mandatory climate model variables and their frequency, to be stored for later use in the conversion and validation phase).
6. Applying the validation methodology using ZTD for the different H-Res model simulations (done by RMI).

The results of this validation are given in Section 4.6.

### 3.7 Methodology of impact study on biogenic emissions

For the CORDEX.be project the BIRA has estimated the isoprene fluxes emitted by vegetation in past and future climate over the European (EURO-CORDEX) domain using the MEGAN-MOHYCAN model (Müller et al., 2008, Stavrou et al. 2014). The model is based on the widely used MEGAN model for biogenic emissions (Guenther et al., 2006, 2012), coupled with the multi-layer canopy environment model MOHYCAN (Müller et al., 2008). The MEGAN algorithm (Eq.1) includes the specification of a standard emission factor  $\varepsilon$  ( $\text{mg m}^{-2} \text{h}^{-1}$ ), representing the biogenic emission at standard conditions (Guenther et al. 2006) for each plant functional type (PFT). The activity factors  $\gamma$  account for the response of the emission to solar radiation, temperature, leaf age, soil moisture, and  $\text{CO}_2$  levels. The  $\gamma_{\text{CO}_2}$  activity factor is not applied for past simulations, and for the future runs two different parameterizations are tested, W2009 and PH2011, based on Wilkinson et al. (2009), and Possell and Hewitt (2011), respectively. LAI in Eq. (1) denotes the leaf area index (LAI).

$$Flux = \varepsilon \cdot \gamma_T \cdot \gamma_{PAR} \cdot \gamma_{age} \cdot \gamma_{SM} \cdot LAI \cdot \gamma_{CO_2} \quad (1)$$

The MOHYCAN model (Müller et al. 2008) calculates the leaf temperature and the attenuation of light as a function of the height inside the canopy, using visible and near-infrared solar radiation values at the canopy top, together with air temperature, relative humidity, wind speed and cloud cover. More precisely, the meteorological input fields driving MEGAN-MOHYCAN are: the downward solar radiation, the cloud cover fraction, the volumetric soil moisture (at four soil layers), the air temperature above the surface, the dew point temperature, and the wind speed directly above the canopy. The emissions are calculated with a time step of 1h at a horizontal resolution of  $0.1^\circ \times 0.1^\circ$ , or about 11 km. Here we first calculate isoprene emissions over 1979-2005 based on the ECMWF ERA-Interim reanalysis data, and investigate the sensitivity to solar radiation changes observed at European stations. Next, we perform simulations using the output of the EURO-CORDEX ALARO-0 regional climate model (Giot et al., 2016) forced by the RCP2.6, RCP4.5 and RCP8.5 scenarios over 2071-2099, and compare with the control emissions over 1976-2005 derived by the same model. The ALARO-0 fields used are temperature, wind, cloud cover fraction, solar radiation downward flux and specific humidity. Furthermore, we incorporate the inhibition effect of isoprene emissions to the enhanced  $\text{CO}_2$  levels of the climate projections. The results of this validation are given in Section 4.14.

### 3.8 Methodology of impact study on agricultural crop performance and yield

The availability of downscaled RCM scenarios allowed for impact assessment of crop performance and production. We compared three scenarios (control model run (base), RCP45 and RCP85) of ALARO-0 runs over the EURO-CORDEX domain at 12.5 km resolution with historical observations (hist). The climatological variables included daily rainfall; mean, minimum, maximum and temperatures; specific humidity; solar radiation; and, wind speed. Agro-climatological algorithms for vapor pressure deficit and potential evapotranspiration were calculated using the FAO Penman-Monteith equation (Allen et al., 1998). Inter-annual variability in potential growing season length was evaluated in cumulative growing degree days using fixed planting dates and crop specific upper and lower threshold temperatures for physiological activity, augmented with day length and vernalisation responses to reflect winter crop development. Climate impacts on arable agriculture were subsequently quantified using REGCROP which is a regional dynamic agrometeorological model geared towards modeling climate impact on biomass production of arable crops (Gobin, 2010, 2012, 2015).

The results that are given in Section 4.13 were evaluated in terms of cumulative growing degrees, actual evapotranspiration, biomass and yield. A summer crop was evaluated to test the overall methodology after which model runs were performed on winter wheat, fodder maize and late potato. The three crops represent the largest share of arable cultivation area in Belgium. From a crop physiological standpoint maize and potato are summer crops while wheat is a winter crop. Wheat and potato are C3 crops, and maize is a C4 crop meaning that their respective responses to increased CO<sub>2</sub> concentrations are different. The C4 photosynthetic pathway has an alleged advantage over the C3 photosynthesis, particularly in drier environments.

### 3.9 Methodology of the impact study on urban impacts

The first urban model described here is the newly-developed surface scheme of Météo-France-Surface Externalisé (SURFEX, Le Moigne 2009, Masson et al. 2013). SURFEX is an externalized surface scheme that can be run either in a coupled mode in which case the atmospheric forcing is provided by the host atmospheric model, or in a stand-alone mode where the atmospheric drivers are derived from observations and fed to the surface scheme such that it is decoupled from the atmospheric part of a GCM. The latter is possible by relying on the algorithmic structure proposed by Best et al. (2004). SURFEX contains various modules allowing one to describe the exchanges of water, momentum, and energy over four surface area tiles: sea, lake, vegetation, and the city. A grid value is then simply an area-averaged value of the different tiles present in the grid cell. Over vegetated areas, SURFEX includes the simple Interactions between Soil, Biosphere, and Atmosphere (ISBA) scheme (Noilhan and Planton, 1989). ISBA solves simultaneously the energy and water budget of the soil and vegetation. Vegetation parameters come from the Ecoclimap database (Masson et al., 2003). Over urban surfaces, SURFEX includes the Town Energy Balance (TEB, Masson 2000) single-layer urban canopy module. Urban canopy is assumed to be an isotropic array of street canyons. TEB simulates heat and water exchanges of three generic surfaces (roof, wall, and road), where heat

transfers are computed through several layers of materials, generally four. Anthropogenic heat and vapor releases from buildings, vehicles, and chimneys can also be added. TEB is forced with literature-based surface thermal parameters and observed or simulated atmospheric and radiation data from above-roof levels. Despite the simplification hypotheses, offline simulations of TEB have been shown to accurately reproduce surface energy balance, canyon air temperature, and surface temperatures observed in dense urban areas - Vancouver and Mexico City (Masson et al. 2002), Marseille (Lemonsu et al. 2004), Basel (Hamdi and Masson, 2008) - during dry and hot seasons. In the study by Pigeon et al. (2008), the evaluation of TEB is extended to two other seasons, fall and winter. In their study, a validation of the parameterization of anthropogenic heat sources against an inventory of energy consumption in the city of Toulouse, France, was also performed. SURFEX can also be run in-line within the ALARO model.

### **3.10 Methodology of impact study on waves and storm surges**

#### **3.10.1 Impact case study: waves and storm surges**

The involvement of RBINS-OD Nature in the modeling of climate change started with the BELSPO CLIMAR project which focused on the physical and bio-geo-chemical aspects of climate change as well as on its socio-economic impact at the Belgian Coast. In the framework of the BELSPO CORDEX.be project, OD Nature activities focus on investigating the influence of climate change on hydrodynamic parameters of the Belgian Continental Shelf (BCS). The influence on storm surges is evaluated at two stations of the BCS. Furthermore, the effect on the significant wave height at two stations of the BCS is assessed. Finally, the effect of climate changes on the wind velocity itself in a station located at the BCS and a station in the northern North Sea are evaluated.

The climate simulations for waves and storm surges have been generated by using the meteorological conditions from the ALARO-0 model of RMI with a 3-hour resolution for the evaluation period (1980-2010), the control period (1976-2005) and the projected scenario RCP8.5 (2069-2099). Note that both the control and projection run of ALARO-0 was forced at the European boundaries by the results of the global coupled earth-system model CNRM-CERFACS-CNRM-CM5. The current climate was also modeled with the ALARO-0 model in the evaluation simulation by forcing with reanalysis data from the ERA-Interim dataset for the period 1980-2010. All model input data was provided in Lambert coordinates and was converted to geographical coordinates as needed for the storm surge model as well as for the wave models. All scientific results are explained in Section 4.15.

#### **3.10.2 Modeling methodology for storm surges with the COHERENS model**

COHERENS V2 is an integrated code with modules for physics, sediment transport, biology and particle tracing. It has been developed in the context of different European and national projects (Luyten, 2016). To conduct simulations for climate scenarios, COHERENS is applied on the North Sea Continental Shelf with a spatial resolution of about 4 km and forced by 3-hourly pressure and wind fields and 15 tidal harmonics at the open boundaries. Special attention is be paid to the Belgian coastal zone where two measurement stations are located that will be subject to a thorough

analysis. A first validation of the COHERENS V2 model was executed, using the atmospheric conditions of the evaluation run and the COHERENS model proved to give satisfactory results.

### 3.10.3 Modeling methodology for waves with the WAM model

The significant wave heights were modeled using the WAM wave model (Günther et al., 1992;; Monbaliu et al., 2000; Bolaños et al., 2011). The WAM model is a third-generation wave model developed by the WAMDI group (1988). It includes “state-of-the-art” formulations for the description of the physical processes involved in the wave evolution. In comparison with the 2<sup>nd</sup> generation model, the wave spectrum has no restrictions and the wind sea and the swell spectrum are not treated separately. The WAM model is implemented on three coupled grids. A coarse WAM grid provides boundary conditions for an intermediate resolution nested WAM model, which is coupled to a local higher resolution model. The coarse grid WAM model extends up to 71°N in order to catch the waves that are generated in this area and travel (as swell) towards the Belgian coast. The westward extension is limited since the Southern North Sea is sheltered by the British Isles. The local model has a resolution of 2.5 km by 3.5 km. The WAM model was not explicitly validated using the ALARO-0 meteorological forecasts.

The WAM model required adaptations for writing the output in NetCDF format. This standard format was chosen by the CORDEX.be consortium for having consistent output from the COHERENS model as well as the WAM model aiming at building a database from the model output.

### 3.10.4 Model data methodology for WAM and COHERENS

A statistical analysis is performed on time series of surges and wave heights using the methods described in Kamphuis (2010). Then, data are extrapolated to extreme values with a certain return period.

To evaluate a time series, first the “extreme events” in the time series are selected. A certain threshold is defined and for each period for which the threshold is passed, the maximum value during that period is used to characterize the extreme event. Note that, according to Kamphuis (2010), the exact value of the threshold is not critical.

A cumulative probability function is made from these extreme events as a function of the maximum values, which is then parameterized by different possible models. In this study, the Normal distribution, Log-Normal distribution, the Gumbel distribution and the Weibull distribution are used. Note that in the Weibull distribution, an additional parameter  $\alpha$  is used. Since these four distributions can be linearized as a function of the maximum values (or of the logarithmic of the maximum values for the Log-Normal distribution), a best fit can be found using a least squares method. For the Weibull distribution, this is done for different values of  $\alpha$ , to find the best fit. The fitted distribution then can be used to extrapolate towards longer return periods.

### 3.11 Methodology of statistical and uncertainty estimation

The aim of this CORDEX.be was to provide coherent climate information for Belgium targeted to end-users, backed by (i) a unified framework for the H-Res climate runs and (ii) uncertainty estimations on the climate-change signal.

Climate change signals were derived for all available climate runs and were put in a table into a CORDEX.be leaflet. More specifically, the climate runs include the CMIP5 GCM and EURO-CORDEX RCM runs to for the different climate scenarios and for the following several meteorological variables: monthly precipitation, extreme precipitation quantiles or precipitation intensity – duration – frequency (IDF) extremes, monthly daily mean, maximum and minimum temperature, number of heat waves, hot days, freezing days, monthly potential evapotranspiration, solar radiation, wind speed. The potential evapotranspiration was calculated from the climate model outputs on temperature, solar radiation, relative humidity, and wind speed, applying and inter-comparing different methods. The climate change signals were obtained for each RCP scenario (RCP8.5, 6.0, 4.5 and 2.6) separately. Comparison moreover was made between the GCM based, RCM based and H-Res based climate change signals. By comparison of the climate change signals of the higher resolution models with the coarser resolution models in which the higher resolution models were nested, the influence of the spatial resolution of the climate model on the climate change signals could be evaluated. By studying the climate change signals per RCP scenario separately, the potential effect of mitigation scenarios became clear. This is an interesting result in view of climate change communication. Based on the model ensemble approach, the total uncertainty in the climate change signals has been quantified. We moreover have split this total uncertainty in its contributing uncertainty sources: the GCM related uncertainty, the RCM related uncertainty, the RCP related uncertainty, the statistical downscaling related uncertainty, the uncertainty related to natural variability, and interaction terms. A variance decomposition method was applied for that purpose. The results of this study can be found further in Section 4.16.

## 4 SCIENTIFIC RESULTS

### 4.1 The performed regional climate simulations

The produced CORDEX.be RCM model simulations are given in Table 1. The availability of this vast amount of data has enabled the successful elaboration of impact studies as presented further. Moreover, the existence of the CORDEX.be data hub allows and facilitates future impact studies. The data from the ALARO-0 model is also freely available to the research community through the international data hub of the Earth System Grid Federation ([ESGF](#)).

Table 1: Climate simulations that were performed (✓) with the regional climate models. The “RCM” indicates runs done over Europe while the “H-Res” runs were over Belgium only. More details are provided on [euro-cordex.be](#).

MODEL	Period	Evaluation	Control	RCP2.6	RCP4.5	RCP8.5
ALARO-0 RMI RCM 50 & 12 km	1950-1976	✓	✓	-	-	-
	2005-2040	-	-	✓	✓	✓
	2040-2070	-	-	✓	✓	✓
	2070-2100	-	-	✓	✓	✓
ALARO-0 RMI H-Res 4-km	1950-2005	✓	✓	-	-	-
	2006-2040	-	-	✓	✓	✓
	2040-2070	-	-	✓	✓	✓
	2070-2100	-	-	✓	✓	✓
COSMO KUL RCM 12 km	1979-2014	✓	-	-	-	-
	1975-2005	-	✓	-	-	-
	2069-2100	-	-	-	-	✓
COSMO KUL H-Res 2.8 km	1979-2014	✓(x3) <sup>3</sup>	-	-	-	-
	1975-2005	-	✓	-	-	-
	2069-2100	-	-	-	-	✓
MAR H-Res 5 km	1950-2015	✓(x3) <sup>4</sup>	-	-	-	-
	1980-1999	-	✓(x2) <sup>5</sup>	-	-	-
	2080-2099	-	-	-	-	✓(x2) <sup>5</sup>
MARH	1981-2003	✓	✓	-	-	-

<sup>3</sup> The H-Res evaluation run with COSMO-CLM at KU Leuven were all forced using ERA-Interim but used three land-use schemes: using urbanization of the year 2000, a vegetation land-use scenario and using the projected urbanization of the year 2060

<sup>4</sup> The H-Res evaluation model runs with the model MAR are performed with four sets of reanalysis datasets: ERA-Interim, ERA-40, ERA20C and NCEP-NCAR-v1.

<sup>5</sup> The H-Res control and projection run of MAR are forced with different two GCMs: NorESM1, CanESM2 and MIROC5.

	<b>2077-2099</b>	-	-	-	-	✓
COSMO UCL H-Res 2.8 km	<b>1979-2014</b>	✓	-	-	-	-
	<b>1975-2005</b>	-	✓	-	-	-
	<b>2070-2100</b>	-	-	-	-	✓
COSMO UCL RCM 12 km	<b>1979-2014</b>	✓	-	-	-	-

## 4.2 Evaluation and climate projection of all H-Res simulations

### 4.2.1 Evaluation of the H-Res simulations over Belgium

Prior to considering the results of the RCM climate projections, it is important to see how well the RCM models are able to reproduce the Belgian climate of the past. If the models agree well with the observations, this gives confidence in the scientific method used to make climate projections.

Figure 7 shows the average winter precipitation over Belgium for the past period 1980-2010 by comparing the observations (central panel, Delvaux et al. 2015) with the evaluation runs of the four H-Res CORDEX.be models. While the average over Belgium of the observations is 2.7 mm/day, the modeled ones range between 2.3 mm/day and 3.1 mm/day and are therefore in good agreement. Moreover the spatial patterns for all models correspond very well with the observed ones and show a clear correlation with the orography. More specifically, in the Belgian regions of higher elevation, more rainfall is observed, as reproduced by the models.

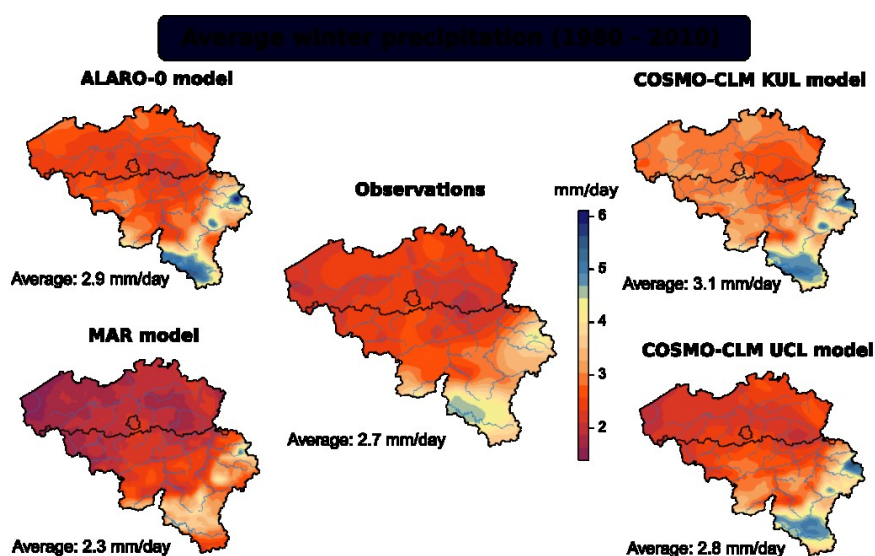


Figure 7: Spatial distribution of average winter (DJF) precipitation (mm/day) for the period 1980-2010. The central panel shows the observations (Delvaux et al. 2015) while the surrounding panels are from the (ERA-Interim) evaluation runs of the four H-Res CORDEX.be models. Averages over Belgium are indicated below the maps.

A similar conclusion can be drawn from the results shown in Figure 8 concerning the comparison of the observed and modeled average annual temperature. While the average over Belgium is 9.9°C, the model results range between 8.6°C and 10.5°C. Also a clear relation with orography is reproduced by the models: The average temperatures are lowest in the regions of highest altitude. For most models, the highest average temperatures are observed in the province of Antwerp.

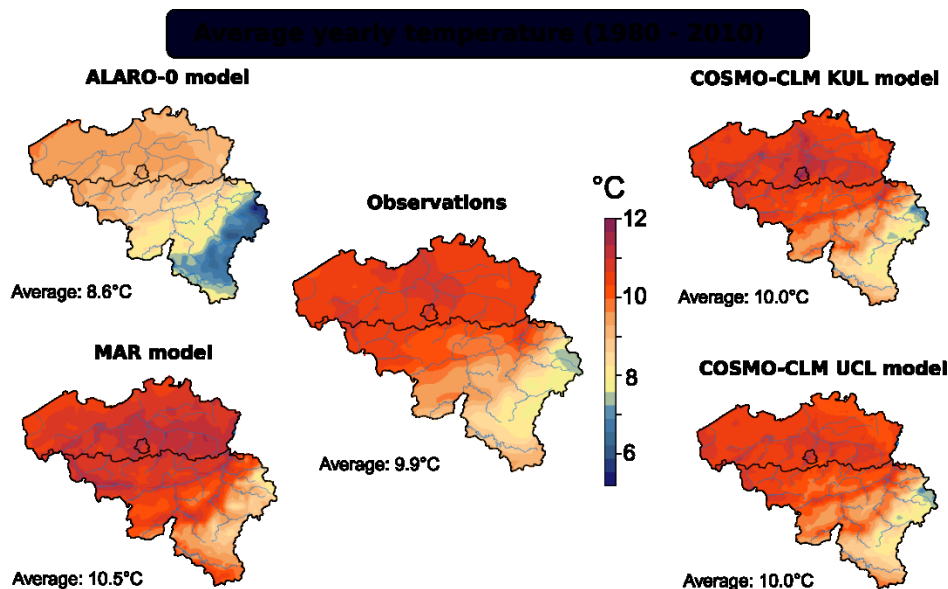


Figure 8: Spatial distribution of average yearly temperature (°C) for the period 1980-2010. The central panel shows the observations (Delvaux et al. 2015) while the surrounding panels are from the (ERA-Interim) evaluation runs of the four H-Res CORDEX.be models. Averages over Belgium are indicated below the maps.

#### 4.2.2 H-Res climate projections over Belgium

Here we provide an overview of a few H-Res climate projections for the period 2070-2100 following the scenario RCP8.5.

Figure 9 shows the spatial distribution of temperature projections. The left four panels give the change in average yearly temperature and results are seen to range between 2.6°C and 3.5°C. All models indicate a clear gradient indicating that climate changes close to the North Sea are lower than the ones present in the South-East of Belgium. The right four panels of Figure 9 show the change in tropical days. A tropical day has a maximum temperature exceeding the 95 percentile of maximum daily temperature. At Uccle, for instance, this means that the temperature exceeds 30°C. On average in the past there are 4.5 tropical days per year everywhere. The climate projections indicate that, averaged over all H-Res models, one may expect an increase of 15 days per year.

Also considered are the changes in winter and summer days under climate change. A winter day is defined as a day with average temperature below a certain threshold. This threshold is chosen such that 25% of all days in the past 30 years are winter days. Similarly in the past the 25% hottest days are termed summer days. Note that the thresholds depend on the spatial location and on the model

used. For instance at Uccle summer (winter) days are days with mean temperature above (below) 15°C (5°C). The expected reduction in winter days, averaged over Belgium and all H-Res models is 50 days while the increase in the amount of summer days is slightly higher on average i.e. 52 days. In other words, the amount of winter days is expected to be reduced to 40 while the amount of summer days will increase to 142.

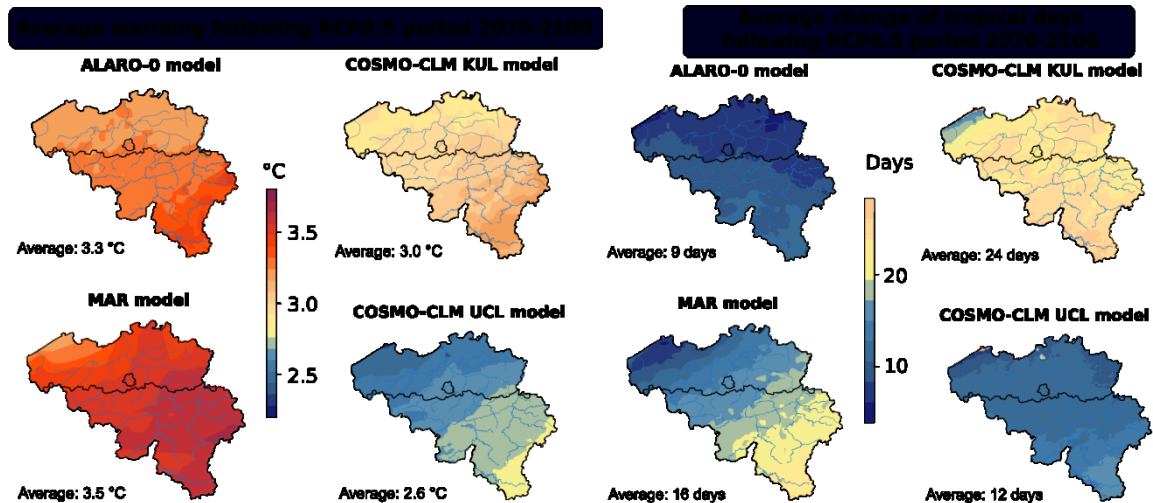


Figure 9: Spatial distribution of climate changes for average yearly temperature (left four panels) and average amount of tropical days per year (right four panels) for the period 2070-2100 following RCP8.5 relative to the control period (1976-2006). The model projections shown are for the four H-Res CORDEX.be models and averages over Belgium are indicated below the maps.

The impacts of climate change on precipitation in Belgium are shown in Figure 10 for three H-Res models. In the left panel the relative increase in winter precipitation is shown to be on average 20% and positive everywhere. Also the change in extreme precipitation (defined as 99 percentile of daily precipitation) is clearly positive and on average 12%.

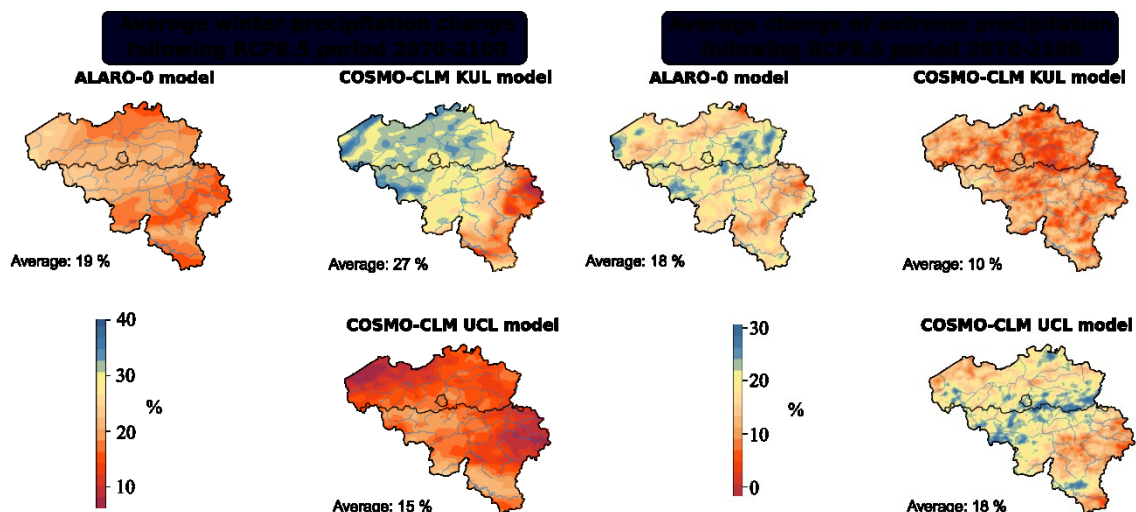


Figure 10: Spatial distribution of relative climate changes for average winter (DJF) precipitation (left four panels) and average change of extreme precipitation (right four panels) for the period 2070-2100 following RCP8.5 relative to the control period (1976-2006). The model projections shown are for three H-Res CORDEX.be models and averages over Belgium are indicated below the maps.

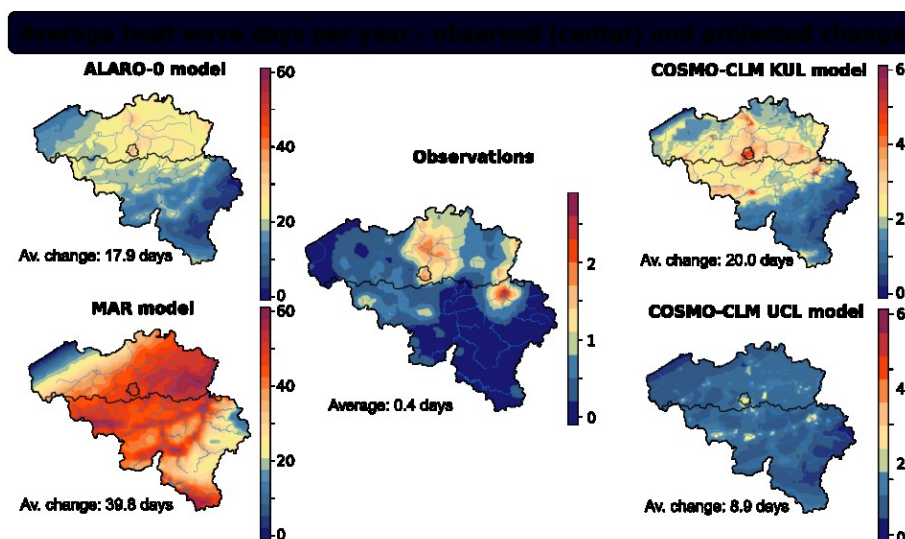


Figure 11: Spatial distribution of observed (central panel) and climate changes of average heat wave days per year, projected for the period 2070-2100 following RCP8.5 relative to the control period (1976-2006). The model projections shown are for the four H-Res CORDEX.be models and averages over Belgium are indicated below the maps.

Finally, here following the definition of Belgian Federal Public health Agency (FPS), are expected to much more frequent and intense in following the RCP8.5 scenario for 2070-2100. Figure 11 shows the spatial distribution of average heat wave days per year, both observed (central panel, Delvaux et al. 2015) and the projected future changes (surrounding four panels). While in the current climate there is less than half a heat wave day per year, this is expected to increase by more than 20 days per year. Increases are even larger over city areas including Brussels, Antwerp and Liège (as best represented by the COSMO-CLM models that include an advanced land-use module). The distribution of the heat wave days as a function of the month of the year is shown in Figure 12. It is clear that future heat waves will become more common both earlier and later in the year.

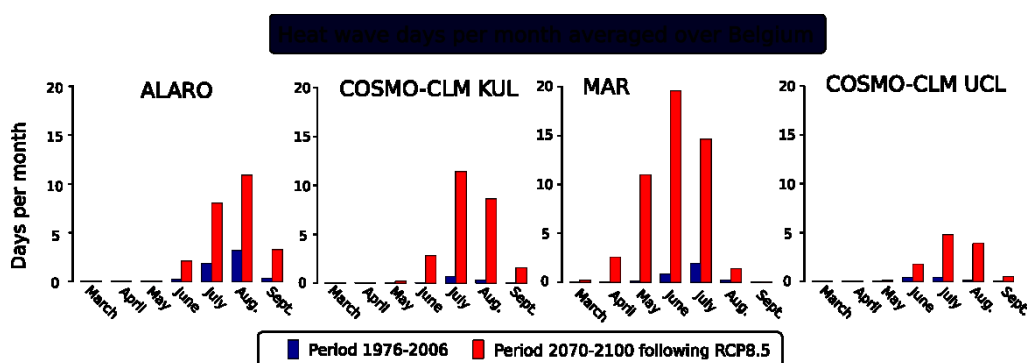


Figure 12: Average amount of heat wave days in the control period (blue columns) and the future period (red columns) as a function of month of the year. These periods are 1976-2006 and 2070-2100 (following RCP8.5). The model projections shown are for the four H-Res CORDEX.be models and are averaged over Belgium.

### 4.3 Evaluation of the regional climate simulations using ALARO-0

#### 4.3.1 Evaluation of the ALARO-0 simulations over Europe

The RMI has finished all EURO-CORDEX runs with ALARO-0 including the RCP2.6 scenario that has become strongly relevant since the Paris Agreement. The simulations were all run at the Tier-1 supercomputer in Ghent. A validation paper based on the ERA-Interim driven EURO-CORDEX runs is published in Geophysical Model Development (Giot et al. 2016). It is concluded that, despite not being tuned for climate purposes, ALARO-0 performs comparably well with respect to the other EURO-CORDEX models. However, in terms of the precipitation bias, ALARO-0 often outperforms all other models due to 3MT physics parameterization scheme (see Figure 13). Moreover, it has been found that ALARO-0 generates consistent results across scales and correctly represents extreme daily precipitation.

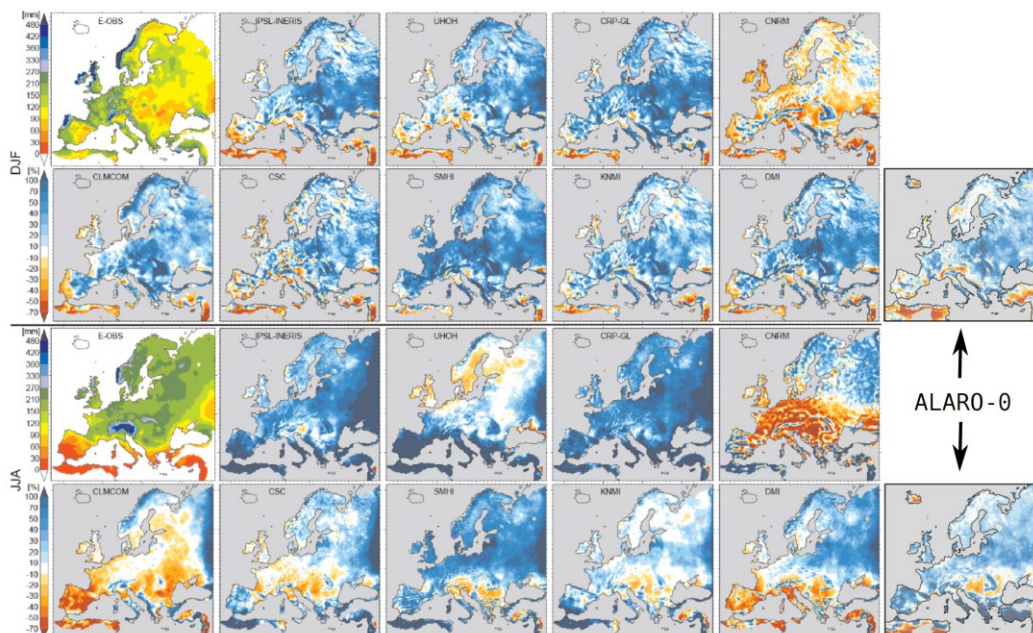


Figure 13: Bias of the ALARO-0 model precipitation against the corresponding biases of the other EURO-CORDEX models (Kotlarski et al., 2014). The upper and lowest two rows are for winter and summer, respectively.

By combining the past and future run, climate change can be studied. Figure 14 shows climate change for temperature and precipitation over Europe according to the ALARO-0 model following RCP8.5. Results for climate projections are in line with results from other CORDEX simulations (Jacob et al., 2014). More specifically, the Scandinavian region has stronger warming in winter compared to Southern Europe, and there is a drying of the Mediterranean region, while precipitation increases in Northern Europe.

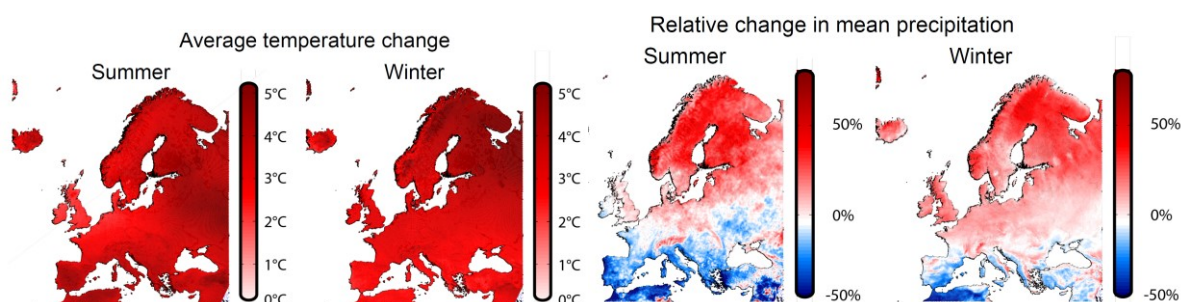


Figure 14: Climate change of period 2070-2100 (RCP 8.5) with respect to control period (1976-2005) obtained with the ALARO-0 model.

## 4.4 Evaluation of the regional climate simulations with COSMO-CLM

### 4.4.1 Coarse-scale and fine-scale climatology

As demonstrated in the previous projects (IWT/CLIMAQs and Belspo/MACCBET), the COSMO-CLM model configured at the convection-permitting scale for Belgium shows a very good skill in the representation of precipitation and cloud properties from in-situ and satellite observations (Brisson et al., 2016a,b). In addition, the H-Res COSMO-CLM model simulations are coupled to TERRA\_URB developed in the MACCBET project. TERRA\_URB enables the representation of the observed urban surface energy balance components from different intensive urban observation campaigns around the world (Wouters et al., 2015; Demuzere et al., 2017). As such, the model setup can reproduce very well the temperature variability in urban areas, including the canopy-layer urban heat island according to in-situ observations, the surface urban heat island according satellite imagery and the boundary-layer urban heat island according tower profiles (Wouters et al., 2016; Trusilova et al., 2016). As a result, the H-Res evaluation run captures very well both the fine-scale and coarse-scale climatology with excellent skill scores compared to state-of-the-art multi-model evaluation initiatives, as seen in Figure 15 and Figure 16 (Wouters et al., 2017).

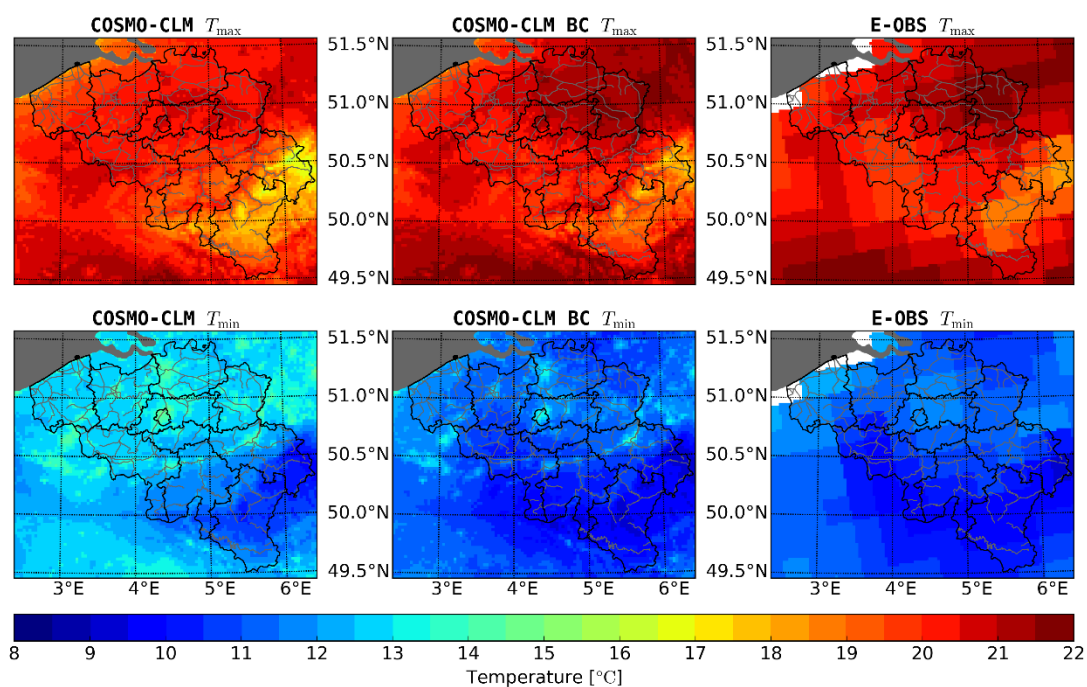


Figure 15: Climatological averages (1980-2014) for daily maximum (top row) and minimum (bottom row) temperatures (Wouters et al., 2017)..

In Figure 15, the averages of the evaluation period (1980-2014) for daily maximum (top row) and minimum (bottom row) temperatures are shown. The results are shown for the extended summer months (beginning of April until the end of September) consistent with the yearly timespan required for the heat stress indicator (see materials and methods). The left, middle and right panels are the model output (COSMO-CLM), the bias-corrected model output (COSMO-CLM BC), and the gridded dataset (E-OBS), respectively.

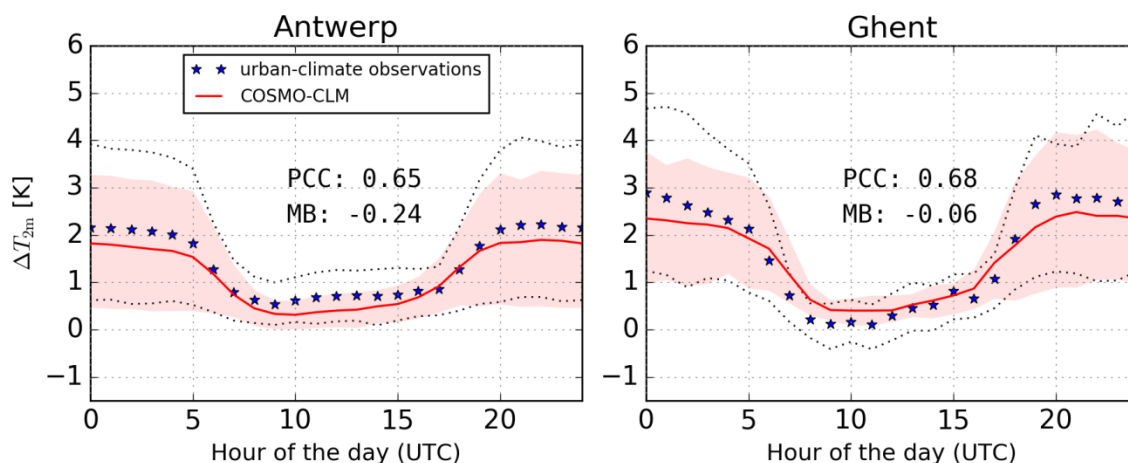


Figure 16: Mean diurnal cycle of the urban heat island for the urban-climate observations (stars) and the COSMO-CLM model (full lines) available during the extended summer periods (April-September) for the years 2012 to 2014 for Antwerp (left) and Ghent (right). Figure adopted from Wouters et al. (2017).

In Figure 16 the diurnal cycle is shown of the urban heat island for the urban-climate observations (stars) and the COSMO-CLM model (full lines) available during the extended summer periods for the years 2012 to 2014 for Antwerp (left) and Ghent (right). The urban heat island for Antwerp (Ghent) is calculated from the temperature difference between the urban station at Royal Lyceum in Antwerp (at Vrijdagmarkt in Ghent) and the rural station at Organic Farm Van Leemputten in Vremde (at Proefhoeve in Melle). The dotted lines (red shaded areas) indicate the range between the 16th and 84th percentile values (percentile levels agree with one standard deviation for a normal distribution) of the observed (modeled) temperatures. The Pearson Correlation Coefficient (PCC) and the mean bias (MB) of the underlying hourly time series are annotated in each panel.

#### 4.4.2 Added value of downscaling precipitation distributions with COSMO-CLM

The model evaluation against observed precipitation intensity distributions for Uccle clearly shows an added value when going to higher resolution modeling, especially regarding precipitation extremes (Vanden Broucke et al., 2017). For daily summer rain intensities, the H-Res setup is clearly superior to the EURO-CORDEX setup for all but the most extreme daily precipitation events (Figure 17, left panel), while both model setups are superior to the ERA-Interim driving model. However, in winter, a significant bias is present in the amount of high intensity daily precipitation events. This bias is positive for the H-Res and negative for the EURO-CORDEX simulations (not shown). For the hourly intensities, the added value of the H-Res simulation over the EURO-CORDEX simulation is more consistent where an increase in performance is seen for all season and time of day subsets. The increase in performance is particularly impressive for summer daytime (Figure 17, right panel). During this particular season/time of day subset, H-Res outperform EURO-CORDEX for all thresholds exceeding the 97<sup>th</sup> percentile (1mm per hour, which occurs about 16 times every summer season).

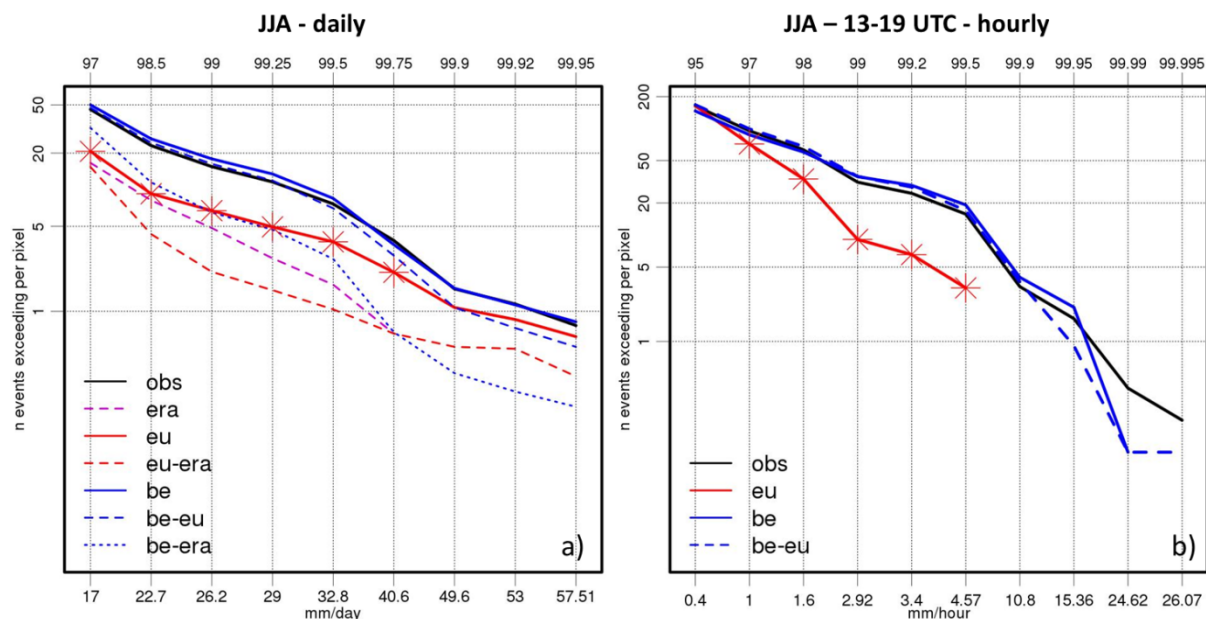


Figure 17: Number of events (for Uccle) exceeding precipitation thresholds for observations and model simulations, on the daily (left panel) and hourly (right panel) timescale. The results are shown for the data from ERA-Interim [era], COSMO-CLM EURO-CORDEX [eu] and COSMO-CLM H-Res [be], and results regridded to the coarser EURO-CORDEX grid (be-eu) and the coarser ERA-Interim grid (be-era). For the COSMO-CLM simulations an asterisk is drawn when the number of events exceeding the threshold in the model simulations differs significantly from the observations ( $p < 0.01$ ).

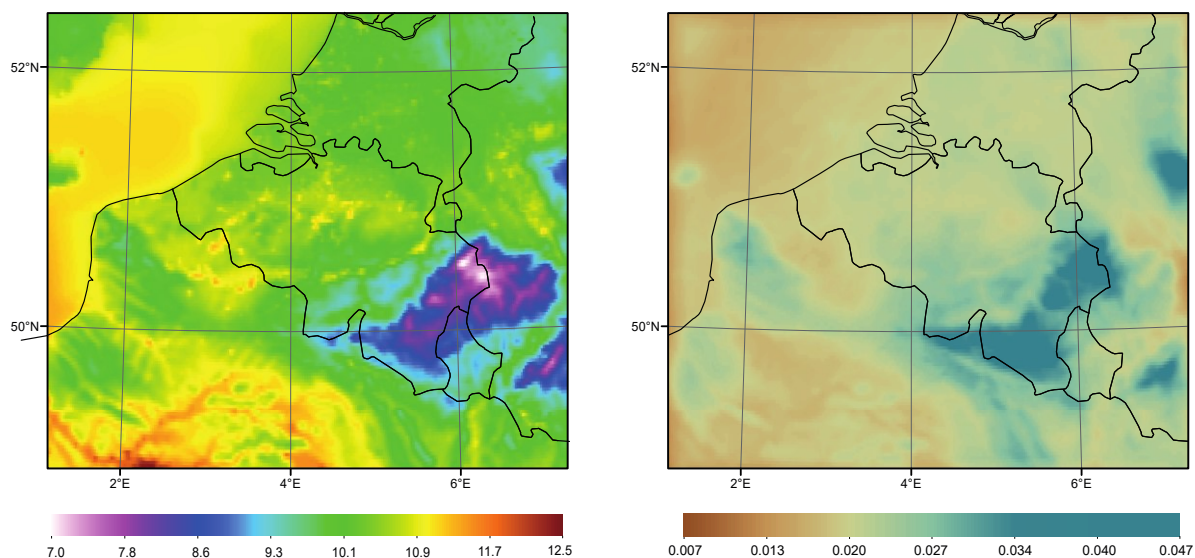


Figure 18: Spatial distribution of the 30-year H-Res evaluation run for the monthly mean 2m temperature (left, °C) and total accumulated precipitation (right, m/day). These results are obtained using the COSMO-CLM model at UCL.

#### 4.4.3 Model evaluation with COSMO-CLM against past climate for Belgium

Figure 18 shows 2m temperature and total precipitation averages for 30-years (1980-2010) for the evaluation simulation following the CORDEX.be-compliant simulations using COSMO-CLM at UCL. The spatial distribution of both temperature and precipitation simulated with COSMO-CLM is, as expected, with high orographic dependency having colder and larger precipitation amounts at higher altitudes such as in the South east of Belgium (see Figure 67 in Annex C) on the order of 8°C and 0.04 mm, respectively. Figure 19 shows the 30-year monthly average of maximum, minimum and mean 2m temperature as well as the monthly mean total accumulated precipitation. Total precipitation

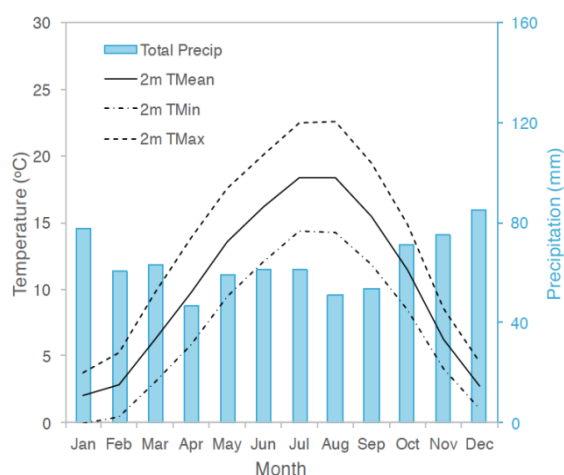


Figure 19: Result from CORDEX.be H-Res evaluation run: 30-year monthly mean 2m temperature (black) and total accumulated precipitation (blue). These results are obtained using the COSMO-CLM model at UCL.

decreases from the first months of the year with slight increases during the summer months where convective precipitation is more prevalent and larger possibility for hail formation and then increases again during the winter period.

In terms of hail formation, it is necessary to evaluate the simulated hail production, specifically hailstones at the surface. Thus, a composite of 32 observed convective cases in Belgium between 2002-2014 were used from previous tests, with more than half having surface hail reports. A subset of these cases is found in Van Weverberg et al. (2014). Observational data was selected from the Wideumont radar (RMI). This dataset contained maximum expected hail-size

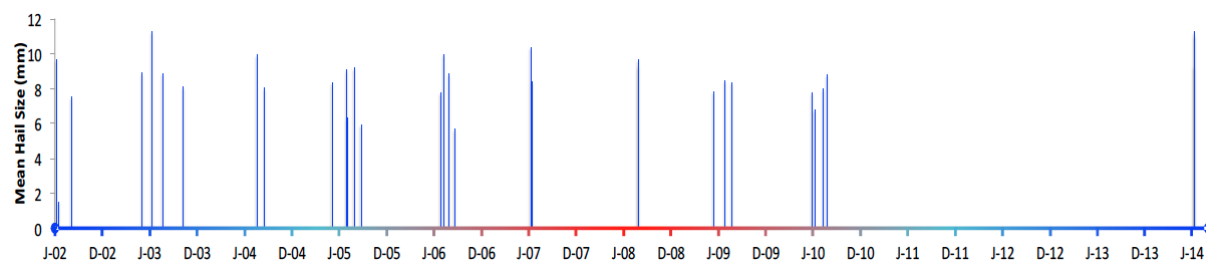


Figure 20: Mean hail size as measured by the Wideumont radar for 32 intense convective cases for the period 2002-2014. The date is shown with the initial month letter of either June or December (e.g. "J" for June) and the year.

measurement (Witt et al. 1998), which are used for the evaluation of the simulated hail. The model was evaluated only within a 240 km range from the radar. Figure 20 shows the dates of the chosen convective cases along with the mean hail size measured by the Wideumont radar. The original test involved the simulations of these hailstorms using the older COSMO-CLM4.8 version with either exponential (exp) or gamma (gam) size distribution within the 2-moment (2m) microphysical parameterization. Thus, the current COSMO-CLM5.0 model was also initialized the same way for these cases (36-hour simulations) for comparison against the older version and also against the chosen dates of the CORDEX.be H-Res evaluation continuous simulation.

Figure 21 shows case-averaged daily distribution of hail size at the surface and area extent (area that contained hail at the surface) within the 240-km radius around the radar for these four simulations against radar observations. As expected larger hail sizes and area extent are simulated using the 2m-exp COSMO-CLM4.8 model due to excessive size sorting as previous studies have shown (Milbrandt and Yau 2005). The COSMO-CLM5.0 case simulations and CORDEX.be H-Res runs have a slightly larger hail size compared to both observations and previous 2m-gam COSMO-CLM4.8 model but not too drastic as the 2m-exp experiments. The area extent of the 2m-gam COSMO-CLM5.0 follows very well radar observations. However, the daily distribution of the CORDEX.be H-Res simulations overestimates (underestimates) its area extent in the early (later) hours of the day.

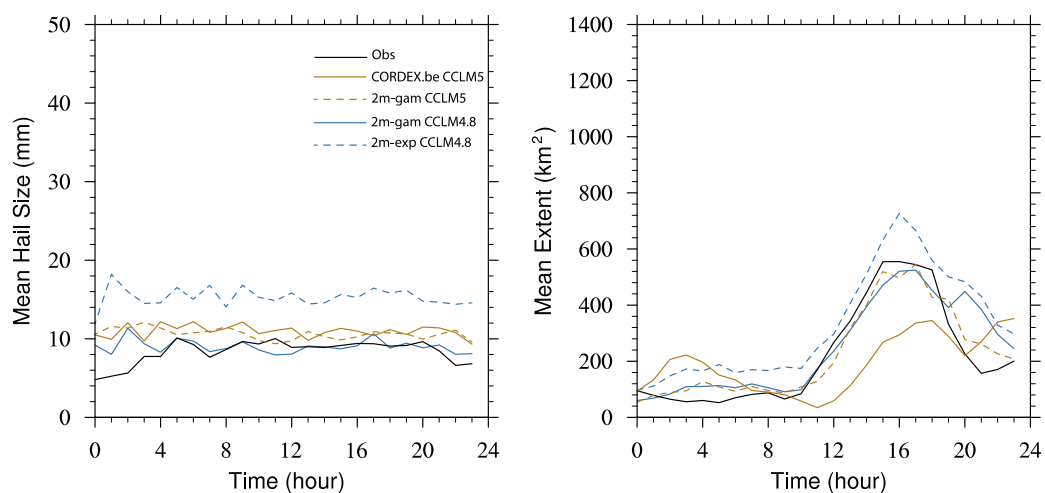


Figure 21: Mean hail size (left) and mean area extent (right) containing hail at the surface for Wideumont radar hail observations (black) compared with CORDEX Evaluation simulations (solid; gold). COSMO-CLM v4.8 and v5.0 simulations with model particle size distribution in exponential (exp) and gamma (gam) functional form is also imposed to compare with previous tests performed in order to evaluate the hail parameterization in COSMO-CLM5.0. These results are obtained using the COSMO-CLM model at UCL.

In Figure 22 different 30-year averages are considered based on the CORDEX.be H-Res evaluation run. Including monthly-mean hail content ( $Q_h$ ), number concentration ( $Q_{nh}$ ) at the surface and an estimation of the vertically integrated hail content ( $T_{qh}$ ). The latter is a measure of the total mass of hail in a column giving an idea of the production of hail within the clouds. The production of hail peaks in the month of July coincides with the hottest month of the year and possibly higher availability of atmospheric water vapor given its higher total accumulated precipitation for that month compared to August (Figure 19). High temperatures and water vapor increase the atmospheric instability and the probability of high updraft speeds, liquid water content, and the larger cloud depth necessary to sustain ice particles within the cloud for hail production. However, higher updraft speeds can cause hail particles to remain up in the cloud for longer periods of time and not to reach the surface. This may explain the fact that higher  $Q_h$  is simulated at the surface in the months of May and June despite having much lower  $T_{QH}$  compared to the month of July. In terms of hail size at the surface, much larger hailstones are reproduced in July than in any other month, as indicated by a lower  $Q_{nh}$ . During the winter months, there is an increase of “hail” content at a much

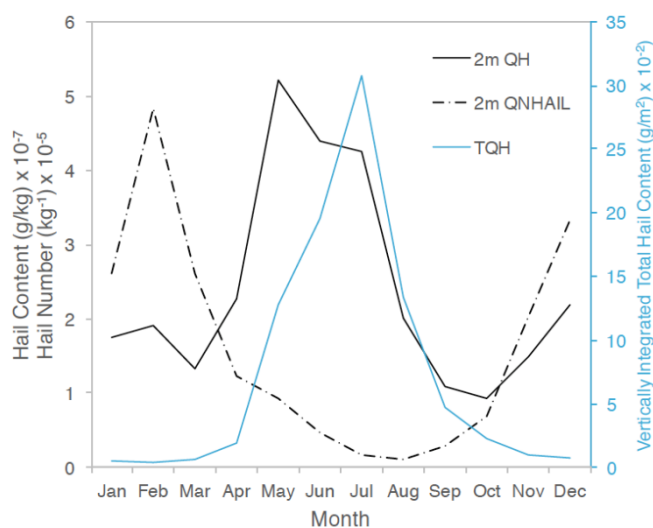


Figure 22: 30-year monthly averages from the CORDEX.be evaluation run. The variables considered are 2m hail content (black; solid), hail number concentration (black; dash), and vertically integrated total hail content (blue; solid). These results are obtained using the COSMO-CLM model at UCL.

higher number concentration which indicates smaller particle sizes at the surface. However, particles with size of the order of 0.6 mm are more suitably called ice pellets.

Even though simulated hail using the CORDEX.be H-Res setup features realistic behaviour, care must be taken when making final conclusions with respect to future projected hail trends, especially regarding daily hail tendencies. Nevertheless, useful information can be obtained from these simulations on how hail changes of deep convective storms can affect other extreme events (e.g. increased hail melting could intensify flooding events) and open the path for further studies in local impact models such as crop damage.

#### 4.4.4 Belgian H-Res climate projections with COSMO-CLM

The following discussion involves the change seen between the control (1976-2005; HIST) and RCP 8.5 climate scenario (2071-2100; RCP85) simulations using the COSMO-CLM model from UCL. Annual mean difference 2m temperature ( $T_{2m}$ ) and relative mean difference 24-hour total accumulated precipitation is shown in the two left panels of Figure 23. As expected, we see an increase in  $T_{2m}$  of about 2.57 °C for the future scenario accompanied by an increase in 24-hour total accumulated surface precipitation of 9.91% independent of any orographic effect on its values.

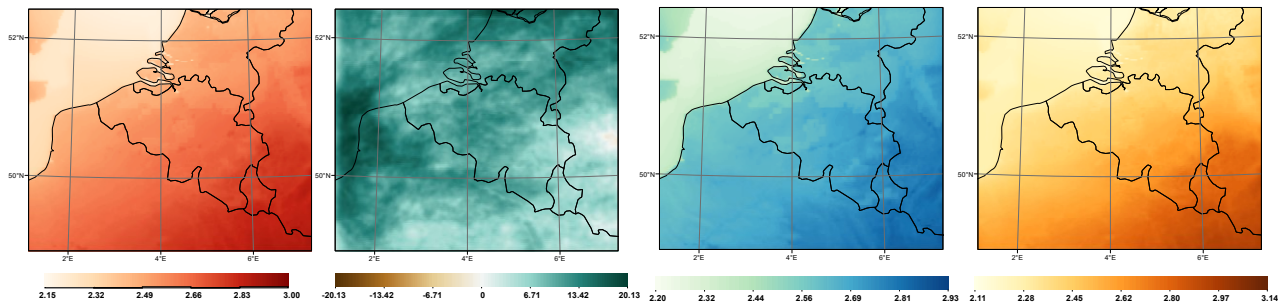


Figure 23: Spatial distribution of H-Res 30-year mean difference (HIST-RCP85) of 2m temperature in °C (far left panel) and relative mean difference of 24-hour accumulated total surface precipitation (second from left) in %, daily minimum (third from left) and maximum (far right) 2m temperature 30-year mean difference in °C.

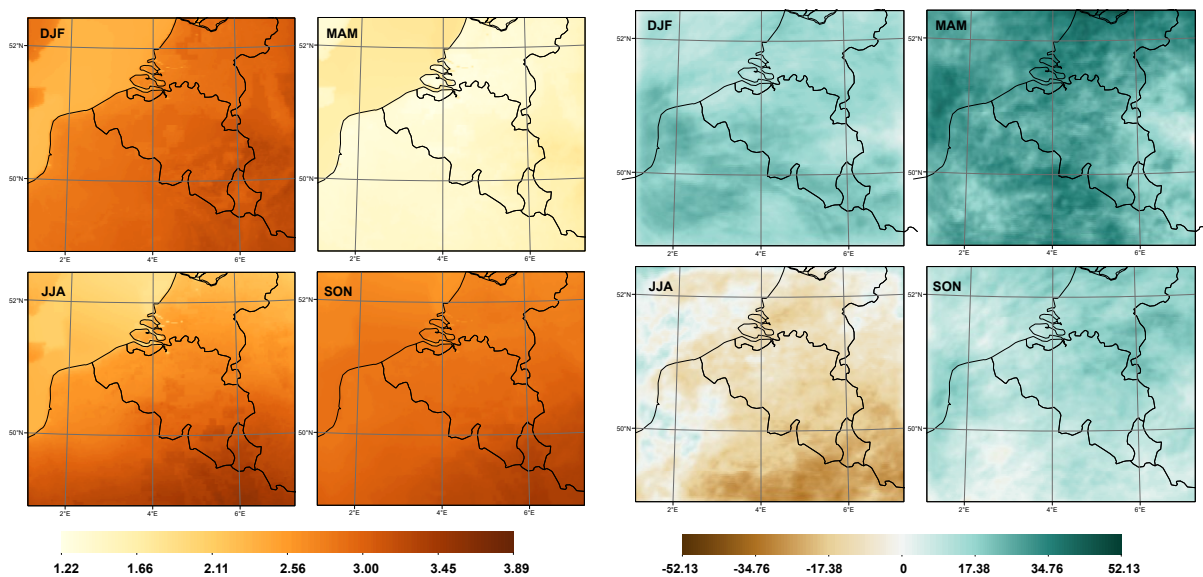


Figure 24: Left four panels: Spatial distribution of 30-year seasonal mean difference of daily maximum 2m temperature in °C. Right four panels: Spatial distribution of 30-year seasonal relative mean difference of 24-hour total accumulated surface precipitation in percent.

Mean annual daily minimum and maximum  $T_{2m}$  also increase with 2.61 °C and 2.50 °C, respectively, in future scenario as shown in the two right panels of Figure 23 with similar magnitudes as its daily mean temperature. However, the magnitude of these changes depends on the season. Daily minimum, mean and maximum  $T_{2m}$  have the lowest increase in the months of March, April, May (MAM) and the largest in the months of September, October, November (SON) as shown in Figure 24 (left four panels)<sup>26</sup> and Figure 25. On the other hand, a decrease of about 13% in 24-hour total accumulated precipitation is projected (right four panels of Figure 24) for the months of June, July, August (JJA) and highest increase in MAM of 26%. The MAM surface precipitation increase coincides

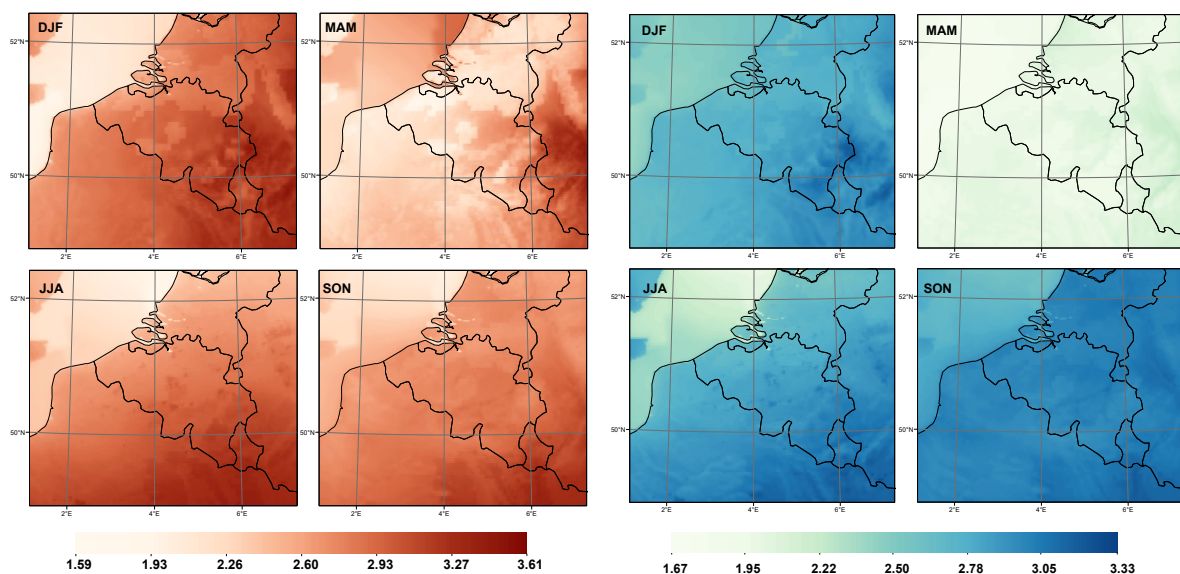


Figure 25: Spatial distribution of 30-year seasonal mean difference of 2m temperature (red-color panels) and daily minimum 2m temperature (blue-colored panels) in °C for the months of December-January-February (DJF), March-April-May (MAM), June-July-August (JJA), and September-October-November (SON).

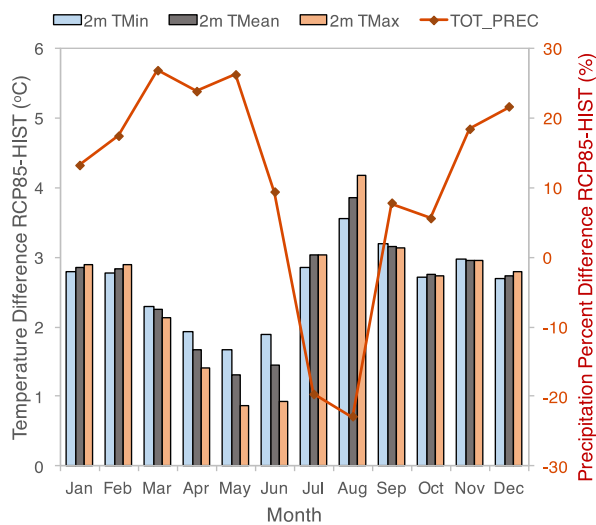


Figure 27: 30-year monthly mean difference of daily mean (grey bar), minimum (blue bar) and maximum (orange bar) 2m temperature in °C, and relative mean difference of 24-hour total accumulated surface precipitation in percent.

with the lowest  $T_{2M}$  increase compared to other seasons.

Summer months (and to some extent some spring and autumn months as well) usually bring more convective-type precipitation with more localized activity than during winter where precipitation is more likely to form due to frontal systems encompassing broader areas. It is interesting to notice that relative difference in 24-hour total accumulated precipitation decreases as the mean difference of daily mean, minimum, and maximum temperature increases during the summer months (Figure 27). This is especially the case in the months of July and August where maximum daily temperatures are simulated to increase by up to 4.5 °C. These much hotter surface temperatures could be the culprit for the decrease in surface precipitation during

this period, possibly indicative of higher evaporation rates within the boundary layer causing less precipitation to reach the surface.

## 4.5 Evaluation of regional climate simulations using MAR

### 4.5.1 Evaluation and projections with MAR over Belgium

The results with the model MAR were provided by ULg and the model setup used to generate the results was given in Section 3.5. The evaluation run (forced with ERA-Interim) is henceforth called MAR-Era and was successfully validated in Wyard et al. (2017a). It is necessary to know the model biases for the current climate before one can interpret future projections. Since meteorological values are known to be nonlinear, it is likely that a part of projected changes/anomalies are bias-dependent. Note that the model description and validation of MAR over Belgium, as specified below, can be found in Wyard et al. (2017a).

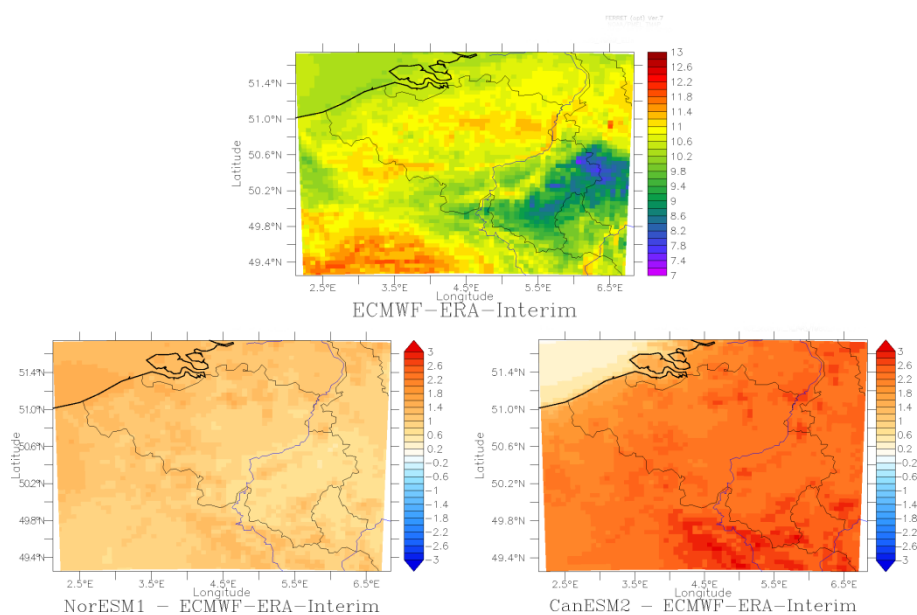


Figure 28: Mean annual temperature anomaly (in °C) over 1980-1999 of MAR forced by NorESM1 (low-left) and CanESM2 (low-right) in relative to the evaluation simulation of MAR (forced by ERA-Interim).

For the period 1980-1999 (Figure 28), MAR forced by NorESM1 (henceforth called MAR-Nor) and MAR forced by CanESM2 (MAR-Can) are respectively  $\pm 1^\circ\text{C}$  and  $\pm 2,5^\circ\text{C}$  warmer ( $\pm 3^\circ\text{C}$  in the South of Belgium) than MAR-ERA for the annual mean temperature.

Regarding the annual mean amount of precipitations over 1980-1999 (Figure 29), MAR-Nor is about 100mm/year wetter over the whole territory whereas MAR-Can is only wetter in the South of Belgium (with biases up to 300mm/year in this area).

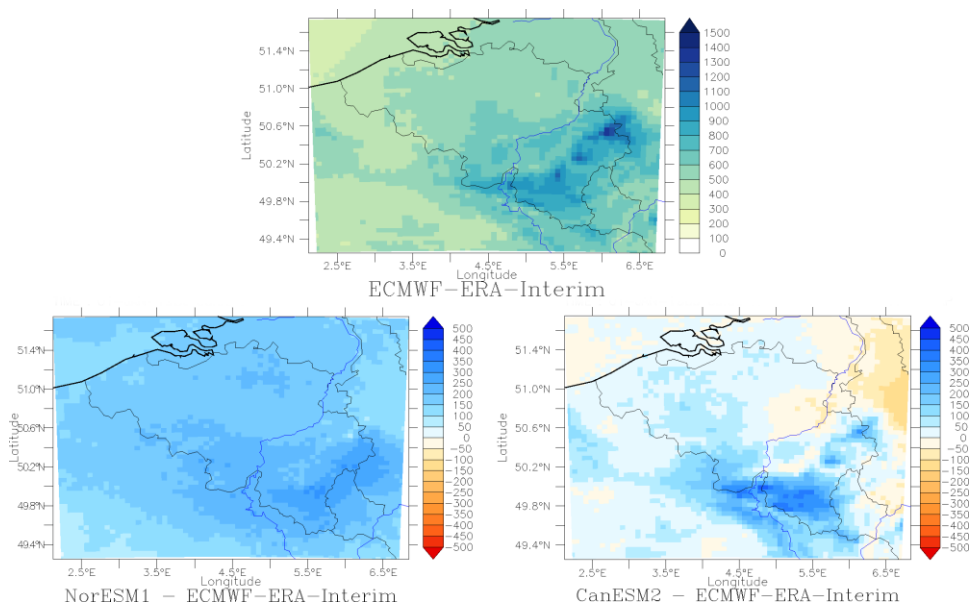


Figure 29: Annual precipitation anomaly (in mm/yr.) over 1980-1999 of MAR forced by NorESM1 (low-left) and CanESM2 (low-right) relative to the evaluation simulation of MAR (forced by ERA-Interim).

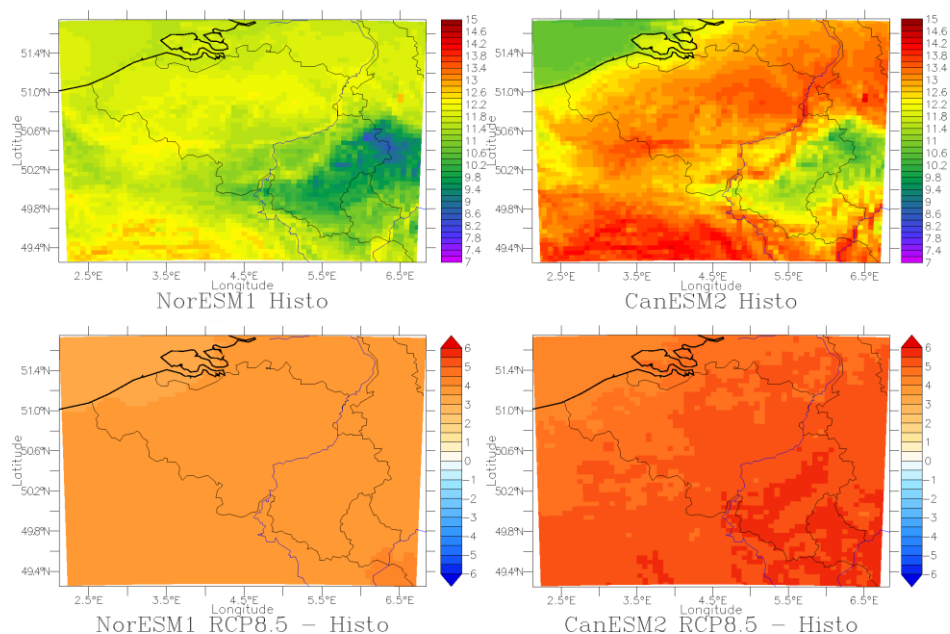


Figure 30: Mean annual temperature (upper panels) and associated climate changes (lower panels) in 2080-2099 simulated by MAR-Nor and MAR-Can using the RCP8.5 experiment relative to the period 1980-1999.

Regarding the future projections using the RCP8.5 scenario, MAR-Nor projects an annual mean temperature increase in the range 2-3°C over 2080-2099 while MAR-Can projects +4-6°C, especially over the Belgian highlands in respect to 1980-1999 (see Figure 30).

#### 4.5.2 Evaluation and projections with MAR over Europe

MAR results were produced over the EURO-CORDEX domain for an evaluation run (called MAR-Era) and validated in Wyard et al. (2017a) and using a forcing from NorESM1 (called MAR-Nor hereafter) as this is the GCM that gives the best results over Belgium as seen in the previous section. The studied periods are 1981-2003 for the MAR-Era and control runs (called “MAR-Nor histo” hereafter) and 2077-2099 for the future experiment RCP8.5 run (called “MAR-Nor RCP8.5” hereafter).

As shown in Figure 31, the simulations of annual mean temperature from MAR-ERA and from MAR-Nor histo give similar results for the 1981-2003 period, except near the boundaries where the bias is higher. The Mediterranean basin and the Scandinavian region are 1°C colder in the Mar-Nor histo than in the MAR-Era.

Concerning the future (the 2077-2099 period), mean annual temperature simulated by MAR-Nor RCP8.5 (Figure 31-D for bias) shows an increase from 2°C to 5°C over all the whole European territory and beyond. North-western Russia exhibits a particular increase in temperature.

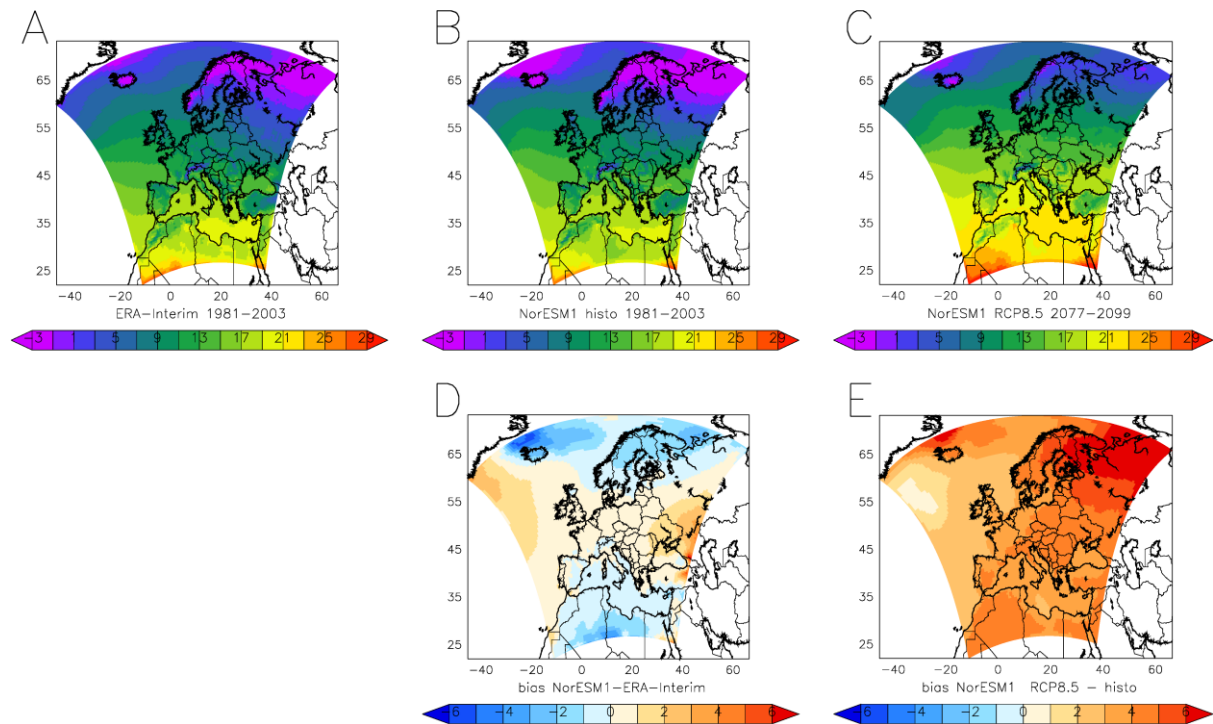


Figure 31: Annual mean temperature (upper panels) for MAR-Era (A) and MAR-Nor histo (B) for the 1981-2003 period and MAR-Nor RCP8.5 (C) for the 2077-2099 period. Lower panels represent bias between respectively MAR-Nor histo and MAR-Era (D) and MAR-Nor RCP8.5 and Mar-Nor histo (E).

As show in the Figure 32, mean annual precipitation amount simulated by MAR-Nor histo (Figure 32-B) is about 100mm wetter over Western Europe during the 1981-2003 period than MAR-Era (Figure 32-A) except over north-western Russia and the western part of the Mediterranean Basin where MAR-Nor histo is about 80mm dryer.

The annual precipitation amount simulated by MAR-Nor RCP8.5 for the 2077-2099 period (Figure 32-C) shows an increase in precipitation over northern Europe especially over ocean and seas compared to the 1981-2003 period (MAR-Era), whereas the annual precipitation amount decreases over the whole Mediterranean Basin during the same period.

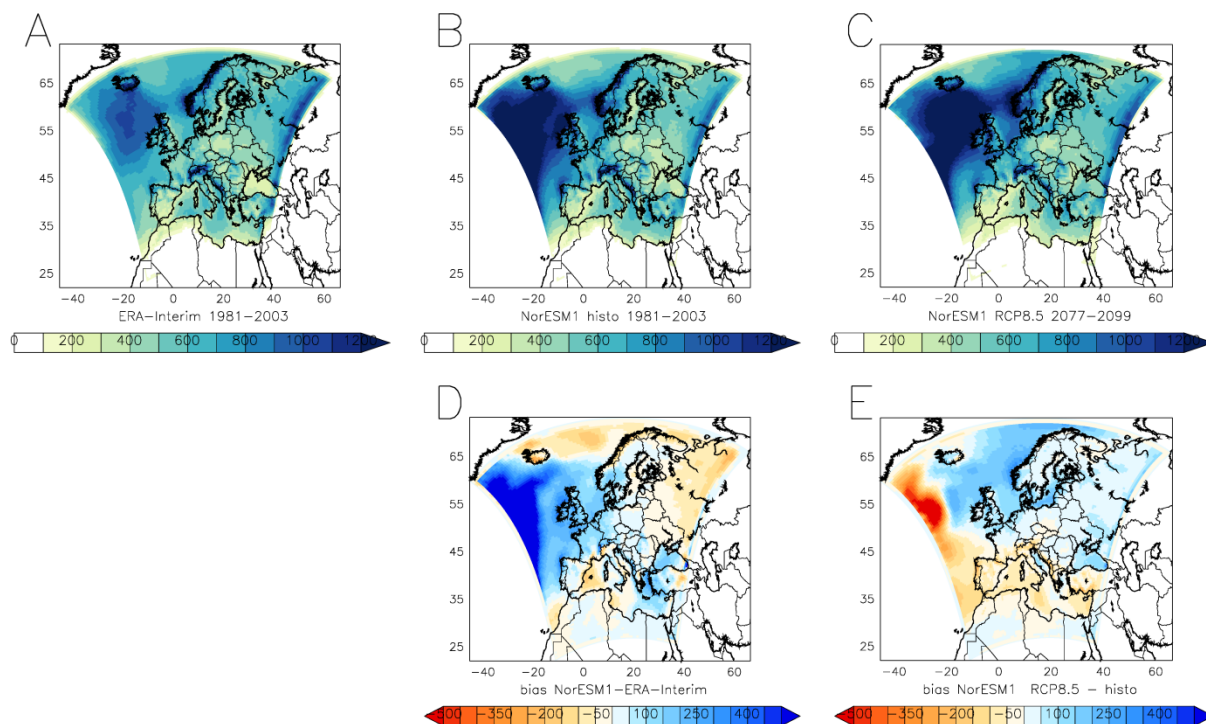


Figure 32: Annual mean precipitation amount (upper panels) for MAR-Era (A) and MAR-Nor histo (B) for the 1981-2003 period and MAR-Nor RCP8.5 (C) for the 2077-2099 period. Lower panels represent bias between respectively MAR-Nor histo and MAR-Era (D) and MAR-Nor RCP8.5 and Mar-Nor histo (E).

## 4.6 Validation of climate simulations using GNSS-derived products

### 4.6.1 Production of a climate-quality GNSS-based tropospheric dataset over Belgium

To match the period for which the climate model run output would be available for the validation, the CORDEX.be working group (WG) on GNSS verification decided to focus the GNSS-based verification on the period 2000-2010 at all location of permanent stations within the model domain (focus on Belgium), providing long-term high-quality data in this period with very high level of availability (i.e. very few gaps). Based on these criteria, about 20 GNSS stations could be identified within the H-Res climate model domains (Figure 33, right). But in order to perform the best GNSS re-processing possible, it was mandatory to perform the GNSS data processing in a global frame. Therefore, about 300 GNSS stations located worldwide were added to the first station selection (Figure 33, left). Then, the historical GNSS data and meta-data have been collected for all these stations. This step was followed by the necessary developments, tests and optimizations to enhance ROB's modeling techniques developed for E-GVAP in order to include all state-of-the-art models for GNSS processing (this is not possible within E-GVAP due to restrictions imposed by the user requirements, e.g. the latency of the products). Once available, this new advanced tropospheric modeling was applied to homogeneously re-process the historical observations from the selected GNSS stations. The reprocessing consumed about 2027 CPU-days and produced about 2Tb of output, which were then used to establish a dataset of climate-quality level GNSS-based products. The

product dataset has a completeness rate over 99%. By autumn 2016, this dataset was available for conversion and for the H-Res climate model validations.

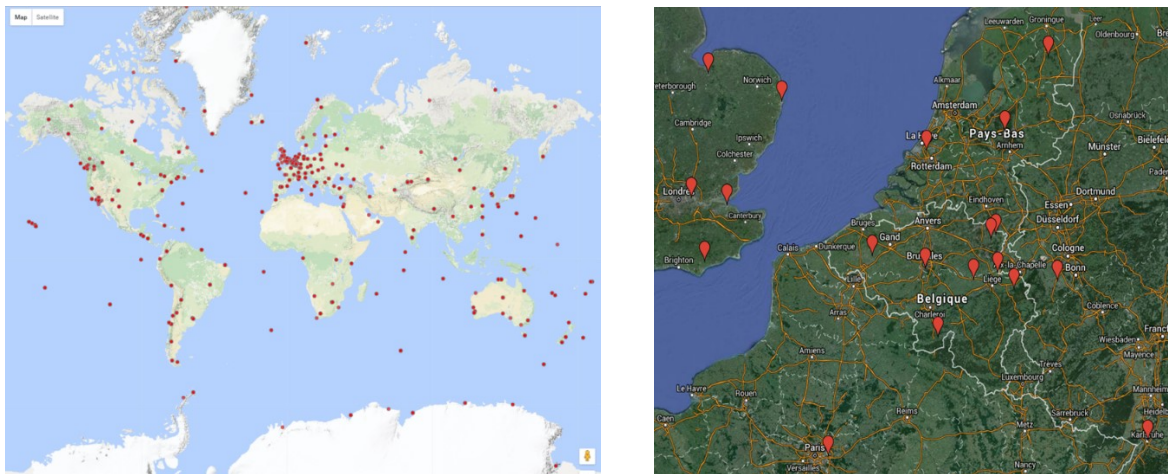


Figure 33: Left: red dots show the location of all continuously operating GNSS stations used for the re-processing. Right: the red markers show the location of the selected GNSS stations which fall within the high-resolution climate model run domains.

#### 4.6.2 Results of the climate model validation using GNSS products

As a first step in the validation of upper-air water vapor for Belgium, the Zenith Tropospheric Delay (ZTD) variable is considered. This variable is available at hourly frequency for the period 2000-2010 from GNSS observations, but were also computed as raw model output following the prescriptions of the CORDEX.be RCM model simulations. The hourly ZTD observed by GNSS were used to study the annual and diurnal cycle of their equivalent in the H-Res climate model.

Figure 34 (right panel) shows the ratio of the ZTD variability between the model data and the observations against the hour of the day. It is clear that the variability ratio is close to one, as it should. In the Figure 34 (left), the anomaly correlation is shown between the hourly observed and modeled ZTD data as a function of the month of the year. For all models there is an annual cycle in the anomaly correlation with a drop in the summer. The origin is not yet known and should be studied in the future. All models, except the COSMO-CLM model from UCL, correlate very well with the observations with correlations usually higher than 70%. The climate simulations with the model MAR and forced with ERA-Interim forcing are better than those using the forcing with NCEP-NCAR-v1 reanalysis, which, in turn are better than with the ERA20C forcing. This result corresponds to expectations: the reanalysis dataset ERA-Interim has integrated an enormous amount of observations, including those from satellite products (Dee et al., 2011). Therefore ERA-Interim is known to being closer to reality than, for instance the older and coarser dataset NCEP-NCAR-v1 (Kalnay et al., 1996). Lastly, ERA-20C, although it covers the entire 20<sup>th</sup> century, it uses only observed surface pressure and marine wind (Poli et al., 2013).

All ZTD time series generated by MAR simulations correlates better with observations than the ZTD from the COSMO-CLM models. Most probably this is caused by contrasting forcing strategies of the different H-Res runs, i.e. the difference in meteorological conditions imposed at the boundaries of the region over Belgium. More specifically, whereas MAR is directly forced at these boundaries by

reanalysis data (i.e. close to observations), COSMO-CLM uses an additional nesting approach. In other words, COSMO-CLM is forced over Belgium by meteorological conditions from its own run on the EURO-CORDEX domain that in turn is forced with reanalysis data at the European boundaries.

Because the ZTD values also contain the effect of the atmospheric dry gases (via the pressure), the natural next step is the validation of the modeled Integrated Water Vapor (IWV). This would allow isolating the effect of the water vapor and studying its annual and diurnal cycle in the H-Res climate models. Moreover a few interesting issues remain that call for further investigation: more specifically, the stark difference in correlations between the two COSMO-CLM simulations.

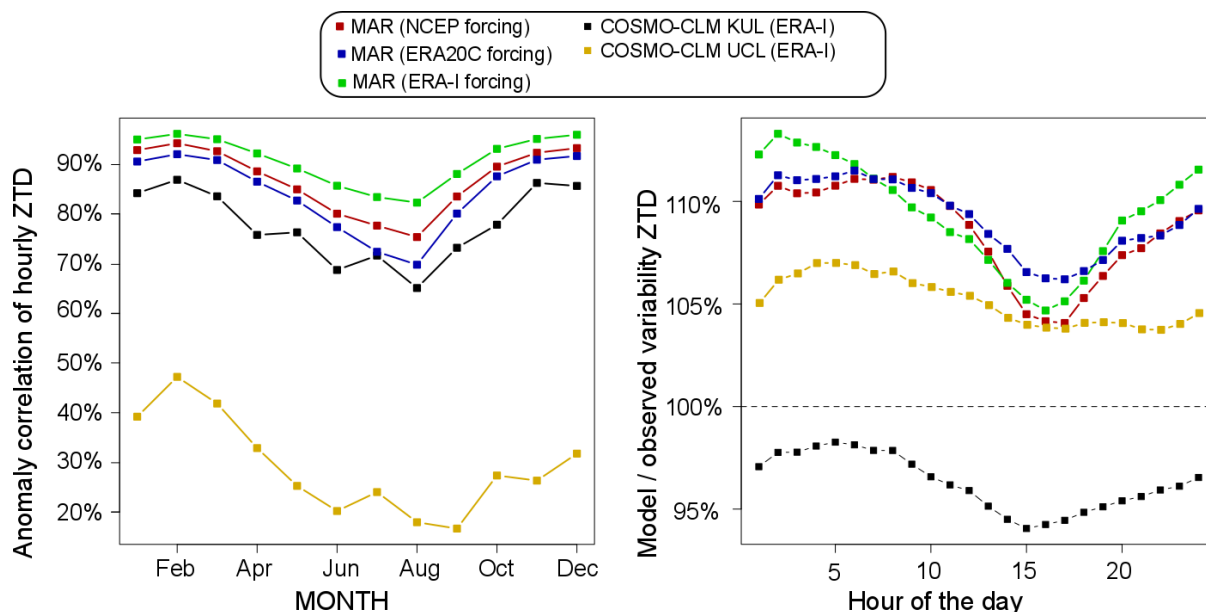


Figure 34: Anomaly correlation (left) and variability ratio (right) of hourly ZTD values between different model simulations and the GNSS-derived observations for the different months of the year. The models considered are the H-Res simulations of COSMO-CLM from KU Leuven (black) and COSMO-CLM from UCL (yellow), both driven by ERA-Interim), and MAR driven by NCEP-NCAR-v1 (red), MAR driven by ERA-Interim (green) and MAR driven by ERA20C (blue). Averages are taken over seven Belgian GNSS stations.

#### 4.7 Climate change impact on extreme precipitation

An interesting question is whether the change in intense/extreme precipitation due to climate change differs between the EURO-CORDEX and H-Res setups. To determine this, we consider the relative change in number of events exceeding precipitation thresholds ranging from moderate to high intensity. Note, however, that both summer and winter seasons are characterized by a significant change in mean precipitation (drier in summer and wetter in winter). Here, we plot the change in occurrence of various precipitation intensities after correcting for this mean signal.

Results show that the change in daily precipitation values does not differ significantly between the EURO-CORDEX and H-Res setups (not shown). Both are also characterized by a large increase in intense daily precipitation events in summer (Figure 35a), while, in winter (not shown) both setups indicate a negligible change in frequency of intense daily precipitation events (after correcting for the significant mean wet signal). A similar lack of difference in sensitivity is seen on the hourly timescale for winter daytime, winter nighttime and summer nighttime. For summer daytime,

however, sensitivity does differ significantly between model setups as shown in Figure 35b. Here, the H-Res setup is characterized by a significantly larger increase in the number of high intensity precipitation events, starting from the 99.5<sup>th</sup> percentile ( $\pm 5$  mm/hour, which in the present day, occurs about 2.7 times every summer season).

Considering the fact that the H-Res setup is vastly superior in simulating present-day hourly rainfall extremes during the summer season (see section 4.1.2), we can conclude that this large increase in intense hourly rainfall event frequency (up to 300% for the most extreme events) is more likely than the more modest increase simulated by the EURO-CORDEX setup. Therefore, this result clearly demonstrates the added value of a high resolution convection-permitting model setup over a lower resolution setup when used in impact studies where hourly rainfall rates are of high importance (e.g. flooding risk).

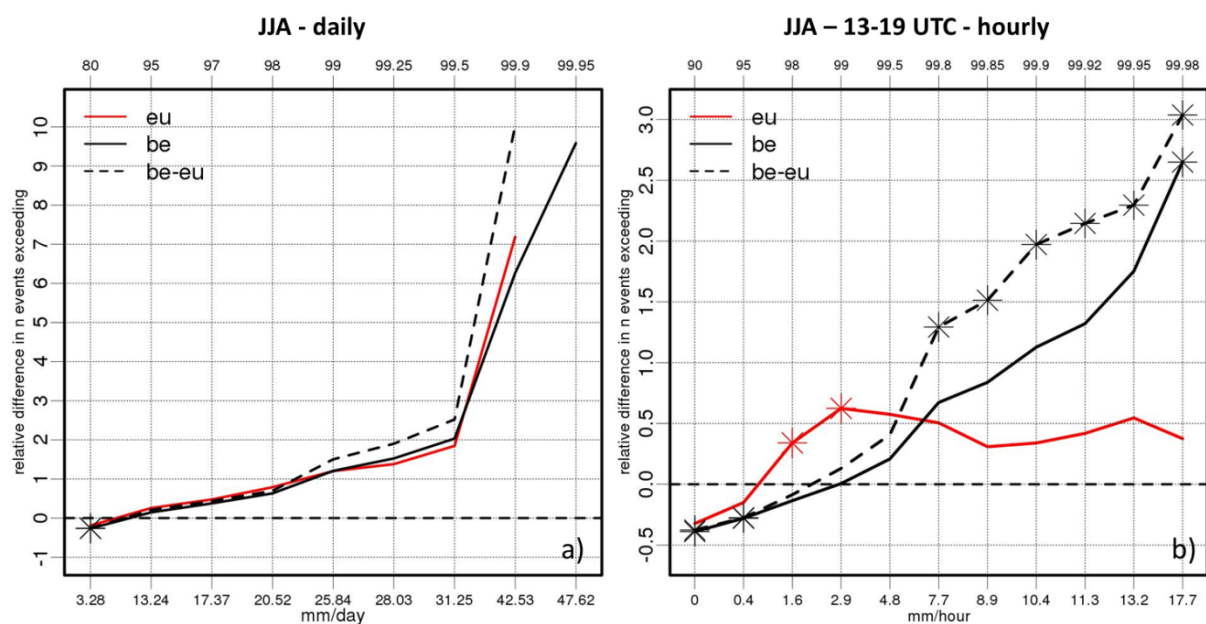


Figure 35: Relative change (due to climate change, 2070-2100 RCP 8.5 versus 1975-2005) in number of events exceeding precipitation thresholds, on the daily and hourly timescale (COSMO-CLM for EURO-CORDEX [eu], COSMO-CLM coupled to TERRA\_URB for H-Res [be], and the COSMO-CLM H-Res regridded to the EURO-CORDEX grid using conservative remapping [be-eu]). A black asterisk is drawn when the relative change in the H-Res simulations exceeds that of the EURO-CORDEX simulations ( $p < 0.01$ ). A red asterisk is drawn when the reverse is true.

In addition to explicitly resolving the deep convection leading to a better representation of extreme precipitation and its climate-change signal, the H-Res simulations also feature the large spatial variability of the (extreme) precipitation under climate change (see Figure 36). Such variability results from the heterogeneous land-cover in terms of orography, soil texture, coastline, and urbanization. This influence of the heterogeneous land-cover is particularly confirmed by the comparison between the H-Res reference urbanization scenario and the vegetation scenario, which demonstrates that the presence of urbanization leads to an overall increase in the precipitation extremes. For the region of Brussels (the 1000km<sup>2</sup> around the city center), urbanization leads to an additional 20% in the total precipitation of intensity exceeding 30mm per day (not shown).

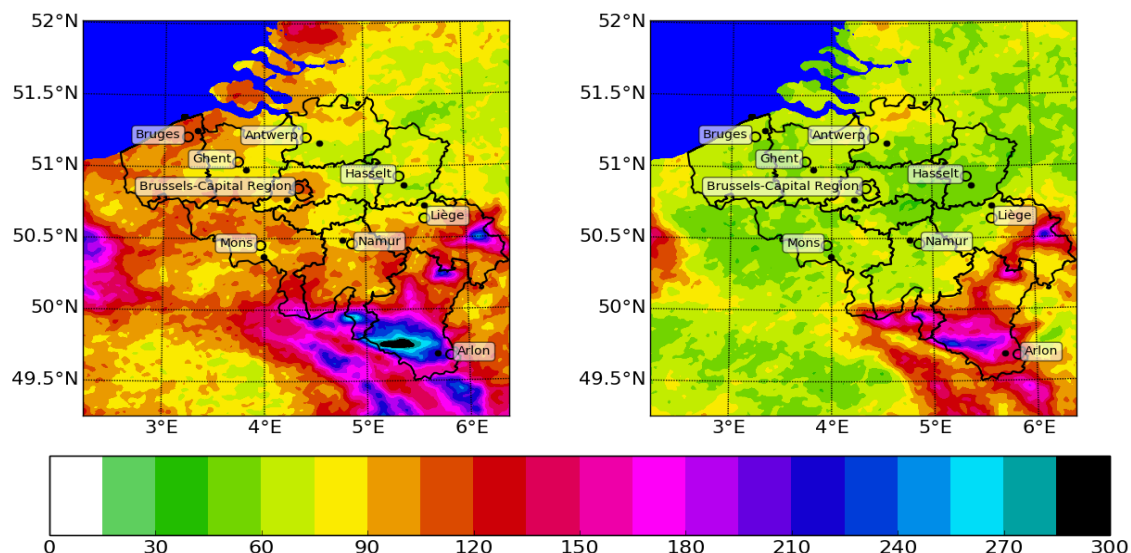


Figure 36: Accumulated annual precipitation with intensity larger than 30mm per day [units: mm per year], averaged for the 30-year H-Res climate simulations (left panel: RCP8.5 future period 2071->2100; right panel: control period 1976->2005) with the COSMO-CLM model coupled to TERRA\_URB. These statistics are based on the 30-year data of the future (left; 2071-2100) and control (right; 1976 - 2005) simulations on the H-Res grid cascade nested in the EC-EARTH member. (Vanden Broucke et al., 2017, in preparation)

#### 4.8 Climate change impact on snow cover

An impact study was done to estimate the impact of climate change on the seasonal snow cover over the Belgium highlands with the RCP8.5 scenario. Figure 37 shows the evolution of the maximum snow height (5-years filtered) in winter (December, January, February – DJF) by considering area only above 500m altitude computed from MAR-ECMWF, MAR-NCEP, MAR-ERA20C, MAR-Nor and MAR-Can simulations from the present period (1960-2010) to the future period (2050-2100).

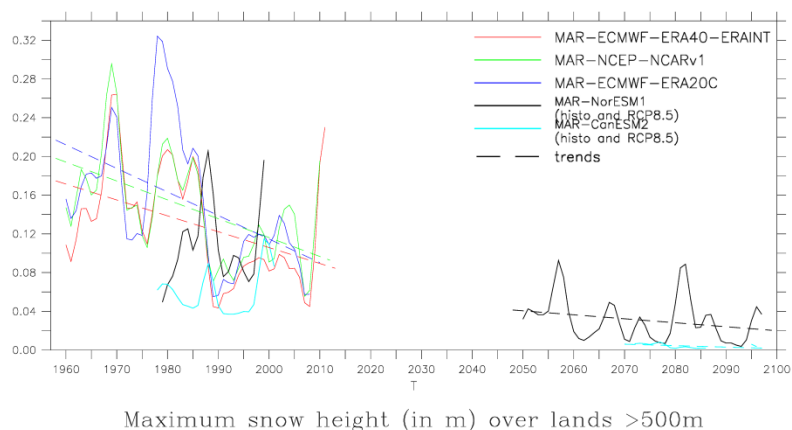


Figure 37: Maximum snow height (5-years filtered) in winter (DJF) over area above 500m altitude from MAR-ECMWF (red), MAR-NCEP (green), MAR-ERA20c (blue), MAR-Nor (bold black), MAR-Can (bold light blue) with control experiment over the period 1960-2010 and rcp8.5 scenario over the period 2050-2100. Trends of all simulations are shown in dashed line.

The 1960-2010 winter evolution of the maximum snow height shows a significant decreasing trend for the MAR-ECMWF, MAR-NCEP, MAR-ERA20C simulations while MAR-Nor and MAR-Can do not simulate any change over the control period.

The MAR-ECMWF, MAR-NCEP, MAR-ERA20C simulations also detected a tipping point at the end of the 1980's. Before 1985, mean winter maximum snow height (5-years filtered) of these three simulations are between 0,164m and 0,196m. After 1985, mean winter maximum snow height (5-years filtered) is rather between 0,092m and 0,113m except at the end of the time series in the 2010's.

For the future, MAR-Nor and MAR-Can using the RCP8.5 scenario project lower winter snow height maxima than these computed with the control scenario. Furthermore, trends of these two simulations show a decrease of the maximum winter snow height over the simulated periods.

The winter snow height maxima simulated by MAR-Can for the end of this century are especially low as a result of the lack of precipitation.

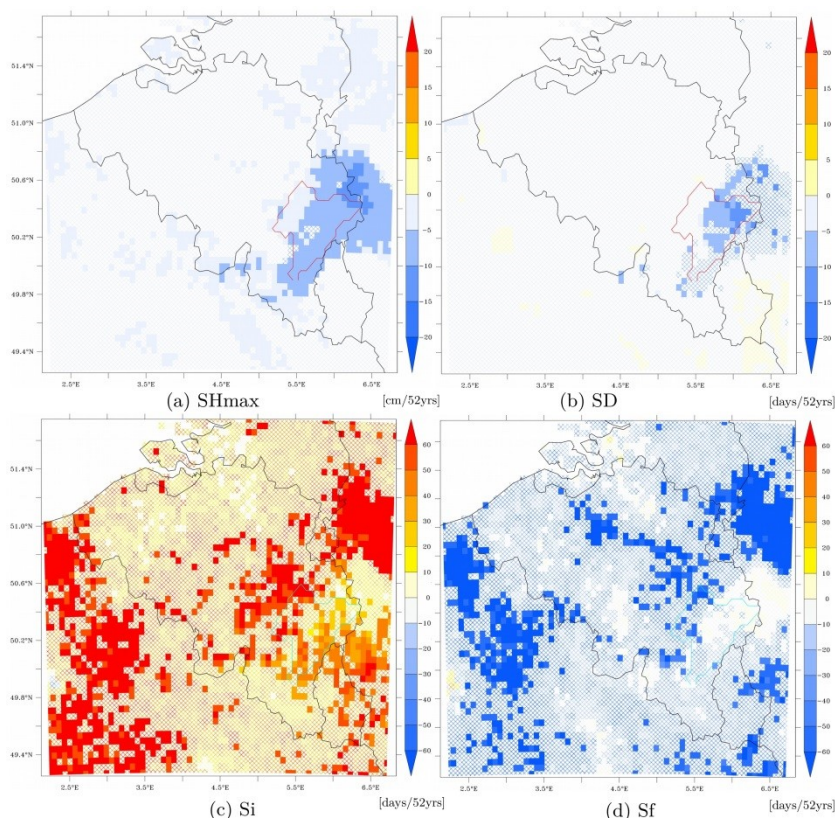


Figure 38: Trends computed from MAR-Era over 1959–2010 in (a) the maximum daily snow depth (SD) in winter (DJF), (b) the number of days per winter with a snow cover of at least 5 cm of thickness (SD), (c) the first day of the year with a snow depth of at least 1 cm (Si), and (d) the last day of the year with snow depth of at least 1 cm (Sf). Filled pixels indicate the places where trends are statistically significant.

By analysing the evolution of the seasonal snow cover in winter over the whole Belgian territory, a significant decreasing trend is identified in all three MAR simulations. According to MAR-ERA, the maximum of daily SH significantly decreases by 5 to 10 cm in 52 years in the Ardennes, and by more than 15 cm in 52 years in the Hautes Fagnes Plateau (see Figure 38a). Considering snow days as days

with a snow cover of at least 5 cm of thickness, the number of snow days significantly decreases up to -15 days in 52 years (see Figure 38b). The onset of the snow cover season (the first day of the year with a snow cover height of at least 1 cm) is delayed up to +60 days in 52 years in some parts of the Ourthe catchment (see Figure 38c). By contrast, the end of the snow cover season (the last day of the year with a snow cover height of at least 1 cm) is shortened up to -60 days in 52 years only in a small part of the Ourthe catchment area (see Figure 38d). Therefore, the duration of the snow cover season seems to shorten throughout the last 52 years. Similar results are found using the outputs of MAR-NCEP1 and MAR-ERA-20C. These results are in agreement with studies carried out in other regions in Europe, such as the low- and medium-elevated parts of the Alps (e.g. Beniston, 2012), or the lowland and coastal regions of Norway (e.g. Dyrddal et al., 2013).

## 4.9 Climate change impact on hail

In Section 4.4.4 an assessment was given of the impact of climate change on temperature and precipitation based on the COSMO-CLM model used at UCL. Here the same climate simulations are used to study the impact of climate change on hail over Belgium. The validation of the model in the context of hail, i.e. the comparison between model and observation was presented in Section 4.4.3.

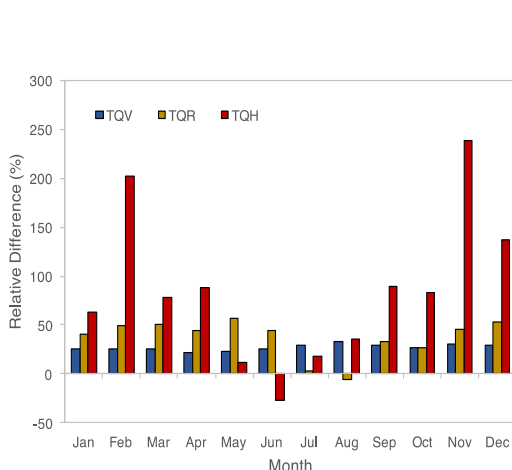


Figure 39: 30-year monthly relative mean difference of precipitable water ( $T_{QV}$ ; blue), vertically integrated total rain content ( $T_{QR}$ ; gold) and total hail content ( $T_{QH}$ ; red).

As mentioned earlier, vertically integrated values are a measure of the total mass of water vapor ( $T_{QV}$ ), rain ( $T_{QR}$ ) or hail ( $T_{QH}$ ) in a column giving an idea of the amount of water vapor or production of rain/hail within the clouds. Figure 39 looks at the relative difference of these variables. Starting with precipitable water ( $T_{QV}$ ), all mean monthly values are larger in the RCP 8.5 future scenario. Many studies have stated that warmer temperatures coupled with larger amounts of atmospheric water vapor may lead to more intensified precipitation and increased frequency of extreme precipitation (Stocker et al. 2013, Diffenbaugh et al. 2005, Meehl et al. 2005, Tebaldi et al. 2007). This does not necessarily translate to increased activity of deep convective storms. However, an increase of atmospheric water vapor in a warmer climate does raise the probabilities of stronger convective storms with an intensification of updrafts speeds due to larger latent heat release within the cloud.

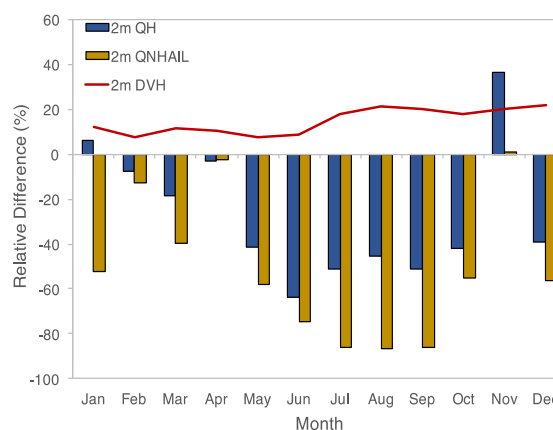


Figure 40: 30-year monthly relative mean difference of 2m hail content (QH; blue bar), 2m hail number concentration (QNHAIL; gold bar), and 2m mean hail size (DVH; red line).

This stronger updraft speeds could sustain hail for longer periods of time, aiding in the growth process of hail embryos and hailstones. From Figure 39 we not only see an increase of total rain of about 33% within the model domain, but also huge increases in hail as well. But the lowest increases are seen in the summer months of about 6%. This is because much smaller amounts of hail are produced in the other months of the year and so increases in their values will result in much larger relative differences.

Increases in hail formation within the cloud will not necessarily mean that more hail will be present at the surface. Stronger updraft speeds can also suggest that hailstones will remain longer higher in the cloud interacting with other hydrometeors (e.g. riming of hail stones) or with cloud edges where air mixing of dry air could hinder hailstone growth. In addition, with a greater fall distance and possibly higher evaporation rates within the column in a warmer climate, it decreases the chances for smaller hailstones to reach the surface. This also means that mass loss from hailstones could pass to other cloud particles such as rain through different microphysical processes (e.g. melting and shedding of hail can produce much larger raindrops). This can have substantial consequences on other natural hazards such as increased risks for flooding.

Figure 40 shows that at the surface hail content and number concentration are smaller compared to the control simulation, an indication that indeed much of the increased hail production within the atmospheric column in the future scenario model domain is not reaching the surface. However, hail number concentration decreased much more than overall hail content. Despite these decreases, hailstones are much larger in the future scenario. Thus, the warmer and wetter environment could potentially be making size sorting more efficient, but this is highly speculative and further analysis need to be made to assess this and also if hail increased production is also assisting in a more efficient production of rain.

Table 2: 30-year annual and seasonal (relative) mean difference for 2m daily mean ( $T_{2M}$ ), minimum ( $TMIN_{2M}$ ), maximum ( $TMAX_{2M}$ ) temperature, 24-hour total accumulated precipitation ( $P_{total}$ ), precipitable water ( $T_{QV}$ ), vertically integrated rain content ( $T_{QR}$ ) and hail content ( $T_{QH}$ ), 2m hail content ( $Q_{H_{2M}}$ ) and number concentration ( $Q_{NHAIL_{2M}}$ ), and mean hail size ( $D_{VH_{2M}}$ )

Variable	Annual Mean	DJF	MAM	JJA	SON
$\Delta T_{2M}$ (°C)	2.57	2.81	1.74	2.79	2.95
$\Delta TMIN_{2M}$ (°C)	2.61	2.75	1.97	2.77	2.96
$\Delta TMAX_{2M}$ (°C)	2.50	2.85	1.47	2.73	2.93
$\Delta P_{Total}$ (%)	9.91	17.34	25.63	-12.72	10.60
$\Delta T_{QV}$ (%)	27.43	27.12	23.00	29.15	28.81
$\Delta T_{QR}$ (%)	32.54	47.70	50.70	10.60	34.61
$\Delta T_{QH}$ (%)	20.99	118.52	25.29	6.11	103.45

$\Delta Q_{H\_2M}$ (%)	-36.91	-19.81	-28.88	-55.74	-27.98
$\Delta Q_{NHAIL\_2M}$ (%)	-45.71	-48.03	-36.80	-80.38	-36.84
$\Delta D_{VH\_2M}$ (%)	11.76	13.54	9.90	14.77	18.40

#### 4.10 Climate-change impact on urban heat stress

A study was performed on the impact of climate change on the urban heat stress using the COSMO-CLM model at KU Leuven. Urban areas, being warmer than their surroundings, are particularly vulnerable to global warming and associated increases in extreme temperatures. Heat waves result in heat-related mortality, reduced work capacity, damage to infrastructure and higher energy usage. Heat waves have become the second most deadly kind of natural disaster for the global society resulting from the effect of temperature on mortality. Particularly for Belgium, an excess mortality of +4000 people has already been recorded during the intense heat-waves between 2000 and 2010. The question arises how much urban heat stress in Belgium will increase under climate change. However, ensemble climate-model projections are generally performed using a too coarse resolution to represent the evolution of temperatures in cities. Detailed heat-stress projections for Belgium are constructed combining the H-Res convection-permitting climate model simulations with statistical analysis of an ensemble of GCMs, both developed within the CORDEX.be project.

The assessment shows that the heat-stress increase for the mid-21st century is twice as large in cities compared to their surrounding rural areas. The exacerbation is driven by the urban heat island itself, its concurrence with heatwaves, and urban expansion. Cities experience a heat-stress multiplication by a factor 1.4 and 15 depending on the scenario (see Figure 41). Remarkably, the future heat-stress surpasses everywhere the urban hot spots of today. The novel insights exemplify the need to combine information from climate models, acting on different scales, for climate-change risk assessment in heterogeneous regions.

More information about these results can be found in Wouters et al. (2017).

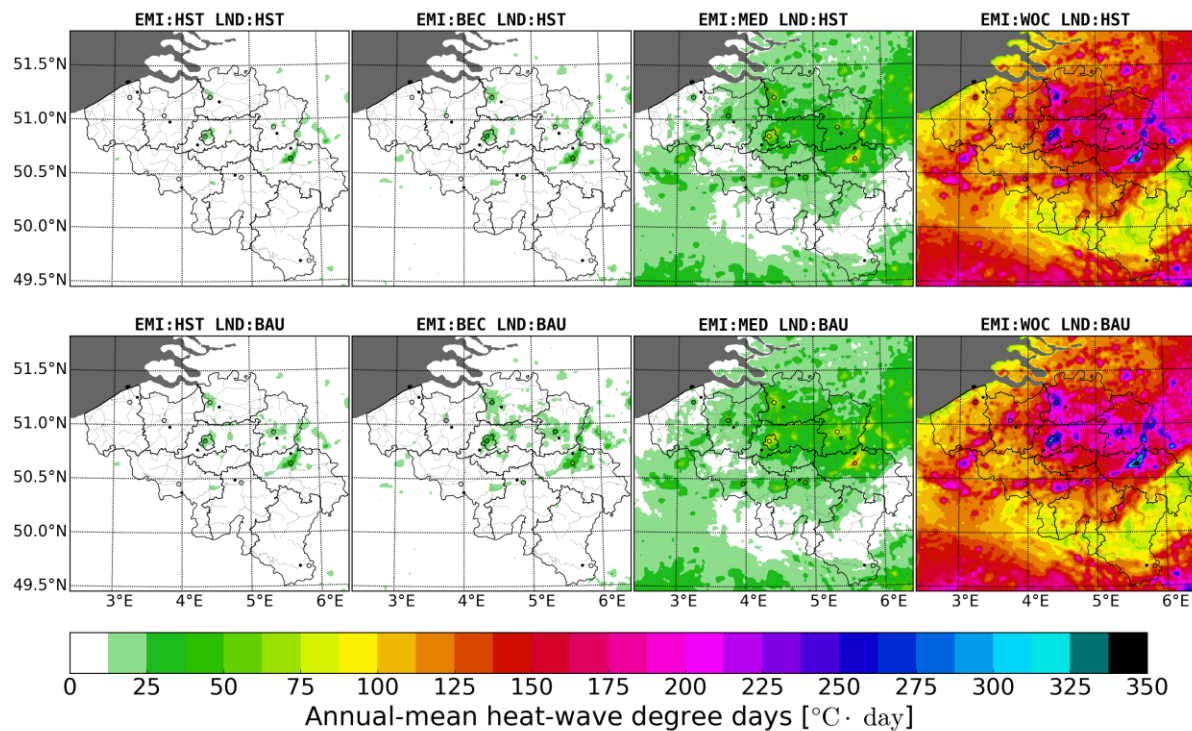


Figure 41: Heat stress in the control period (1981-2010) and the projected period (2041-2070) based on H-Res urban LaND-use climate simulations HiSTorical 2000 and Business-As-Usual 2060) and the ensemble EMIssion scenarios (HiSTorical, BEst Case, MEDian, and WORst Case).

#### 4.11 Climate change impact on the heat waves

The H-Res simulation of the ALARO-0 model with 4-km resolution was used as forcing of the SURFEX model in order to study the impact of climate change on the amount and intensity of heat waves. The resolution of these urban runs was 1 km and this allowed the comparison of three different locations around Brussels, each featuring three different environments and measurement stations. More specifically, Brussegem is a rural station, Uccle a sub-urban one while Molenbeek is located in a densely populated environment in the city center.

Figure 42 represents the number of heatwaves per year for 25 years at three different locations in the Brussels Capital Region. The green bars represent observations between 1981 and 2005; the blue bars the heat waves simulated with SURFEX at 1 km resolution, forced by the control runs of ALARO-0 between 1981 and 2005; and, finally, the red bars represent the HWs simulated by SURFEX and forced by the RCP8.5 scenario for the 2075-2099 period. Note that there is no forcing with the evaluation run such that no year-to-year correspondence can be expected. Comparing the control simulation to the observations, the model is seen to overestimate the number of HW in the rural station but a good correspondence is obtained for the other two stations. For the future period, an increase with factor 4.2, 3.4 and 3.0 in the number of heat waves is projected in Brussegem, Uccle and Molenbeek, respectively.

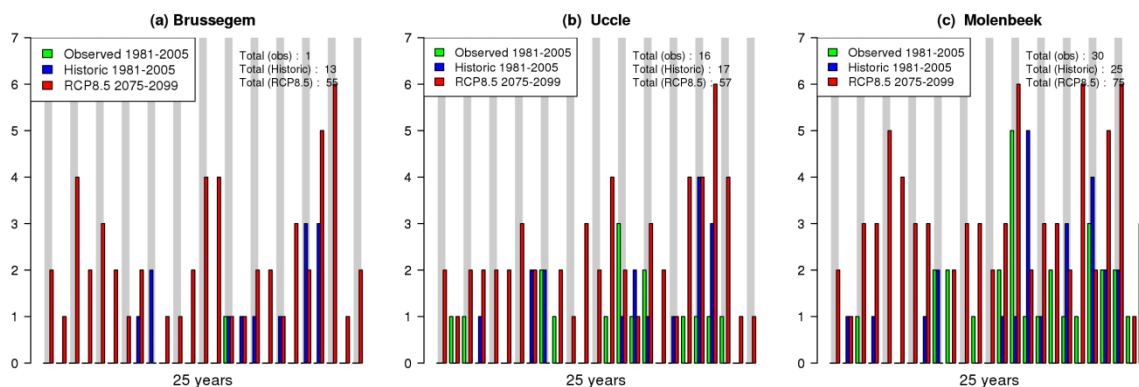


Figure 42: The number of yearly heatwaves at three different locations in the Brussel Capital Region. Indicated are observed heat waves (green), simulated with SURFEX for the evaluation period (blue), and for the projected period (red, RCP8.5 scenario) for the 2075-2099 period.

Figure 43 represents the minimum cumulated intensity (MIN\_C\_I) of heat waves with respect to their duration at the Molenbeek station. Here MIN\_C\_I is the summed excess minimum temperature above 18 °C during a heat wave. Again green represents the observations, blue the control simulations and red the RCP8.5 simulations. The main result here is that, although a strong increase in the number of heat waves is found, the majority of these events is of short duration (< 10 days) and with low intensity. Note that there will also be a slight increase in the number of very long heat waves which will then be even more extreme.

In Table 3 an overview is given of the most important heat wave features. Most notably 86.7% of observed HWs have a duration of less or equal than 10 days, 80.0% for the control and 65.3% for the future.

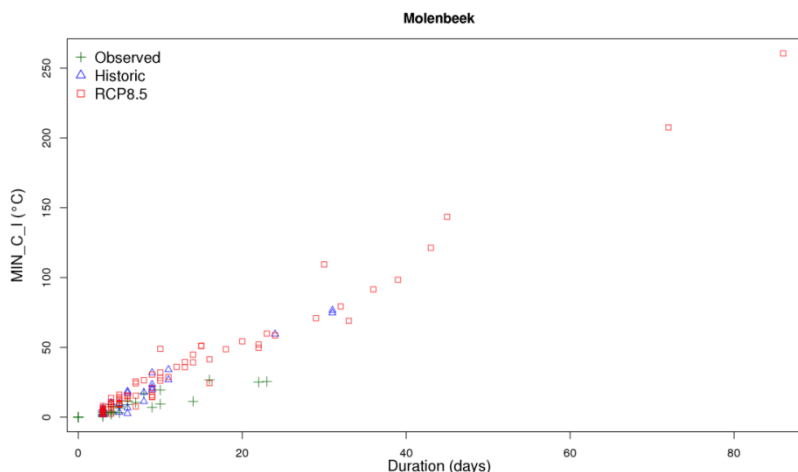


Figure 43: Heat wave duration against the minimum cumulated intensity (MIN\_C\_I) of heat waves at the Molenbeek station. Where the MIN\_C\_I is the sum of each  $T_{min}$  minus 18 °C during a HW event if  $T_{min}$  is > 18 °C. Indicated are observed heat waves (green), simulated with SURFEX for the evaluation period (blue), and for the projected period (red, RCP8.5 scenario) for the 2075-2099 period.

Table 3: Overview of the different heat wave features for the period 2070-2100 following the RCP8.5.

Climate run (period)	Number of HW/year	Average cumulated intensity during the night of HWs ( $\pm\sigma_{\text{mean}}$ )	Average cumulated intensity during the day of HWs ( $\pm\sigma_{\text{mean}}$ )	Average duration of HWs ( $\pm\sigma_{\text{mean}}$ )
Observations (1976-2005)	1.2	8.7 ( $\pm 1.3$ )	12.7 ( $\pm 2.0$ )	6.9 ( $\pm 1.0$ )
Control (1976-2005)	1.0	19.7 ( $\pm 4.2$ )	13.0 ( $\pm 3.2$ )	8.8 ( $\pm 1.6$ )
Future (2070-2100)	3.0	34.5 ( $\pm 5.1$ )	18.5 ( $\pm 2.9$ )	13.0 ( $\pm 1.7$ )
Future/Control	3.0	1.8	1.4	1.5

## 4.12 Climate change impact on urban environment

### 4.12.1 Impact on urban heat stress

The heat-stress results based on urban convection-permitting model climate simulations support the view that there will be a strong increase in the risk of heatwave-related problems, especially for citizens' mortality because of more extreme future heatwaves. They further offer new insights on the relation between heatwave-related problems, urbanization and climate change. Especially by explicitly resolving the inter-urban heterogeneity, it reveals the propagation heat-stress increase under climate change towards the scales of the cities. It also indicates its dependency to the city size and imperviousness, and to other local environmental aspects such as distance from the coastline, soil texture and orography. As such, local hot spots of heat stress are identified, and particularly the role of urban heat islands and their concurrence with heatwaves. Moreover, the high resolution reveals the additional role of local land-use change indicating that urban expansion results in a further amplification of heat-stress increase under climate change. With respect to previous coarser heat-stress assessments, the current results obtained from urban convection-permitting modeling clearly provide supplementary climate information that is important for the local stakeholders. It also holds great promise for urban-climate assessment with respect to other risks related to climate change propagating to the city scales, especially urban-induced precipitation, urban wind and dry islands, and their consequences on urban hazards (flooding and wind gusts), power generation and diseases.

The detail in the heat-stress results highlight the important role of the local governments and organisations for becoming sustainable and resistant against global warming with combined mitigation and adaptation strategies. From a climate science perspective, four pillars need to be addressed simultaneously, namely (1) cutting down carbon emissions (meeting the targets of the Paris Agreement), (2) rolling back urban expansion, (3) avoiding local heat generation, and (4) increasing the heat resistance against global warming, especially in the urban areas. They can be achieved with compact urban design that fits high-rise buildings, green space, and vehicle-restricted traffic networks into existing cities and villages. 'Green' infrastructure consisting of trees, green (and white) roofs, and sunshades should further provide additional cooling of buildings and the public

space, but also ‘blue’ infrastructure with urban lakes, waterflows (rivers, streams), fountains, spray systems and storm-water reservoirs. The advantage of the above heat-reducing strategies is that they are so-called “no-regret” measures, since they will in any case lower energy costs under climate change and improve the overall cities’ attractiveness by enhancing the quality of living, working, accessibility, recreation and health (e.g., avoid air conditioning, reserve public space for tree and biking lanes, avoid urban flooding etc.).

Future interdisciplinary research needs to pursue optimal pathways for future urbanization, for which heat-reducing strategies apply to the multiple scales of climate change on the one hand and of policy-making on the other hand. It is clear from the results that urban convection-permitting and local-impact modeling should serve as key tools. Further details can be found in Wouters et al. (2017).

#### 4.12.2 Evaluation of model simulations with 100-m resolution over Brussels

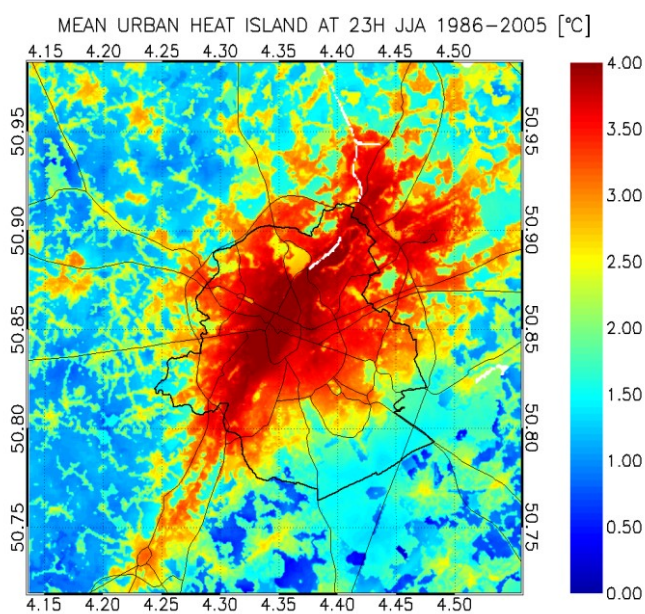


Figure 44: The average Urban Heat Island of Brussels during all summer periods (June-August) for the years 1986-2005 at 23h, the moment of maximum UHI intensity.

The impact of climate change on the city of Brussels was performed using the UrbClim model, developed at VITO. As input for this model the regional climate models of the CORDEX.be consortium were used, in order to obtain reference and future time series of urban heat island (UHI) intensity. At the start of the project, it was decided that VITO would focus on modeling the urban heat island and related parameters for the city of Brussels, at an unprecedented horizontal resolution of 100m. During the first year of the project the UrbClim model has been set up for the city of Brussels and simulations have been performed for a reference period (1986-2005), driven with ERA-Interim reanalysis data (Figure 45). A validation has been performed with observation data from 3 measurement stations, yielding excellent error statistics.

#### 4.12.3 Evaluation of model simulations with meter resolution over Brussels

However, when assessing outdoor heat stress in public areas, air temperatures are only a part of the story. Other parameters like radiation load, humidity and wind speed also play a large role to define the thermal comfort of people. Therefore, we have developed a new downscaling technique, involving radiation calculations based on the 3D city model of Brussels, to calculate heat stress at a meter-scale spatial resolution, which drastically increases the relevance and usefulness of the data for policy makers. The effect of heat stress on a human body can be quantified by the Wet Bulb

Globe Temperature (WBGT), an internationally recognized thermal comfort index. Figure 46 shows the mean WBGT for Brussels and a part of the city center during a particularly hot day in the summer of 2003. The meter-scale resolution allows quantifying and visualising the cooling effect of building shadows, trees, parks and water bodies. Moreover, since the WBGT index is also embedded in Belgian legislation regarding heat stress at work, it is possible to calculate potentially lost working hours for outdoor workers due to obligatory work breaks.

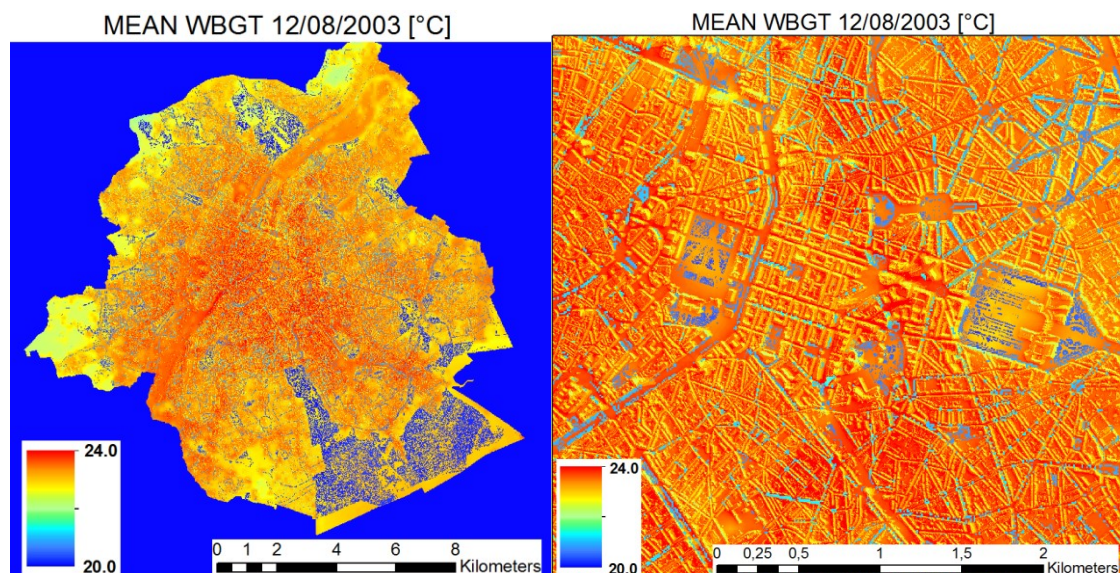


Figure 46: The mean Wet Bulb Globe Temperature on 12 August 2003 for the entire Brussels area (left) and a zoom on the center of the city (right). These results were obtained using the UrbClim model.

#### 4.12.4 Impact of climate change on thermal comfort parameters over Brussels

In the final phase of the project, the objective was to couple UrbClim, including the downscaling, to the output from the regional climate models of the CORDEX consortium. Only the ALARO-0 EURO-CORDEX simulations were available on time to still perform our time-consuming simulations within the timing of the CORDEX project. Therefore, these results can be seen as a demonstration of the feasibility and added value of such a coupling. Simulations were performed for the reference period (1986-2005) and a future period (2081-2100) following the RCP8.5 emission scenario. The ALARO-0 results were found to have a substantial negative bias of over 2°C in the near-surface air temperatures, which is corrected for by use of the ERA-Interim driven results.

Table 4 shows the annual average value in dense urban areas of a set of heat stress, energy use and productivity loss indicators for both the reference and the future summer (June-August) periods. According to these results, the average UHI intensity of Brussels is not going to change a lot due to climate change, which is reported before in related research. Nevertheless, the amount of heat stress for people living in the city of Brussels is expected to rise significantly. When calculating the number of Heat Wave Days (days for which the minimum temperature exceeds 18°C and the maximum temperature exceeds 30°C), we see a fourfold increase towards the end of the century.

Also the amount of time the temperature exceeds 25°C (expressed in Cooling Degree Days, an indicator for air-conditioning and energy use) will more than double. Based on WBGT thresholds

from the Belgian government for different types of work, we have calculated the amount of obligatory work breaks for every type, expressed in the Lost Working Days indicator. Clearly, climate change will have a significant impact on the outdoor productivity in the city of Brussels, as we see a huge raise in these numbers towards the end of the century. Note that these numbers are based on the results of only one model and one emission scenario, so they should be interpreted in this regard.

*Table 4: Potential impact of climate change on indicators for heat stress, energy use and productivity losses for dense urban areas (soil sealing > 90%) in Brussels.*

	1986-2005	2081-2100 (RCP8.5)
<b>UHI intensity [°C]</b>	3.7	3.9
<b>Heat Wave Days</b>	4.2	15.9
<b>Cooling Degree Days</b>	28.2	74.0
<b>Lost Working Days</b>		
→ <i>Light work</i>	0.9	2.6
→ <i>Medium-heavy work</i>	1.1	3.4
→ <i>Heavy work</i>	3.0	6.3
→ <i>Very heavy work</i>	8.8	15.6

In addition, work has been done with the UrbClim model on Delhi (India), in the framework of the BELSPO postdoc fellowship held by Richa Sharma, and for which CORDEX.be was the “host” project. The model has been validated with both air temperature measurements and thermal infrared satellite imagery. Simulations of urban growth have been performed, together with future climate simulations (RCP8.5 scenario), allowing to evaluate the effect on the local urban climate stemming from (1) global climate change and (2) local land cover changes. Figure 47 shows their combined impact on the annual average number of Heatwave Days (thresholds defined by the present-day 98<sup>th</sup> percentile values). The inhabitants of the city face a huge increase in the amount of heat stress by the end of the century. The results of this study are used to raise awareness of urban managers for the extreme heat threats that their city will face and prepare adaptation plans accordingly.

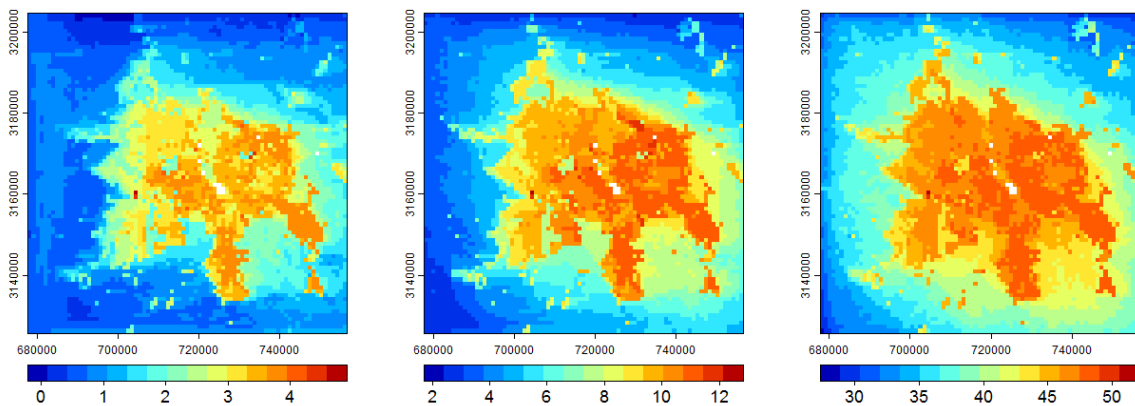


Figure 47: The number of Heatwave Days in Delhi and surroundings for the present (1986-2005), near (2026-2045) and far (2081-2100) future.

### 4.13 Climate change impact on agricultural crop performance and yield

Agricultural production risk is to a great extent determined by weather conditions and is therefore expected to be influenced by projected climatic time series. Projected rainfall and evapotranspiration for RCP4.5 and RCP8.5 showed that the projected water balance is negative during the summer months pointing at increased drought (Figure 48).

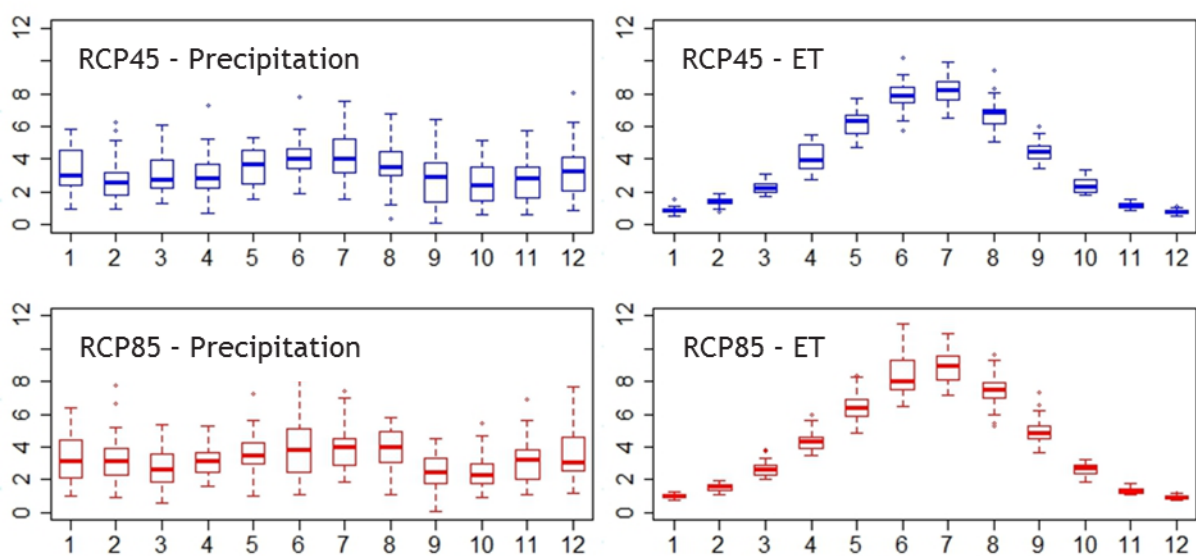


Figure 48: Daily precipitation (P) and evapotranspiration (ET) for the RCP4.5 and RCP8.5 scenarios.

The temporal overlap between projected climatological conditions and crop stages in the arable cropping system were determined using a modeling framework that coupled phenology to the soil water balance and crop growth (Figure 49). The modeling framework demonstrated a clear dual shift in both phenology, approximated by growing degree days, and projected meteorological patterns, approximated by actual evapotranspiration, rainfall and temperature. The impacts of temperature stress (heat, frost) and water stress (drought, waterlogging) reduced crop growth, whereas increased CO<sub>2</sub>-concentrations had a positive effect on crop yields. The interaction between these

effects depended on the crop type, the cropping season and the field conditions. The effects of fertilisation and water use efficiency under increased CO<sub>2</sub> concentrations did not compensate for the impact of projected adverse temperature and water stress on agricultural crops. Summer crops experienced increased drought stress particularly when sensitive crop stages coincided with dry spells (Figure 48).

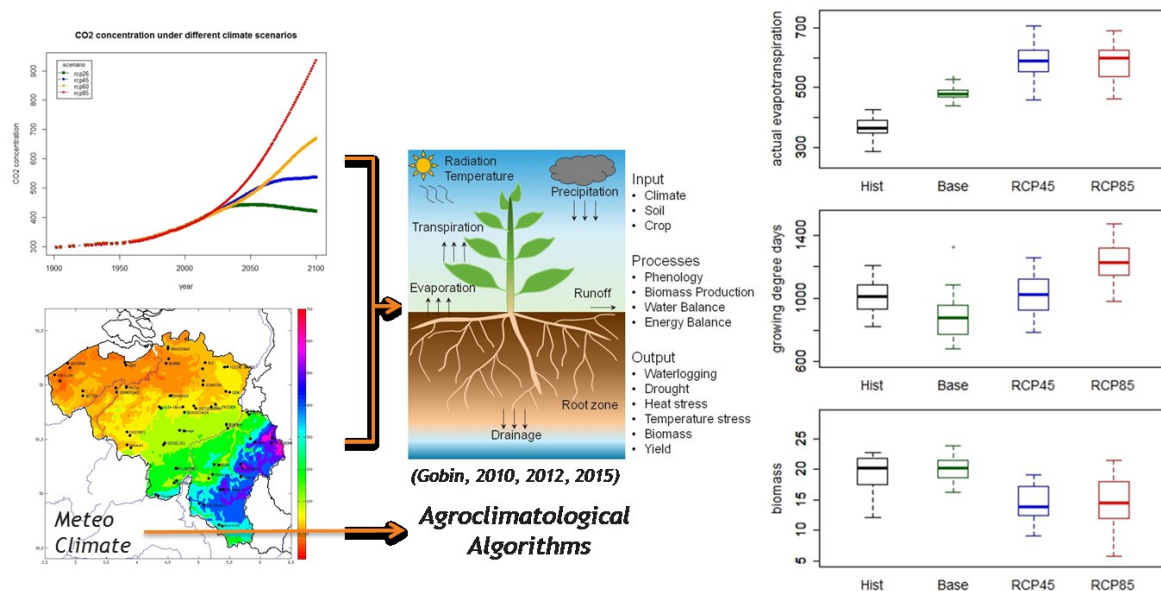


Figure 49: Climate impact on crop evapotranspiration, growing degree days and biomass production of a summer crop for observations (Hist) and control run (base), RCP45 and RCP85 scenarios.

Overall a larger variability was projected for biomass production and yields under RCP4.5 and RCP8.5 as compared to current production levels (Figure 50). An increased winter precipitation resulted in a larger soil water reservoir to be explored during spring by the winter wheat root system. Despite a C4 photosynthetic pathway which is more suited to drier environments, fodder maize yields expressed in fresh above ground biomass declined and their variability increased. Late potato yields declined remarkably under a projected climate and their variability increased spectacularly.

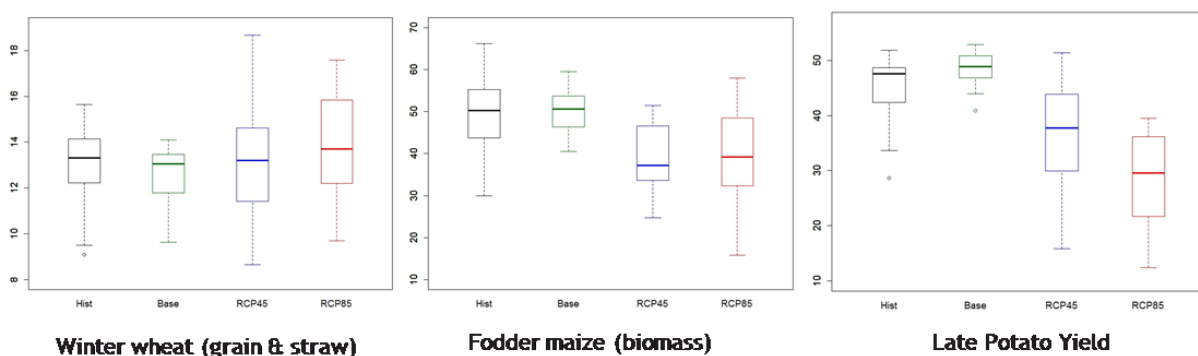


Figure 50: Climate impact on winter wheat, fodder maize and late potato (ton/ha) for observations (Hist) and control run (base), RCP45 and RCP85 scenarios.

#### 4.14 Climate change impact on isoprene emissions over Europe

Two evaluation simulations were performed to calculate past isoprene emissions over the period 1979-2005, both driven by ERA-Interim ECMWF reanalysis meteorological fields (Dee et al., 2011). Because these fields are constrained by meteorological observations, the derived isoprene emissions constitute our “best” estimate. Moreover, to better account for the effects of solar radiation changes over Europe that might not be captured by the ECMWF solar radiation fields, in the SSR simulation we have corrected the modeled short-wave radiation by using ground-based solar radiation observations over 1979-2005 (Sanchez-Lorenzo et al., 2013). Four simulations were conducted using the meteorology of the EURO-CORDEX ALARO-0 model, one for the period 1976-2005 (ALARO-HIST) and three for the period 2071-2099 following the climate scenarios RCP2.6, RCP4.5 and RCP8.5. These simulations are summarized in Table 5.

*Table 5: Performed simulations using the MEGAN-MOHYCAN model driven by meteorological conditions from either ECMWF or ALARO. The mean fluxes over Europe and over Belgium are given in Tg/yr and in Gg/yr, respectively. The percentage changes (in italics) are calculated with respect to the control simulations. Two schemes for CO<sub>2</sub> inhibition are the Wilkinson et al. (2009) parameterization (“W2009”) and the Possell and Hewitt (2011) parameterization (“PH2011”).*

Performed simulations		Flux over Europe (Tg/yr)	Flux over Europe accounting for CO <sub>2</sub> inhibition		Flux over Belgium (Gg/yr)	Flux over Belgium accounting for CO <sub>2</sub> inhibition	
			W2009	PH2011		W2009	PH2011
<b>ECMWF</b>	1979-2005	6.2	-	-	14.0	-	-
<b>SSR</b>	1979-2005	6.2	-	-	14.3	-	-
<b>ALARO-HIST</b>	1976-2005	4.6	-	-	10.1	-	-
<b>ALARO-RCP2.6</b>	2071-2099	5.0	4.8 (-4%)	4.3 (-14%)	10.5	10.1	9.0
<b>ALARO-RCP4.5</b>	2071-2099	6.1	5.4 (-11%)	4.4 (-28%)	11.6	10.3	8.4
<b>ALARO-RCP8.5</b>	2071-2099	8.4	5.8 (-31%)	4.1 (-51%)	15.3	10.5	7.5

The distribution of the isoprene emissions is similar for the ECMWF, SSR and ALARO-0 simulations (Figure 51), with higher isoprene emissions in Southern Europe and over central Russia. Compared to the ECMWF simulation, the use of observed solar radiation fields yields only slightly higher emissions over the entire domain, but leads to up to 10% higher emissions in Eastern Europe, due to stronger brightening suggested by the observations. The use of ALARO-0 climate data results in lower mean

emission flux over Europe (by 23%), due to the negative temperature bias in ALARO-0 (Giot et al. 2016) with respect to ECMWF temperature fields, except over Ukraine, Poland and Belarus.

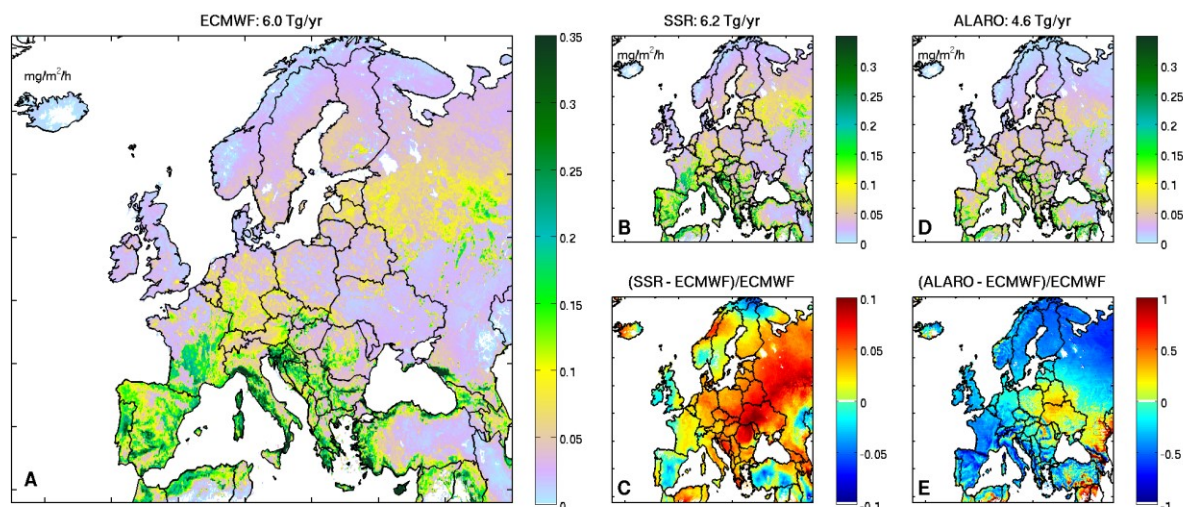


Figure 51: Mean isoprene emission flux (in  $\text{mg}/\text{m}^2/\text{h}$ ) calculated by ECMWF (A), SSR (B) and ALARO-0 (D) simulations. The relative difference between the SSR and ALARO-0 simulations with respect to the ECMWF results is illustrated in panels C and E, respectively.

The isoprene emission trends over 1979-2005 based on ECMWF, SSR and ALARO-0 simulations are shown in Figure 52. The isoprene emissions increased almost uniformly during this period. Although the emission trend is weaker using the ALARO-0 climate input, the patterns are similar in the three simulations. The strongest emission trends (up to 3%/yr) are calculated over northern France, southern Belgium, and southern Turkey, while the weakest trends (less than 1%/yr) appear over Spain, Turkey, Sweden, and central European Russia.

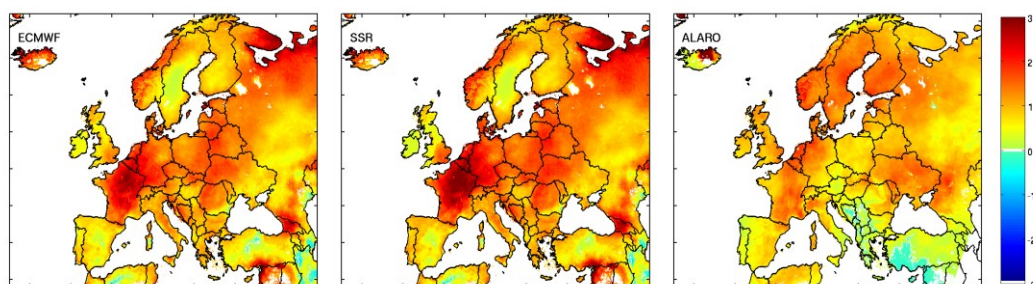


Figure 52: Isoprene emission trend (in % per year) between 1979 and 2005 according to 3 historical runs, ECMWF (left), SSR (middle) and ALARO-0 (right).

The isoprene emission distribution over Europe and over Belgium calculated based on ALARO-0 meteorological fields is illustrated in Figure 53. All climate scenarios suggest a flux increase over the European domain with respect to the control simulation, which amounts to 6% in RCP2.6, 33% in RCP4.5, and 82% in the RCP8.5 simulation. Similar but somewhat weaker increases are found over Belgium, 4% in RCP2.6, 15% in RCP4.5 and 51% in RCP8.5. The highest emissions in Belgium are found over the Ardennes and Campine forests (Figure 53), whereas central and western Belgium remains to be a low-isoprene-emitting region due to the dominance of urban centers, pasture and

croplands. The distribution of the relative change in the future scenario emissions with respect to the control run is shown in Figure 54 (upper panels).

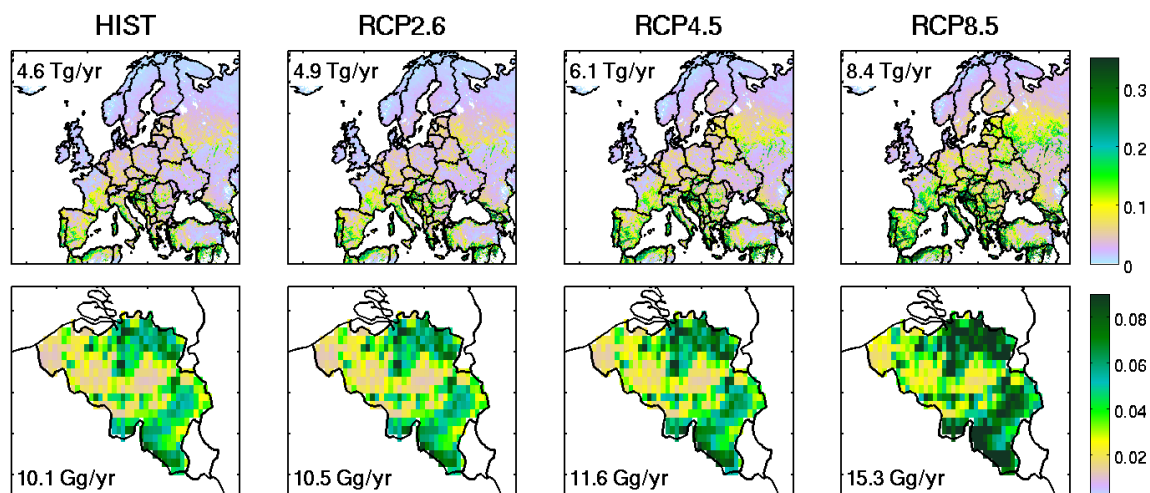


Figure 53: Isoprene fluxes over Europe and Belgium for the control run ALARO-HIST and for the 3 RCP scenarios (calculation without accounting for CO<sub>2</sub> inhibition effects), and are thus only influenced by the changes in future climate as predicted by the ALARO-0 model.

Whereas the RCP2.6 simulation suggests weakly higher isoprene emissions (up to 20%), the RCP4.5 and RCP8.5 simulations suggest isoprene emission increases that locally reach 40% and 110%, respectively. The enhanced future isoprene emissions in the central Russian region are mainly a result of strongly increasing temperatures, somewhat counteracted by decreasing insolation. In the Mediterranean region, similar isoprene emission increases are the result of a combination of less strong temperature increases, solar brightening and increased soil moisture stress due to the dryer future climate in this region, which slightly reduces the isoprene flux.

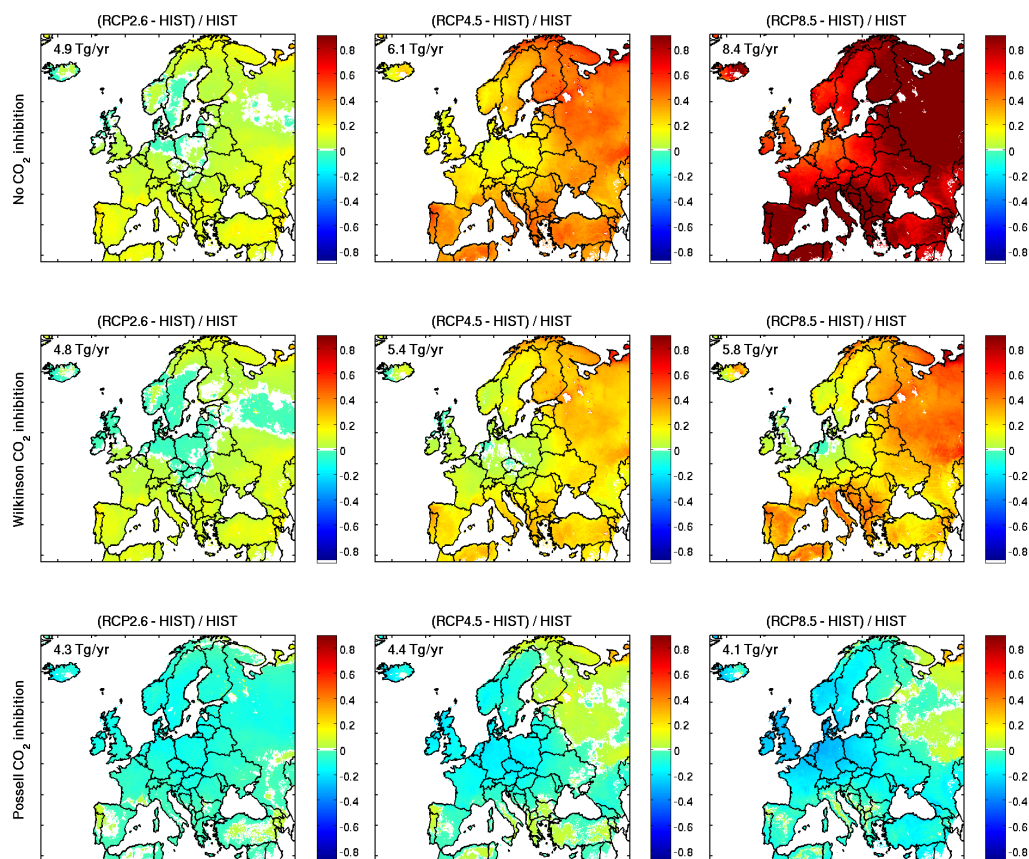


Figure 54: Relative isoprene emission increments compared to the Control ALARO-0 run for 3 RCP scenarios considering no CO<sub>2</sub> inhibition (top row), considering moderate CO<sub>2</sub> inhibition according the parametrization of Wilkinson et al. (2009) (middle row) or considering strong CO<sub>2</sub> inhibition according to the parameterization of Possell and Hewitt (2011) (bottom row). The average annual isoprene emission for each run is given on the left upper corner of every map.

When accounting for the inhibitory effect of future CO<sub>2</sub> levels on isoprene production the estimated isoprene fluxes are found to be lower than in the standard future simulations (Table 5, Figure 54). Because CO<sub>2</sub> is uniformly distributed, the spatial patterns of the emission changes are not influenced by including the CO<sub>2</sub> inhibition parameterization. Relative to the standard future simulations (in which the CO<sub>2</sub> inhibition effect is neglected), the future isoprene emission decreases by 4%, 11% and 31% in RCP2.6, RCP4.5 and RCP8.5, respectively, when applying the Wilkinson et al. (2009) parameterization, whereas the decrease is stronger when the Possell and Hewitt (2011) parameterization is used (-14%, -28%, -51%). It should be acknowledged, however, that due to the limited amount of measurements, both parameterizations bear large uncertainties. By the end of the century, the isoprene emissions in Belgium will remain very close to the present value, ranging

between +4% and -26%, depending on the used parameterization (Table 5, Figure 55).

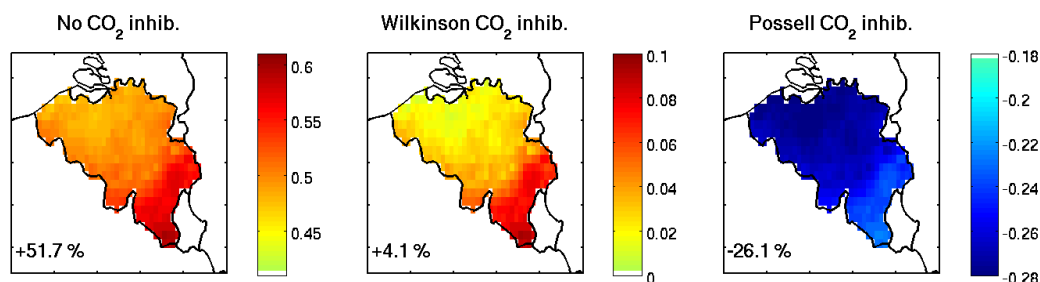


Figure 55: Same as Figure 54 for Belgium. Relative isoprene emission increments compared to the control ALARO-0 run for the RCP8.5 scenario, considering no CO<sub>2</sub> inhibition, moderate CO<sub>2</sub> inhibition (Wilkinson et al. 2009), or strong CO<sub>2</sub> inhibition (Possell and Hewitt (2011)).

## 4.15 Climate change impact on storm surges and waves

### 4.15.1 Climate change impact on wind

As wind is one of the main drivers of storm surges and waves, at first, an analysis of wind speed and wind direction was carried out. Then we analyse storm surges and waves following the same methodology. More specifically, extreme events are identified following the method described in Kamphuis (2010), to fit them following a Weibull cumulative distribution and then extrapolate for longer return periods using a least squares method (See Section 3.10.4).

The impact of climate change on wind is analyzed at two stations: Ostend and a station located in the Northern part of the North Sea where the wind regimes can differ significantly from the Southern part.

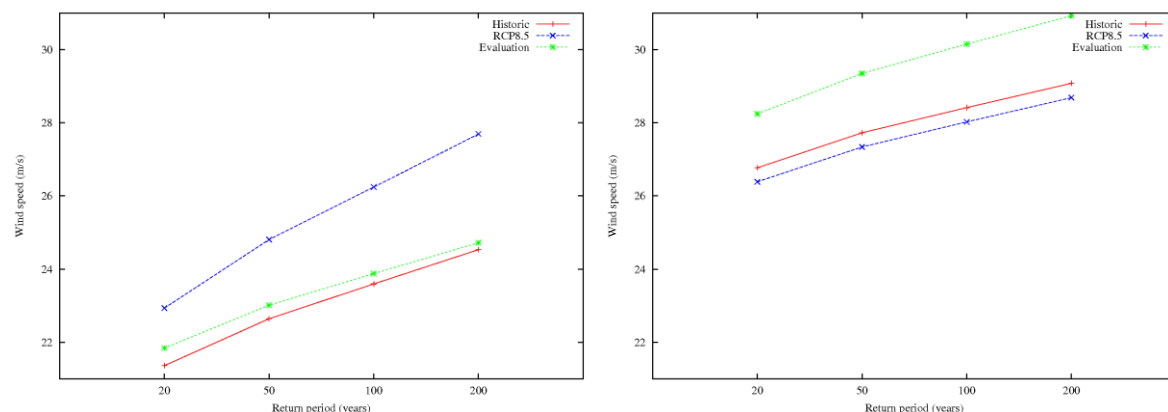


Figure 56: Maximum wind speed for a certain return period at Ostend (left) and at a Northern North Sea station (right) for different simulation periods. Shown are the results from the control or “historic” simulation (red line), the RCP8.5 projection (blue line) and the evaluation simulation (green line).

The wind speeds for the control and evaluation runs are more or less the same. While for the climate simulations, it is higher at Ostend (Figure 56 left panel).

Compared to Ostend, the magnitude of the wind speed in the Northern part of the North Sea is larger (see Figure 56 right panel). However, the evaluation and control run are not close to each other. This highlights the importance of the possible forcing variations between different models (ERA-Interim or CNMR global earth system). In the Northern part of the North Sea the return periods for the climate projection are below the ones of the evaluation and control. This illustrates the importance of spatial differences in climate and the need for carrying out further analysis (at different locations in the North Sea). This also indicates that results for the climate scenario with respect to control runs have to be treated with caution.

Moreover, an analysis of the wind direction for the evaluation run, the control run and the climate run has been carried out. No significant changes between the three simulations are noticed.

#### 4.15.2 Climate change impact on storm surge

For climate studies we focus on storm surges rather than on water elevations as the latter results from both the effect of wind and tides. High water levels can result from the combination of strong winds at high tides which is a timing effect. For climate studies, it is necessary to get rid of this timing effect. So, a storm surge is defined as the sole effect of wind on the water elevation. Storm surges are computed by subtracting time series of tide-only simulations from the full runs including both wind and tides.

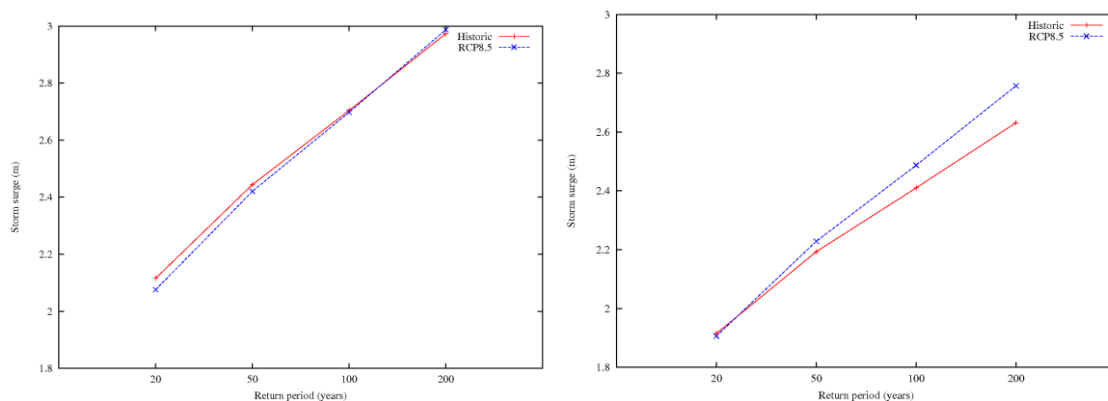


Figure 57: Maximum storm surge for a certain return period at Ostend (left) and at Westhinder (right) for different simulation periods. Shown are the results from the control or “historic” simulation (red line) and the RCP8.5 projection (blue line).

As shown in Figure 57 (left panel) the effect of climate change on the return levels of storm surges at Ostend is small although the change in wind speed at Ostend is larger than in the Northern part of the North Sea. One possible explanation for that is a nonlinear effect of the wind on storm surges.

Figure 57 (right panel) shows the return periods for the station Westhinder which is located in the Belgian part of the North Sea, a little bit more offshore than the Ostend station. The effect of climate change at Westhinder is a bit larger than at Ostend. This highlights spatial differences even at small scale and illustrates the need for analysing the impact of climate change at a larger number of stations.

### 4.15.3 Climate change impact on waves

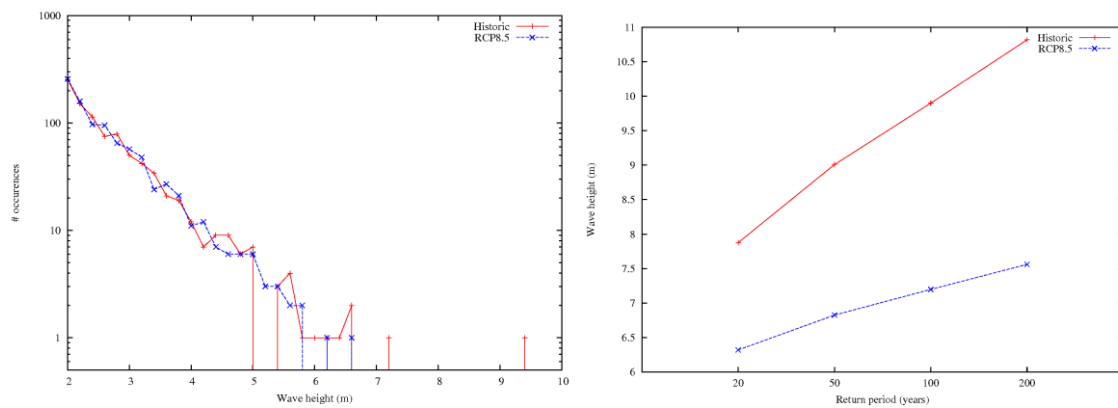


Figure 58: The frequency (left) and return levels (right) of maximum values of significant wave height at Westhinder for different simulation periods. Shown are the results from the control or “historic” simulation (red line) and the RCP8.5 projection (blue line).

The frequency of maximum wave height during extreme events is shown in the left panel of *Figure 58*. An outlying extreme event is present for the control run (dated December 1994). Although the WAM model is extensively validated with UKMO winds, this indicates that further validation of the model is needed for the current forcings (control run). The effect of this one event on the maximum wave height for a certain return period is unclear. However, such outliers can influence the results of a linear regression by least squares method and other more robust regression methods could be tested.

The right panel of *Figure 58* shows that the future climate scenario shows a decrease of extreme wave heights. As further validation of the WAM model is needed, the focus on values obtained should not be too high. The existence of an outlier is a possible reason for this strong increase. Further analysis of the role of storms and outliers is needed. Another possible reason for this is the decrease of wind speed for winds from the northern part of the domain. The winds coming from the North-West zone of the North Sea are generating the largest waves.

## 4.16 Statistical interpretation and uncertainty estimation

### 4.16.1 Validation of model results with different model resolutions

Here the question is addressed how the climate change signal changes as a function of the resolution of the climate model. More specifically, the results of the H-Res simulations will be compared to the RCM and GCM climate runs.

Results show that the high-resolution ALARO-0 and COSMO-CLM models reveal an added value to capture sub-daily precipitation extremes during summer compared to the driving GCMs and reanalysis data. Further validation of historical climate simulations based on design precipitation statistics derived from intensity–duration–frequency (IDF) curves shows indeed a better match of the convection-permitting model results with the observations-based IDF statistics. Results moreover indicate that one has to be careful in assuming spatial scale independency of climate

change signals for the delta change downscaling method, as high-resolution models may show larger changes in extreme precipitation. These larger changes appear to be dependent on climate model, since such intensification is not observed for the ALARO-0 model.

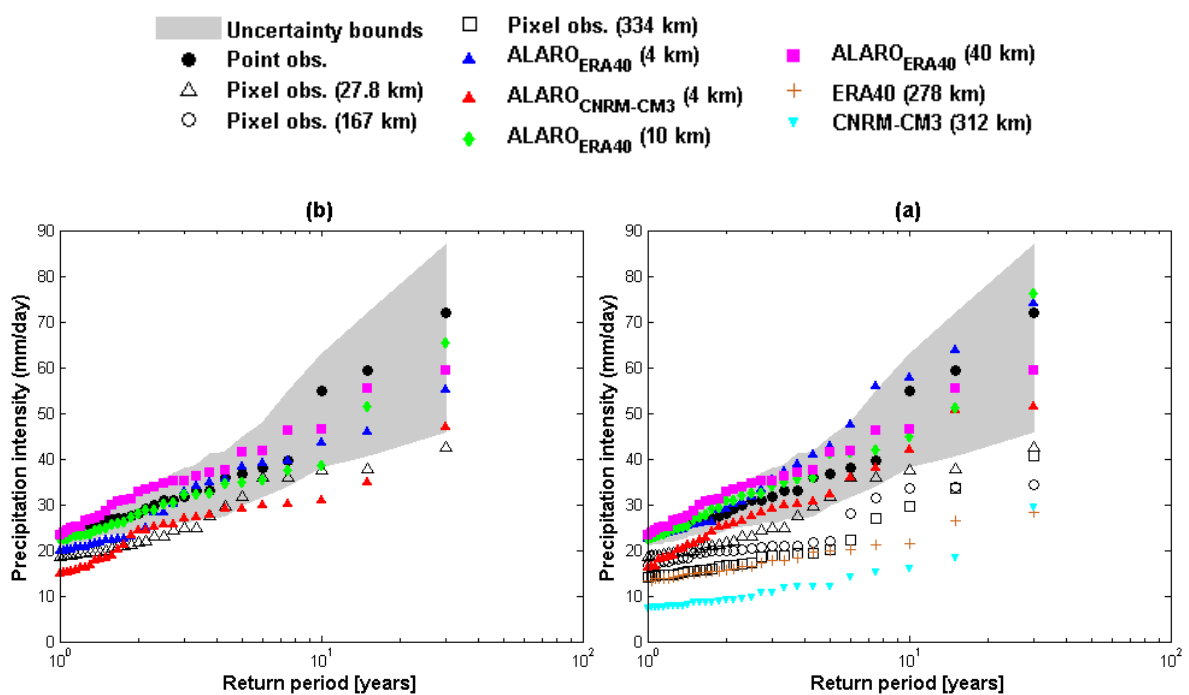


Figure 59: Validation of the native (a) and aggregated (b) daily precipitation quantiles (1961–1990) for the ALARO-0 model and its driving GCM or reanalysis data based on Uccle observations, for the summer season (shaded areas show at-site confidence intervals for the point observations using the bootstrap-based 95% confidence intervals)

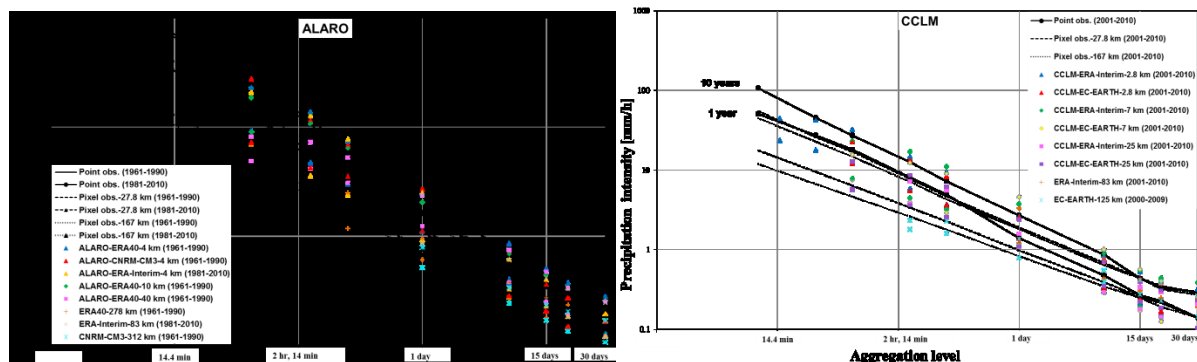


Figure 60: Comparison of historical IDF relationships based on point and pixel interpolated Uccle observations, with COSMO-CLM, ALARO-0 and the driving GCM or reanalysis results for the summer season (IDF curves for the E-OBS pixel data were extrapolated for the sub-daily timescales based on extreme value distribution)

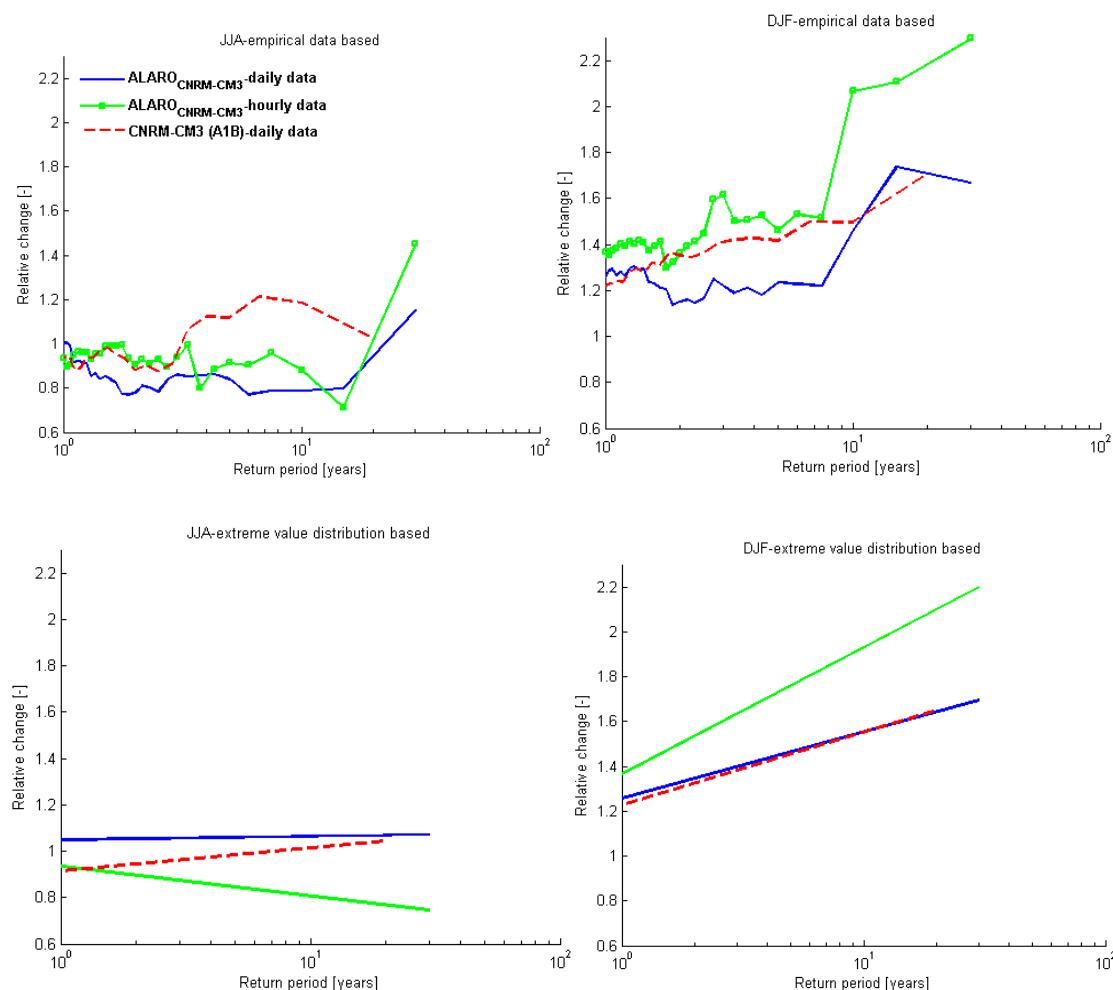


Figure 61: Change factors for daily and hourly precipitation quantiles computed using the ALARO<sub>CNRM-CM3</sub> 4 km and the driving CNRMCM3 (A1B) for the summer (left-column panels) and winter (right-column panels) seasons, obtained from the empirical data (top panels) and after use of the extreme value distributions (bottom panels)

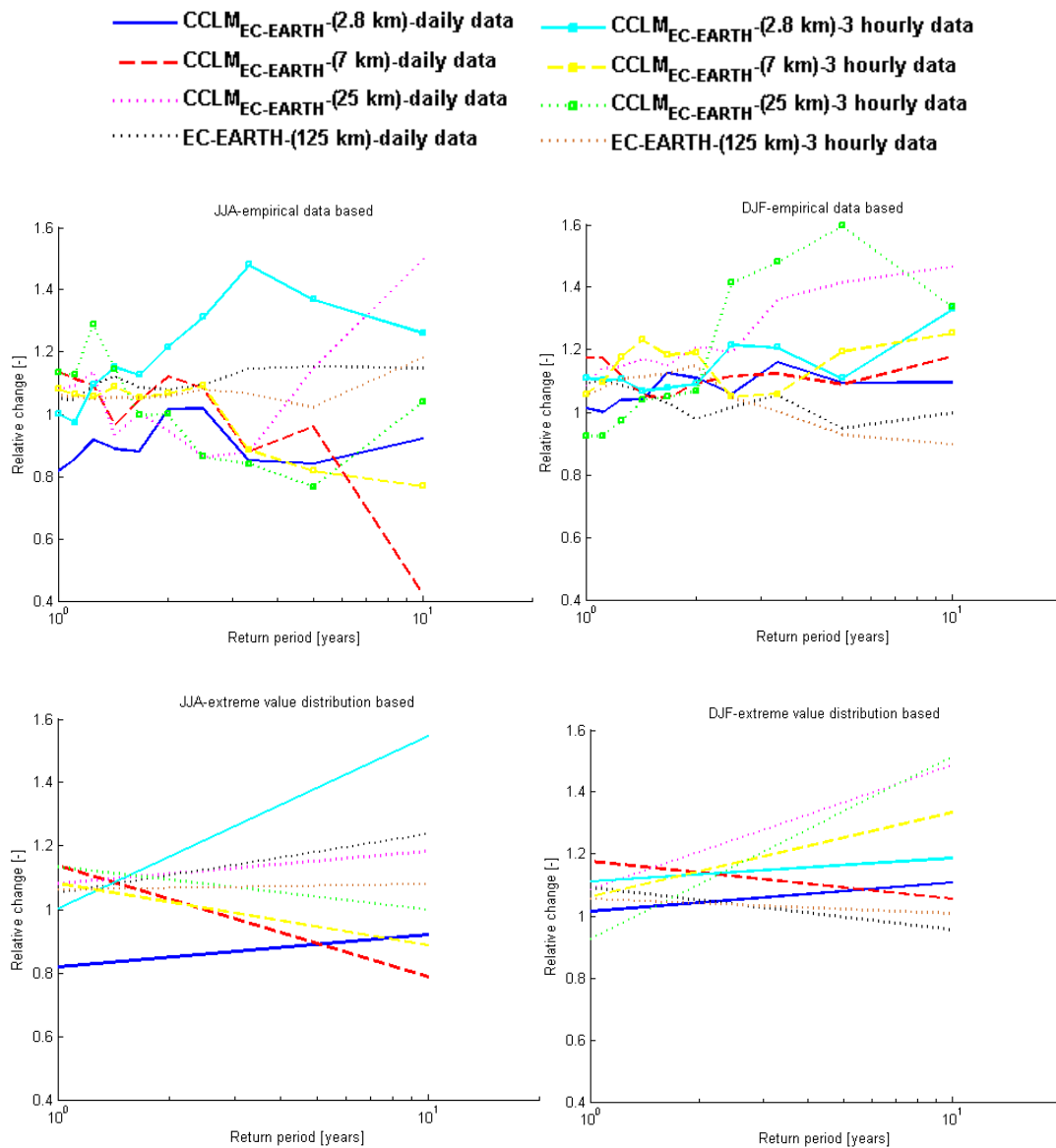


Figure 62: Change factors for daily and 3-hourly precipitation quantiles computed using COSMO-CLMEC-EARTH 2.8, 7, and 25 km for the summer (left-column panels) and winter (right-column panels) seasons, obtained from the empirical data (top panels) and after use of the extreme value distributions (bottom panels).

That the finer resolution models may show larger rainfall intensities was also confirmed after analysing 88 RCM runs available for 0.11 and 0.44 spatial resolutions from the EURO-CORDEX project. This comparative analysis shows higher design precipitation intensities by the finer resolution runs. The results reveal that making a temporal stationarity assumption for the climate system may lead to underestimation of design precipitation quantiles up to 70% by the end of this century. This again confirms the importance to incorporate fine resolution models in the analysis, as

done in our CORDEX.be approach, and to consider statistical downscaling that accounts for the scale dependency.

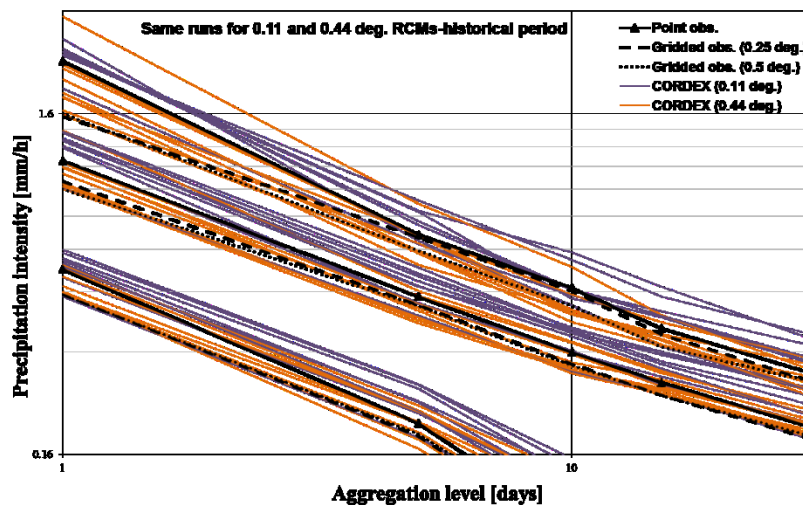


Figure 63: Comparison of the current climate IDF curves between the EURO-CORDEX RCMs of 0.11 and 0.44 resolutions

#### 4.16.2 Climate change signals for with different model resolutions and the impact of statistical downscaling:

The results of the statistical downscaling of the available ensemble set of CMIP5 GCM runs, EURO-CORDEX RCM runs and the two H-Res runs (ALARO-0 and COSMO-CLM) studied so far, show a clear tendency of the expected extreme precipitation intensities for the future to increase. Considering the higher intensities of precipitation (return periods higher than 1 year), the amount of increase is higher for smaller time scales and larger return periods. The precipitation intensity with hourly time scale and 10-year return period may increase up to about 100%. Furthermore, the increase in the design storm intensities as derived from the CMIP5 ensemble increases with the CO<sub>2</sub> concentrations in the emission scenarios, ranging from 37% in the RCP2.6 scenario to 64% in the RCP8.5 scenario. The changes moreover are found to depend on the return period and the aggregation level, with an amplification for larger return periods and smaller aggregation levels.

The results of this study indicate that the statistics based on historical or current meteorological conditions (e.g. IDF curves for extreme precipitation) are not sufficient to represent future precipitation patterns. They emphasize the necessity of upgrading the statistics, e.g. upgrading the IDF-curves for designing, operating and maintaining municipal water management infrastructures in the future.

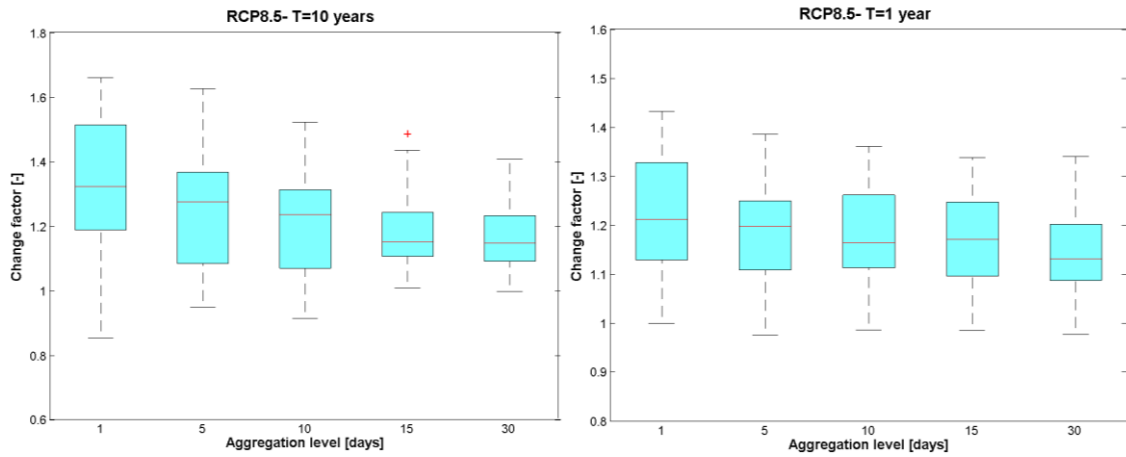


Figure 64: Change factors of the EURO-CORDEX 0.11 RCMs for design precipitation, for different durations and return periods

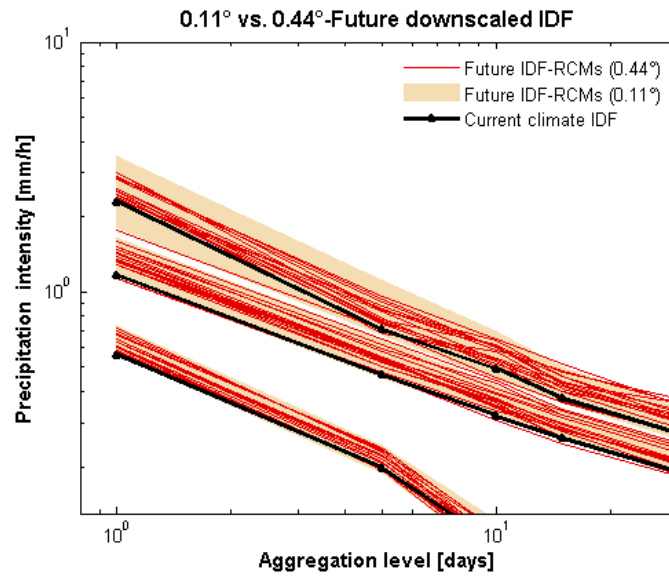


Figure 65: Comparison between the future IDF curves of the 0.11 and 0.44 RCMs with same model runs (current climate IDF curves based on the station observations are shown in black color)

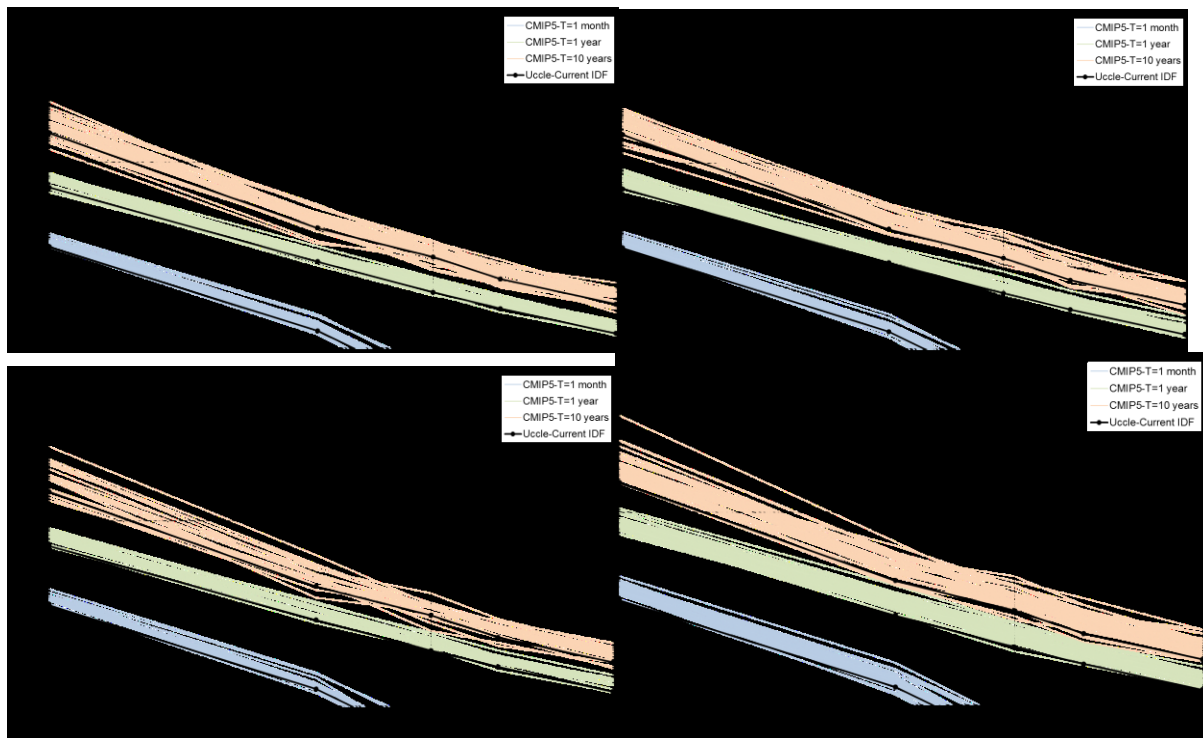


Figure 66: Future IDF curves (2071–2100) after quantile perturbation based on the CMIP5 GCMs versus the historical climate IDF curves (1961–1990) at Uccle

#### 4.16.3 On the importance of the different uncertainty sources

The variance decomposition approach identifies the local or RCM as the most dominant component of uncertainty in design precipitation changes, followed by the uncertainties related to the GCMs and RCP scenarios. For the EURO-CORDEX 0.11 ensemble, the choice of RCM roughly contributes between 17% and 50% to the total uncertainty, while the RCM contribution for the 0.44 ensemble peaks up to 69%. This means that one can give slightly higher trust to the higher changes obtained from the higher resolution RCMs than from the coarser models. The uncertainty analysis also reveals a greater role of the boundary forcing (i.e., GCM) compared to the future greenhouse gas scenario (i.e., RCP). Again, it shows the importance to incorporate the higher resolution models, as done in the CORDEX.be approach.

When the GCM uncertainty is studied separately, based on a larger ensemble of 140 CMIP5 GCM runs including 15 GCMs, 3-10 GCM initial conditions and 4 RCPs, it is found that the choice of GCM model is the major contributor (up to 65% for some cases) to intense precipitation change uncertainty for all return periods (1 year, 10 years) and aggregation levels (1-, 5-, 10-, 15-, 30-day). However, uncertainties related to the GCM initial conditions and RCPs of up to 38% and 23% respectively are found in some cases. The sensitivity analysis reveals that the GCM, RCP and GCM initial condition uncertainties are greatly influenced by the set of climate model runs considered, especially for more extreme precipitation at finer time scales.

Potential evapotranspiration (ETP) is next to precipitation another important variable for impact analysis in hydrology, water engineering, agriculture and other disciplines. Therefore, a specific task

was devoted to the analysis of the bias in ETP climate change signals. This was derived from seven simple temperature- and radiation-based methods (Blaney–Criddle, Hargreaves–Samani, Schendel, Makkink, Turc, Jensen-Haise, Tabari) and compared with that from the standard Penman–Monteith FAO 56 method on the basis of 12 out of the CMIP5 GCM runs. The results show the lack of conformity on the amount of ETP changes between the simple and standard methods, with biases of over 100% for some simple methods. The uncertainty affiliated with ETP methods for monthly ETP changes is smaller but of comparable magnitude to GCM uncertainty, which is usually the major source of uncertainty, and larger for daily extreme ETP changes. This outcome emphasizes the imperative of addressing the uncertainty associated with ETP methods for quantifying the hydrological response to climate change.

## 5 CONCLUSIONS AND RECOMMENDATIONS

### 5.1 General CORDEX.be conclusions

The CORDEX.be has created a platform for interaction between the Belgian modeling groups. This platform is used to produce and intercompare the Belgian simulations and to situate them with respect to the international CORDEX (“COordinated Regional Climate Downscaling Experiment”) ensembles. This information is provided to the stakeholders to show that the data from any of the Belgian simulations are consistent with the other Belgian CORDEX.be simulations and with the CORDEX ensemble. A website [euro-cordex.be](http://euro-cordex.be) has been created and will be maintained and updated with new results and serve as a link between the Belgian activities and the international ones of the CORDEX project. Also a CORDEX.be data hub was created at RMI and is accessible for future impact studies.

A large set of regional climate model (RCM) simulations were produced (see Table 1) over Europe and Belgium. Climate simulations with different models cover different greenhouse-gas scenarios and different future periods. Moreover, the simulations over the European domain have a resolution of 12.5 km while convection-permitting resolutions of below 5 km are available over a domain covering Belgium. More specifically, the simulations covering the evaluation period are closest to reality and can be used to compare with observations. With respect to the future scenarios, the period that is mostly covered is 2070-2100 following the RCP8.5 scenario, but simulations with the ALARO-0 model cover 2006-2100 for three scenarios (RCP2.6, RCP4.5 and RCP8.5).

#### *Model Validation*

As a first step long climate “evaluation” climate model were compared with past observations and GNSS-derived products. Such validation step is indispensable as it should give confidence in the use of the models for climate change purposes. All models were found to reproduce well the climate of the past.

An extensive validation of the climate simulations was performed by comparing the evaluation simulations with gridded and station observations. A positive validation is a necessary condition to put confidence in the use of the climate model for future climate projections.

With respect to the H-Res model runs over Belgium, while the average observed precipitation is 2.7 mm/day, the modeled ones range between 2.3 mm/day and 3.1 mm/day and are therefore in good agreement. Also for temperature, observations and models agree well with the largest bias being -1.3°C for the ALARO-0 for the average yearly temperature.

Different publications addressed the validation of the different model runs. More specifically Giot et al. (2016) presents the validation of ALARO-0 over the European domain. Despite not being tuned for climate purposes, ALARO-0 performs comparably well with respect to the other EURO-CORDEX models. In terms of the precipitation bias, ALARO-0 often outperforms all other models. The H-Res COSMO-CLM simulation over Belgium shows a very good skill in the representation of precipitation and cloud properties from in-situ and satellite observations (Brisson et al., 2016a,b). Moreover, a coupling of COSMO-CLM with TERRA URB enables the representation of the observed urban surface energy balance components from different intensive urban observation campaigns around the world

(Wouters et al., 2015; Demuzere et al., 2017, Wouters et al., 2017). Also, the COSMO-CLM precipitation intensity distributions for Uccle clearly shows an added value when going to higher resolution modeling, especially regarding precipitation extremes (Vanden Broucke et al., 2017). It was demonstrated that the COSMO-CLM model incorporating a 2-moment microphysical scheme provides realistic behavior in the simulation of hail. Finally, the model MAR was successfully validated over the Belgian domain for temperature and precipitation (Wyant et al., 2017a). Apart from the model validation against surface observations, also an upper-air variables was validated. More specifically a comparison was performed of the Zenith Tropospheric Delay (ZTD), which is a measure for the upper-air moisture content, between the model and GNSS-derived observations. All models capture well the diurnal and annual cycle of ZTD, as well as the variability and almost all correlate well with the observations, especially during winter.

The data from the ALARO-0 model is also freely available to the research community through the international data hub of the Earth System Grid Federation (ESGF).

### *Climate projections*

The CORDEX.be results for climate change are compare and position with respect to the ones that are found in international initiatives (CMIP5 and CORDEX), in order to provide an estimation of the uncertainties. Therefore an overview table is established that includes the climate change numbers from different climate projections for Belgium (Termonia et al., 2018). The uncertainty information in included in this table through “low” and “high” scenarios, that enables to the stakeholder to choose its decision-relevant climate information. Such table brings together all relevant information and reduces the fragmentation of the climate information at the Belgian level.

Focusing on the future period 2070-2100 for the scenario with the largest greenhouse gas emissions (RCP8.5), the most prominent impacts of climate change (averaged over the H-Res climate runs and over Belgium) include:

- The change in average yearly temperature ranges between 2.6°C and 3.5°C. A clear spatial gradient with climate changes close to the North Sea lower than the ones present in the South-East of Belgium.
- The climate projections indicate that, averaged over all H-Res models, one may expect an increase from 4.5 tropical days in the past to 19.5 days per year in the future.
- The amount of winter days is expected to be reduced from 91 to 40 while the amount of summer days will increase from 91 to 142.
- The relative increase in winter precipitation is on average 20% and positive everywhere in Belgium.
- The change in extreme precipitation (defined as 99 percentile of daily precipitation) is positive everywhere and on average 12%.
- The precipitation intensity with hourly time scale and 10-year return period may increase up to 100%.
- Heat waves, as defined by the Belgian Federal Public health Agency (FPS), with a current-day frequency of half a heat wave day per year, are expected to increase by more than 20 days per year. Moreover, increases will be even larger over city areas including Brussels, Antwerp and

Liège. It is clear that future heat waves will become more common both earlier and later in the year.

From the local impact models, the main impacts are:

- For the Brussels urban environment:
  - Significant increase of heat stress for people living in the city of Brussels, up to twice as large as in the surrounding rural areas.
  - Significant impact on the outdoor productivity due to thermal discomfort. More specifically, a doubling of lost working days may be expected.
  - A doubling of days when air-conditioning is intensively used, impacting the urban energy consumption.
- An increased variability for biomass production and yields. Average yields for fodder maize and late potatoes will also decline.
- Severely reduced winter snow height maxima (above 500m altitude).
- An increase of 51% of biogenic emissions from isoprene with the highest emissions in the Ardennes and Campine forests (disregarding the CO<sub>2</sub> inhibition effect).
- Indications exist that there will be less hail events but increase of mean hail size.

Based on interactions and feedback with stakeholders, different applications are ongoing that demonstrate the use of the climate data (e.g. Vanderhoeven et al., 2017).

## 5.2 Climate change impact on extreme precipitation

By comparing model simulations with observations over Belgium it was shown in Section 4.7 that regionally downscaled high-resolution models clearly outperform lower resolution simulations in the context of simulating heavy or extreme precipitation on the daily and hourly timescale, especially in summer. The reason for this improvement is the fact that high grid resolutions are necessary to explicitly resolve deep convection, amounting to more realistic summertime convective cloud dynamics. This finding clearly shows the added value and necessity of regional downscaling when assessing the impact of climate change on extreme precipitation.

The high resolution simulations for Belgium project a more severe future increase in heavy and extreme precipitation events on the hourly timescale, when compared to their lower resolution counterpart. For example, high resolution modeling predicts that hourly precipitation events exceeding 18 mm/hour, which currently occur about once every 10 years for any given location in Belgium, will become 3 times as frequent, while low resolution simulations project an increase in frequency of only 50% for this type of event. This result thus clearly demonstrates the added value of high resolution regional climate modeling in impact studies related to high intensity short duration precipitation events and their societal impact (e.g. flash flooding, damage to crops and infrastructure, soil erosion). They also provide further evidence that climate change could have a significant impact on the precipitation climatology over Belgium, and underscore that we need to adapt our infrastructure to deal with the negative consequences of heavy or extreme short-duration precipitation.

### 5.3 Climate change impact on snow cover

As shown in Section 4.8, over the period 1959-2010, all simulations using the MAR model show decreasing trends of the maximum snow height during winter in the Ardennes. The number of days with at least 5cm of snow accumulation is reduced up to -15days / 52 years and the beginning of snow season is delayed up to -60 days / 52 years in the highest parts of the Ardennes Massif. Regarding hydroclimatic conditions favouring floods in winter, these results induce that the number of days favourable to floods due to snow melting combined with rainfall events is decreasing over the considered period. Unfortunately, these results also induce a negative impact on winter tourism since there will be less snow for gliding sports. These trends are likely to continue in the future.

### 5.4 Climate change impact on urban environment: heat waves, urban heat stress and thermal comfort parameters

The presented results in Section 4.11 provide further evidence that we need to start adapting our cities to heat stress and climate change. Cooling the public space and the buildings of a city by implementing green and blue infrastructure, constructing green roofs, shade elements, etc. instead of using air-conditioning systems yields significant energy savings and makes a city more attractive. New infrastructures that are already adapted to the coming climate change will in the end lead to lower costs and higher efficiency. The advantage of these measures is that they are so-called “no-regret” measures; they will always help to improve the quality of living and the attractiveness of a city.

### 5.5 Climate change impact on biogenic emissions

In Section 4.14 the isoprene emissions have been calculated from vegetation over the EURO-CORDEX domain based on reanalysis data and on the output of a RCM. The estimated emission fluxes over Europe are found to increase by up to 83% in the RCP8.5 projection, and moderate increases are calculated in the RCP2.6 and RCP4.5 cases. In Belgium, the emission increase relative to the present day emissions due to the climate change is estimated at 51% in the extreme RCP8.5 scenario, but is much lower in the RCP2.6 (4%) and RCP4.5 (15%) simulations. The inclusion of the CO<sub>2</sub> inhibition results in an overall decrease in the estimated fluxes, which counteracts the increase due to climate change. It should be acknowledged, however, that the present study does not account for the potentially non-negligible effects of land use changes and CO<sub>2</sub> fertilization on the estimated emissions. Furthermore, the role of isoprene emissions on the atmospheric composition in a future climate depends also on the evolution of other emission sources (e.g. NO<sub>x</sub>) with which isoprene interacts, leading to ozone formation. The non-linearity of tropospheric ozone chemistry and the strong decline of anthropogenic emissions over Europe expected to occur during the 21st century as a result of regulations, is expected to modify the relationship between surface ozone and meteorological parameters. To assess these effects, simulations of the atmospheric composition using a high-resolution atmospheric model would be necessary.

## 5.6 Climate change impact on agricultural crop performance and yield

A regional dynamic agro-meteorological model (Gobin, 2010, 2012) was employed to simulate climate impacts on biomass production of arable crops. The physical basis relies on quantified relationships between weather and yield at the regional scale. Daily meteorological inputs and subsequent mathematical descriptions of bio-physical crop growth processes allow for establishing climate-related stress occurrences during the growing season. The model has been used to calculate meteorological and climate impacts on Belgian arable yields at the regional scale. The focus has been predominantly on time-series analysis and inter-scenario comparisons. Weather series belonging to a future climate show a larger projected variability in crop productivity, which is not compensated for by CO<sub>2</sub> fertilisation.

## 5.7 Climate change impact on waves and storm surges

The results analysis provided in Section 4.15 focuses on the impacts of climate change on wind, storm surges and wave heights and summarized here. Further analysis of these results is ongoing, in particular concerning the validation of the waves model with the meteorological forcing applied and concerning the effect of outliers in the wind distribution. Simulations using the ALARO-0 model for the projection scenarios RCP2.6 and RCP4.5 will also be carried out. Moreover, the simulations with the RCP8.5 scenario for the periods 2010-2069 forced by ALARO-0 are planned.

The analysis of wind speed focuses on two stations: Ostend and a station located in the Northern part of the North Sea. At Ostend, the control and evaluation runs provide quite similar results. The climate run indicates a moderate increase of the wind speed extremes at Ostend. For the station located in the northern part of the North Sea, the evaluation run contains larger wind speed extremes than the control run. For the climate projection run, wind speed extremes are slightly reduced as compared to the control run. These differences are attributed to the different forcings of the ALARO-0 model for the control and evaluation runs. As expected, the southern and northern parts of the North Sea show different wind climate.

The maximum storm surge extremes are similar for the control and climate runs. Differences appear on small spatial scales as well as nonlinear effects of the wind.

The climate run shows a decrease of the maximum significant wave height extremes. However, two remarks must be taken into account. First of all, a validation of the WAM model for the forcings of the ALARO-0 must be performed. Secondly, changes in the wind speed in the northern part of the North Sea may have an impact on the wave heights on the Belgian Continental Shelf.

## 5.8 GNSS-based model validation of the H-Res climate model runs

Within CORDEX.be the standard climate model validation procedure has been complemented with a pioneering approach: the validation based on GNSS-derived products (ZTD and IWV). In order to obtain the observed ZTD and IWV, the necessary re-processing activities (developments and runs) have been carried out at ROB, thereby provided the CORDEX.be consortium with a climate-quality GNSS-based tropospheric dataset. This dataset could be readily converted into a dataset of Integrated Water Vapor (IWV). In parallel, ZTD and IWV data were extracted from the H-Res climate models for inter-comparison. The ZTD datasets was then used for the GNSS-based validation

procedure, i.e. to validate and study e.g. the annual and diurnal cycle of the water vapor in the atmosphere.

Almost all H-Res models showed a remarkable good correlation with observations and are able to reproduce the variations of variability in the diurnal and yearly cycle.

During the course of this project, several recommendations have been identified that should be taken into account for any future GNSS-based climate model run validation in Belgium (also valid for Europe). Amongst them:

- When identifying the set of high-quality GNSS stations falling within the climate model domains, it came out that we can significantly extend the model validation if the model output were available after 2010. This would not only provide longer time series for the currently selected stations (i.e. more than 17 years instead of 10 years) but also include much more GNSS stations providing high-quality observations. For example, with a requirement of GNSS observation for a period longer than 10 years in the period 2000-2017, we could add about 60 more GNSS stations in Belgium, with a total about 150 GNSS stations in the complete high-res climate model domains. This would directly enhance the statistical confidence in the results obtained, but also enhance the understanding of the studied phenomena, hence potentially enhance the physics in the models, by e.g. better studying the spatial discrepancies in the model domains.
- During the course of another project (supplementary researcher “Development of Key Performance Indicators (KPIs) and Decision Models for Geodetic GNSS Positioning” at ROB), it was found that, even if the quality of the GNSS re-processing carried out for CORDEX.be was excellent, the quality of the GNSS tropospheric products provided within CORDEX.be can still benefit of integrating the developments done in that project into the enhanced processing strategy developed for CORDEX.be. This should be considered for any further activities similar to CORDEX.be.
- It was also identified that the GNSS-based and model output datasets can be used well beyond the “simple” validation, but also for more in-depth studies like studying the extremes and the super-CC relationship (goal of a recently proposed BRAIN.be pioneer project).

## 5.9 Conclusions stakeholders meeting

Delivering Climate Services is a networking effort requiring the collaboration of different experts at different levels of the climate-services chain, from the scientific to the stakeholders' level with frequent interactions between the levels. CORDEX.be is a networking and modeling effort to produce the foundations of Climate Services for Belgium. However, different steps still are required to close this chain for Belgium, more specifically, there is a need for:

- a more thorough analysis of the enormous amount of produced data in order to establish a coherent picture of the climate-change impacts on Belgium. For instance, the impact of climate change on drought and forest fires is an important issue to investigate for Belgium. These were not directly studied within the CORDEX.be project but the CORDEX.be data could certainly serve to study these. Droughts are relevant in the context of water availability and agriculture, and require an impact study by season.

- integrating the current and future impact analysis into the design of Belgian adaptation policy measures by vulgarizing the most prominent CORDEX.be results and continuing contacts at the different levels of the climate services chain.

In order to start a dialogue with the stakeholders community on the usefulness of the CORDEX.be results, a one-day stakeholders meeting was organized at RMI at the end of the project. There were about eighty participants, more than half of which were stakeholders. These included people from both the private and public sector, with the public sector ranging from the federal, the regional up to the city level.

Here are a few key messages that have been drawn from the interaction with stakeholders:

- Most impact studies done within CORDEX.be address the future period 2070-2100 for which the climate-change signal is mostly well pronounced. Most stakeholders, however, are interested in climate changes with time horizon of maximally 30 years. Studies at this time horizon must involve a full uncertainty analysis, based on both local, regional and global climate studies.
- There is a need to list climate impacts that will potentially be affecting Belgium, in order of impact severity, per season and per time range (20 up to 100 years). This could be supplemented with maps that show the spatial distribution and should be written in an understandable language for the general public.
- The risks of future multi-component disasters should be addressed. For instance the risk of a combined storm surge (coastal flooding) and river flooding, or, having a severe drought two years in a row?
- There is a need to translate the climate impact, mostly expressed in numbers and graphs, into a language for general public. For instance, a change in frequency of alert phases (and pollution peaks) or expressed in frequency of well-known high-impact storms such the “Pukkelpop” storm.

## 6 DISSEMINATION AND VALORISATION

### 6.1 Stakeholder meetings during the project

Three stakeholder meetings were organized for the CORDEX.be project and one was organized in September 2017. On 29-4-2015, five stakeholders were invited with the aim of selecting our two case studies. In this meeting Johan Brouwers and Claire Collin suggested “sensitivity maps” and “invasive species”, respectively, as good candidates for case studies. Claire and Johan helped organize two other meetings: one on sensitivity maps (2-9-2015 afternoon) with Ruimte Vlaanderen (Jozefien Hermy and Anneloes Van Noordt) and one on invasive species (2-9-2015 noon) with Belgian Biodiversity Platform (Sonia Vanderhoeven) and Service public Wallonie (Etienne Branquart). An impact assessment of climate change on invasive species should involve specific output from RCM or H-Res runs, from which experts could assess the future probability of establishment and/or physiological response of specific plant or animal species. Based on a literature study a list of 20 meteorological variables has been compiled and distributed. Maps of these variables will be worked out in the context of the BELSPO-funded TRIAS project (Vanderhoeven et al, 2017) to allow for expert judgement.

Apart from these three stakeholder meetings a CORDEX.be project presentation was given at the VMM conference concerning the MIRA report (17-9-2015). RMI co-organized a climate meeting for re-insurance company Swiss Re at Uccle (28-10-2015) where CORDEX.be was advertised.

### 6.2 Final CORDEX.be stakeholders meeting 26-09-2017

In order to start a dialogue with the stakeholders community on the usefulness of the CORDEX.be results, a one-day stakeholder meeting was organized at the end of the project. There were about eighty participants, more than half of which were stakeholders. These included people from both the private and public sector, with the public sector ranging from the federal, the regional (Walloon, Flanders, Brussels) up to the city level. The fact that around 60% of the invitees confirmed their participation shows the large interest in the theme of climate services and the engagement in the dialogue with climate experts. The meeting presentations and pictures can be found [here](#). The meeting drew media attention from the [national VRT television](#) and the written [press Het Nieuwsblad](#).

The meeting was organized having in mind that the stakeholders would express their needs regarding climate information. Therefore, the first part of the meeting was intended for a general public and featured different stakeholders presentations. The second part was composed of four parallel break-out sessions: urban climate, agriculture, air quality and hydrology. In order to stress the potentially dramatic impact of climate change on the Belgian population, a national-television weather man, Frank Deboosere, presented a hypothetical weather forecast for an intense heat wave. This 13-day heat wave was taken out of future simulation of the year 2063, generated with a regional model that is also used for weather forecasting purposes. This “weather forecast” was followed by a thorough explanation to what extent this was (not) a real weather forecast.

Based on scientific results, the presentations highlighted that climate change will pose new challenges associated with a range of weather-related hazards (e.g. sea-level, extreme flooding, heat

waves and droughts) that strongly impact nature and society. Belgium is a particularly vulnerable region due to its dense population, large urbanization and a large low-lying area close to the sea. Impact studies done within CORDEX.be addressed extreme precipitation, heat waves and urban heat stress, snow height, agriculture, hail and biogenic emissions.

### 6.3 Follow-up meeting

The objective/intention of the follow-up meeting was to present the status of the CORDEX.be project to the follow-up committee. Additionally, since all nine partners were present, this occasion was used to see whether the impact modeling groups had started their work or were ready to start their work and to identify critical points. Any identified issues such as delays in the climate runs due to problems within the models were discussed in small meetings later on. The project partners were requested to develop case studies involving high-impact. Producing statistics for hail (UCL) was raised as a priority because of its large climate impact.

### 6.4 Scientific publications in international journals

- Bauwens, M., Stavrakou, T., Müller, J.-F., Van Schaeybroeck, B., De Cruz, L., De Troch, R., Giot O., Hamdi, R., Termonia, P., Laffineur, Q., Amelynck, C., Schoon, N., Heinesch, B., Holst, T., Arneth, A., Ceulemans, R., Sanchez-Lorenzo, A., and Guenther, A., “Recent past (1979-2014) and future (2070-2099) isoprene fluxes over Europe simulated with the MEGAN-MOHYCAN model” Submitted to Biogeosciences.
- Brisson E, Weverberg KV, Demuzere M, et al (2016) How well can a convection-permitting climate model reproduce decadal statistics of precipitation, temperature and cloud characteristics? *Clim Dyn* 1–19.
- Brisson, E., Demuzere, M. & van Lipzig, N. P. Modeling strategies for performing convection-permitting climate simulations. *Meteorologische Zeitschrift* 25, 149–163 (2016b).
- De Ridder, K., B. Maiheu, D. Lauwaet, I.A. Daglis, I. Keramitsoglou, K. Kourtidis, P. Manunta and M. Paganini, 2016. Urban Heat Island Intensification during Hot Spells—The Case of Paris during the Summer of 2003. *Urban Science*, 1.
- Demuzere, M., Harshan, S., Järvi, L., Roth, M., Grimmond, C.S.B., Masson, V., Oleson, K.W., Velasco, E., Wouters, H. Impact of urban canopy models and external parameters on the modeled urban energy balance in a tropical city. in review for *QJRMS* (2017).
- De Troch, R.: The application of the ALARO-0 model for regional climate modeling in Belgium: extreme precipitation and unfavorable conditions for the dispersion of air pollutants under present and future climate conditions, PhD Thesis, 9 May 2016
- Fettweis, X., Franco, B., Tedesco, M., van Angelen, J. H., Lenaerts, J. T. M., van den Broeke, M. R., and Gallée, H.: Estimating the Greenland ice sheet surface mass balance contribution to future sea level rise using the regional atmospheric climate model MAR, *The Cryosphere*, 7, 469-489, 2013.
- Fettweis, X., Wyard, C., Doutreloup, S., Belleflamme, A: Noël 2010 en Belgique : Neige en Flandre et pluie en Haute-Ardenne, *Bulletin de la Société Géographique de Liège* (accepted). *Bulletin de la Société géographique de Liège* 68 (2017).

- Giot, O., Termonia, P., Degrauwe, D., Troch, R. D., Caluwaerts, S., Smet, G., Berckmans, J., Deckmyn, A., Cruz, L. D., Meutter, P. D. and others: Validation of the ALARO-0 model within the EURO-CORDEX framework, *Geosci. Model Dev.*, 9(3), 1143–1152, 2016.
- Hamdi, R., F. Duchêne, J. Berckmans, A. Delcloo, C. Vanpoucke, and P. Termonia, 2016: Evolution of urban heat wave intensity for the Brussels Capital Region in the ARPEGE-Climat A1B scenario, *Urban Climate*, 17, 176-195.
- Hamdi, R., O. Giot, R. De Troch, A. Deckmyn, and P. Termonia, 2015: Future climate of Brussels and Paris for the 2050s under the A1B scenario. *Urban Climate*, 12, 160-182.
- Hosseinzadehtalaei, P., Tabari, H., Willems, P. (2016), Quantification of uncertainty in reference evapotranspiration climate change signals in Belgium, *Hydrology Research*, 47(5), nh2016243
- Hosseinzadehtalaei, P., Tabari, H., Willems, P. (2017), Uncertainty assessment for climate change impact on intense precipitation: How many model runs do we need?, *International Journal of Climatology*, In revision
- Lauwaet D., De Ridder K., Maiheu B., Boëne W., Demuzere M., Verdonck M.-L., 2017. Effectiveness of green and blue infrastructure to mitigate heat stress in the city of Ghent. *Urban Climate*, in preparation.
- Prein, A.F. Wolfgang Langhans, Giorgia Fosser, Andrew Ferrone, Nikolina Ban, Klaus Goergen, Michael Keller, Merja Tölle, Oliver Gutjahr, Frauke Feser, Erwan Brisson, Stefan Kollet, Juerg Schmidli, Nicole P. M. van Lipzig, Ruby Leung (2015). A review on regional convection-permitting climate modeling: Demonstrations, prospects, and challenges, *Rev. Geophys.*, 53, 323–361.
- Saeed, S., Brisson, E., Demuzere, M., Tabari, H., Willems, P., Van Lipzig, N. (2017). Multidecadal convection permitting climate simulations over Belgium: Sensitivity of future precipitation extremes. *Atmospheric Science Letters*, 18 (1), 29-36.
- Sharma, R., Hooyberghs, H., Lauwaet, D., De Ridder, K., 2017. Climate Change and Urban Heat Island – Short term and long term projections for Delhi, *International Journal of Climatology*, in preparation.
- Sharma, R., Lauwaet, D., Hooyberghs, H., De Ridder, K., 2017. Assessing the Urban Heat Island of Delhi (India) with the urban climate model, *UrbClim, Theoretical and Applied climatology*, in review.
- Tabari, H., De Troch, R., Giot, O., Hamdi, R., Termonia, P., Saeed, S., Brisson, E., Van Lipzig, N., Willems, P. (2016), Local impact analysis of climate change on precipitation extremes: are high-resolution climate models needed for realistic simulations?, *Hydrology and Earth System Sciences*, 20, 3843–3857
- Tabari, H., Taye, M.T., De Troch, R., Termonia, P., Saeed, S., Brisson, E., Van Lipzig, N., Willems, P. (2015), Local impact analysis of climate change on precipitation extremes: Are high-resolution climate models needed for realistic simulations?, Submitted.
- Tabari, H., Taye, M.T., Willems, P. (2015), Water availability change in central Belgium for the late 21th century, *Global and Planetary Change*, 131, 115-123.
- Termonia, P. B. Van Schaeybroeck, L. De Cruz, R. De Troch, S. Caluwaerts, O. Giot, R. Hamdi, S. Vannitsem, P. Willems, H. Tabari, E. Van Uytven, P. Hosseinzadehtalaei, N. Van Lipzig, H. Wouters, S. Vanden Broucke, J.-P. van Ypersele, P. Marbaix, C. Villanueva-Birriel, X. Fettweis, C. Wyard, C. Scholzen, S. Doutreloup, K. De Ridder, A. Gobin, D. Lauwaet, T. Stavrakou, M.

- Bauwens, J.-F. Müller, P. Luyten, S. Ponsar, D. Van den Eynde, E. Pottiaux, “The CORDEX.be initiative as a foundation for climate services in Belgium”, submitted to Climate Services.
- Trusilova, K., Schubert, S., Wouters, H., Früh, B., Grossman-Clarke, S., Demuzere, M., and Becker, P. The urban land use in the COSMO-CLM model: a comparison of three parameterizations for Berlin. *Meteorologische Zeitschrift* 25, 231–244 (2016)
  - Vanden Broucke S., Wouters H., Demuzere M., Van Lipzig N. 2017, The added value of convection-permitting simulations in representing mean and extreme climate and climate change over Belgium. (In preparation).
  - Van Schaeybroeck, B.; Vannitsem, S.: Assessment of calibration assumptions under strong climate changes, *Geophys. Res. Lett.*, 43, 1314–1322, 2016.
  - Wouters, H., Demuzere, M., De Ridder, K. & van Lipzig, N. P. The impact of impervious water-storage parametrization on urban climate modeling. *Urban Climate* 11, 24–50 (2015).
  - Wouters, H. M., Blahak, U., Fortuniak, K., Maiheu, B., Camps, J., Tielemans, D., and van Lipzig, N. P. M. The efficient urban canopy dependency parametrization (SURY) v1.0 for atmospheric modeling: description and application with the COSMO-CLM model for a Belgian summer. *Geoscientific Model Development* 9, 3027–3054 (2016).
  - Wouters, H., K. De Ridder, Lien Poelmans, Patrick Willems, Parisa Hosseinzadehtalaei, Hossein Tabari, Johan Brouwers, Sam Vanden Broucke, N.P.M. van Lipzig, and M. Demuzere. Heat stress under climate change twice as large for cities as for rural areas: a study for a densely populated mid-latitude maritime region (2017), *Geophys. Res. Lett.*, 44, 1–11.
  - Wyard, C., Scholzen, C., Fettweis, X., Van Campenhout, J. and François, L. (2016), Decrease in climatic conditions favouring floods in the south-east of Belgium over 1959–2010 using the regional climate model MAR. *Int. J. Climatol.* 37(5), 2782-2796 (2017a).

## 6.5 Contributions to conference proceedings & national publications

- De Troch, R., Giot, O., Hamdi, R., Saeed, S., Tabari, H., Taye, M. T., Termonia, P., Van Lipzig, N., Willems, P., 2014. Overview of a few regional climate models and climate scenarios for Belgium. Tech. rep., Royal Meteorological Institute of Belgium.
- Giot, O.; Termonia, P.; De Troch, Rozemien; Caluwaerts, Steven; Smet, Geert; Deckmyn, Alex ; Gerard, Luc; Van Ginderachter, Michiel; De Meutter, Pieter; Degrauwe, Daan ; De Cruz, Lesley ; Hamdi, Rafiq; Duerinck, Annelies; Berckmans, Julie ; Van den Bergh, Joris; Van Schaeybroeck, Bert: ALARO-0 used to perform EURO-CORDEX simulations, *ALADIN-HIRLAM Newsletter* 4, 74-79, February 2015.
- Tabari, H., Hosseinzadehtalaei, P., Willems, P., Saeed, S., Brisson, E., Van Lipzig, N. (2016), How will be future rainfall IDF curves in the context of climate change?, *Sustainable Hydraulics in the Era of Global Change: Proceedings of the 4th IAHR Europe Congress (Liege, Belgium, 27-29 July 2016)* (Ed. Sébastien Erpicum, Bejanmin Dewals, Pierre Archambeau, Michel Piroton), CRC Press, 796-803; ISBN print 978-1-138-02977-4, ebook 978-1-4987-8149-7.
- Wyard, C., Fettweis, X., & Erpicum, M. (2015). Etude de l'évolution de l'enneigement dans les Hautes Fagnes (Belgique) au cours des cinquante dernières années à l'aide du modèle climatique régional MAR. In M., Erpicum (Ed.), *Actes du XXVIIIe colloque annuel de l'Association*

Internationale de Climatologie : Modélisations et variabilités. Liège, Belgique: ULg. <http://hdl.handle.net/2268/18398>.

- Wyard, C., Fettweis, X., Belleflamme, A., Doutreloup, S., & Erpicum, M. (2017). Reconstruction de l'évolution du rayonnement solaire reçu en surface en Europe Occidentale sur la période 1900-2014 à l'aide du modèle atmosphérique régional MAR. In S., Dahech & S., Charfi (Eds.), Actes du XXXe colloque de l'Association Internationale de Climatologie : Climat, ville et environnement. <http://hdl.handle.net/2268/212993>.

## 6.6 Outreach to the scientific community

- P. Termonia presented the CORDEX.be project at a plenary talk at the International Conference on Regional Climate ICRC-CORDEX 2016.
- Invited lectures were held by An Gobin on different occasions in the agriculture sector, notably at the provincial centres of different crops in Flanders (PCA, Inagro), at Agrolink Flanders, and at the ministry of agriculture (ILVO). CORDEX.be was portrayed as an important project relevant for future climate impact.
- The framework of the CORDEX.be project has been advertised several times by Eric Pottiaux within the COST Action ES1206 "Advanced Global Navigation Satellite Systems tropospheric products for monitoring severe weather events and climate" (GNSS4SWEC) as well as within the EUMETNET EIG GNSS water Vapor Program (E-GVAP), with a specific focus on the GNSS re-analyses and the corresponding verification of the high-resolution atmospheric runs (see list below).
- Van Lipzig, N.P.M., 2014. The regional climate studies group at KULeuven. Introduction presentation at the panel meeting of the Regional Hydroclimatological Projects. 7th International Scientific Conference on the Global Water and Energy Cycle, 16 July 2014, The Hague, The Netherlands.
- Vanderhoeven, S. et al. (2017). Tracking Invasive Alien Species (TriAS): Building a data-driven framework to inform policy. Research Ideas and Outcomes, 3, e13414.

## 6.7 Outreach articles for the general public

- Termonia, P., R. Hamdi, B. Van Schaeybroeck, P. Willems, N. Van Lipzig, J.-P. van Ypersele, P. Marbaix, X. Fettweis, K. De Ridder, A. Gobin, T. Stavrakou, P. Luyten, E. Pottiaux, Combineren van regionale downscaling expertise in België: CORDEX en verder (CORDEX.be), Science Connection 50.
- Van Lipzig, N.P.M., 2016. Why climate science needs high-performance computing: Demonstrations, prospects and challenges. HPC Tier-1 inauguration, KULeuven, 17 October 2016, Leuven, Belgium.
- Van Lipzig, N.P.M., 2016. Klimaatverandering in Vlaanderen, huidige waarnemingen en klimaatscenario's tot 2100. Klimaatworkshop, Klimaatadaptatie in de landbouw, UGent 29 september 2016, Gent, België.
- Van Lipzig, N.P.M., 2016. Klimaatscenario's voor België op hoge resolutie. Voorstelling van het MIRA Klimaatrapport 2015: over waargenomen en toekomstige klimaatveranderingen. Vlaamse Milieumaatschappij, 11 Maart 2016, Aalst, België.

- Van Lipzig, N.P.M., 2015. Why Limit Global Warming to 2°C? Preface on lecture by H.E. Denise Bauer, Ambassador of the United States of America to Belgium. Earth Day @ KU Leuven, 22 April 2015, Leuven, Belgium.
- [KMI nieuwsbrief 2017](#).
- Wyard, C. (December 2016). Plus de pluie, mais pas plus d'inondations ... . FNRS news, December 2016. <http://hdl.handle.net/2268/206990>.
- Wyard, C. and Fettweis, X. (February 2017). Montée des eaux : Un nouveau modèle de simulation climatique. Le 15e Jour du Mois, 261. <http://hdl.handle.net/2268/207517>.
- Wyard, C. and Fettweis, X. (March 2017). Changement climatique : conséquences en Ardenne. Au fil de l'eau : Bulletin de liaison du Contrat de Rivière de l'Amblève et de la Rour - Über Wasser : Verbindungsbroschüre des Flussvertrags Amel und Rur, 32, pp.18-19. <http://hdl.handle.net/2268/208938>.
- EGU 2017 Press conference: Cities' resilience to a changing climate (<http://www.egu.eu/news/337/#cities>) with follow-up outreach at: EGU Blog: [Heat waves in cities getting worse under climate change](#), Keri McNamara May 10, 2017 Atmospheric Sciences, Climate, Conferences, EGU, EGU GA 2017, Energy, Resources and the Environment, General Assembly.
- Newsletter, Der Standard, Austria: Forscher: [Hitzebelastung in den Städten wird künftig exorbitant steigen](#).
- 
- [Press release of KU Leuven](#) and related [video](#): "Steden puffen vaker onder extreme hitte als gevolg van klimaatverandering", H. Wouters, M. Demuzere and N. Van Lipzig.
- Blogosphere of American Geophysical Union (AGU), "[Heat stress escalates in cities under global warming](#)". Outreach article on Wouters et al. (2017), Geophys. Res. Lett., 44, 1–11.

## 6.8 Posters & Presentations

- Bauwens, M., T. Stavrakou, J.-F. Müller, J. Berckmans, R. De Troch, L. De Cruz, O. Giot, R. Hamdi, P. Termonia, and B. Schaeybroeck, "Effect of climate change and CO<sub>2</sub> inhibition on isoprene emissions in Europe calculated using the ALARO-0 regional climate model", poster at EGU General Assembly, Vienna, 23–28 April 2017.
- De Troch, R., B. Van Schaeybroeck, P. Termonia, P. Willems, N. Van Lipzig, J.-P. van Ypersele, P. Marbaix, X. Fettweis, K. De Ridder, A. Gobin, T. Stavrakou, P. Luyten, E. Pottiaux,, "Combining the regional downscaling expertise in Belgium: CORDEX and beyond", poster at Belgian Geography days, 13-14 November 2015.
- Gobin A., Van Schaeybroeck B., Termonia P., Willems P., Van Lipzig N., Marbaix P., Van Ypersele J.-P., Fettweis X., De Ridder K., Stavrakou T., Luyten P., Pottiaux E., "Climate impacts on agricultural biomass production in the CORDEX.be project context", poster at European Geosciences Union General Assembly 2016, 17-22/04/2016, Vienna, Austria
- Pottiaux, E.: presentation at COST Action ES1206 GNSS4SWEC Final Workshop, ESTEC, Noordwijk, 21-23 February 2017.

- Scholzen, C., & Fettweis, X. (2016, April). First steps of the regional climate model MAR over the Euro-CORDEX domain. Paper presented at the European Geosciences Union General Assembly 2016, Vienna, Austria. <http://hdl.handle.net/2268/196182>.
- Pottiaux, E., P. Termonia, B. Van Schaeybroeck, P. Willems, N. Van Lipzig, J.-P. van Ypersele, P. Marbaix, X. Fettweis, K. De Ridder, A. Gobin, T. Stavrakou, P. Luyten, “GNSS Re-processing for the verification of Belgian High-resolution climate model runs”, poster at 2nd workshop of the COST Action ES1206, 1-15 may 2015.
- Sharma, R., Hooyberghs, H., Lauwaet, D., De Ridder, K., 2016. WUDAPT: The global database of land use at local scales – Climatological applications in the developing world; presentation at WUDAPT Workshop 2016, Chinese University of Hong Kong (CUHK), Hong Kong (5 December 2016).
- Sharma, R., Lauwaet, D., Hooyberghs, H., De Ridder, K., 2016. Boundary layer climate modeling of a tropical megacity, presentation at NAACLIM Final Meeting, Met Office, Exeter, UK (4 October 2016).
- Sharma, Richa; De Ridder, Koen; Hooyberghs, Hans; Lauwaet, Dirk, 2016. APPLICATION OF URBCLIM FOR AN ASIAN TROPICAL CITY – THE CASE OF DELHI, poster at the Living Planet Symposium 2016, Prague.
- Stavrakou, T., J.-F. Müller, M. Bauwens, J. Berckmans, S. Caluwaerts, R. De Troch, L. De Cruz, O. Giot, R. Hamdi, P. Termonia, and B. Schaeybroeck, “High resolution isoprene emission over Europe in past and future climate”, poster at EGU General Assembly, Vienna, 17-22 April, 2016.
- Termonia P., Van Schaeybroeck B., De Ridder K., Fettweis X., Gobin A., Luyten P., Marbaix P., Pottiaux E., Stavrakou T., Van Lipzig N., Van Ypersele J.-P., Willems P., “CORDEX.be: COmbining Regional climate Downscaling EXpertise in Belgium”, poster at European Geosciences Union General Assembly 2016, 17-22/04/2016, Vienna, Austria.
- Termonia P., Van Schaeybroeck B., Willems P., Van Lipzig N., Van Ypersele J.-P., Marbaix P., Fettweis X., De Ridder K., Gobin A., Stavrakou T., Luyten P., Pottiaux E., “CORDEX.be: COmbining Regional climate Downscaling EXpertise in Belgium”, presentation at The International Conference on Regional Climate ICRC-CORDEX 2016, 17-20/05/2016, Stockholm, Sweden.
- Van Schaeybroeck, B. P. Termonia, P. Willems, N. Van Lipzig, J.-P. van Ypersele, P. Marbaix, X. Fettweis, K. De Ridder, A. Gobin, T. Stavrakou, P. Luyten, E. Pottiaux, “CORDEX.be: COmbining Regional climate Downscaling EXpertise in Belgium”, poster at workshop on Uncertainty Quantification in Climate Modeling and Projection, ICTP, Trieste, Italy, 13-17 July 2015.
- Van Schaeybroeck B., Termonia P., De Ridder K., Fettweis X., Gobin A., Luyten P., Marbaix P., Pottiaux E., Stavrakou T., Van Lipzig N., Van Ypersele J.-P., Willems P., “The CORDEX.be initiative as a foundation for climate services in Belgium”, presentation at European Geosciences Union General Assembly 2017, Vienna, Austria.
- Wouters, H., Demuzere, M., Van Lipzig, N., De Ridder, K., Blahak, U. (2015). Urban parametrization for a regional climate model: applications for Belgium. MACCBET final symposium, presentation, Brussels, 1 june 2015.
- Wouters, H., H., Demuzere, M., De Ridder, K., Blahak, U., Van Lipzig, N. (2015). Modeling the seasonal dependency of contributions to urban heat islands in Belgium. International Conference on Urban Climate, poster, Toulouse, 19-24 july 2015
- Wouters, H., H., Demuzere, M., De Ridder, K., Van Lipzig, N. (2015). The impact of impervious water-storage parametrization on urban climate modeling. In : Geophysical Research Abstracts,

- 17, abstr.nr. EGU2015-9483-1. European Geosciences Union General Assembly, poster, Vienna, 12 - 17 April 2015
- Wouters, H., H., Van Lipzig, N., Poelmans, L., Willems, P., Brisson, E., De Ridder, K., Demuzere, M., Blahak, U. (2015). The impact of urban land-use change and global climate change on the heat stress in Belgium. CLM Community Assembly, presentation , Luxembourg, 29 september - 2 october 2015.
  - Wouters, H., Matthias Demuzere, Ulrich Blahak, Nicole van Lipzig, Koen De Ridder, Krzysztof Fortuniak, Bino Maiheu, Johan Camps, Daniël Tielemans, Jürgen Helmert, Gianluca Mussetti, Matthias Raschendorfer, Jan-Peter Schulz. News on TERRA\_URB, the urban land-surface parametrization of the COSMO(-CLM) model. COSMO/CLM/ART user seminar, poster, Offenbach (Germany), 7-9 march 2016.
  - Wyard, C., Fettweis, X., & Erpicum, M. (2015, April 16). Snow cover evolution during the last fifty years in the Hautes Fagnes (Belgium) using the regional climate MAR model. Paper presented at EGU General Assembly 2015, Vienna, Austria. <http://hdl.handle.net/2268/180843>.
  - Wyard, C., Fettweis, X., & Erpicum, M.. (2015, November 13). Snow cover evolution and its impact on flooding in the Ourthe River catchment (southeast of Belgium) over the period 1958--2014 using the MAR model. Paper presented at The 6th Belgian Geography Days, Etterbeek, Belgium. <http://hdl.handle.net/2268/189437>.
  - Wyard, C., & Fettweis, X. (2016, April 19). Decrease in hydroclimatic conditions generating floods in the southeast of Belgium over the last 50 years. Paper presented at European Geosciences Union General Assembly 2016, Vienna, Austria. <http://hdl.handle.net/2268/196181>.
  - Wyard, C., & Fettweis, X. (2016, June 08). The MAR model performances over Belgium. Paper presented at The 1st MAR Workshop, Liège, Belgium. <http://hdl.handle.net/2268/199021>.
  - Wyard, C., Fettweis, X., & Scholzen, C. (2016, August 29). How reliable are the models to study recent climate change? A study of heat/cold waves and radiative fluxes trends over 1900-2010 using the model MAR in Belgium. Poster session presented at 15th International Swiss Climate Summer School 2016 "Climate Risks - Coping with Uncertainties", Grindelwald, Switzerland. <http://hdl.handle.net/2268/201970>.

## 7 REFERENCES

- Acosta-Michlik L et al. (2011) Multiscalar and Multiagent Modeling Framework for Assessing Sustainable Futures in a Globalised Environment (MULTIMODE), Final Report, (BELSPO, Research Programme Science for a Sustainable Development, Brussels), Technical report.
- Ainsworth, E.A. and Long, S.P., 2005. What have we learned from 15 years of free-air CO<sub>2</sub> enrichment (FACE)? A meta-analytic review of the responses of photosynthesis, canopy properties and plant production to rising CO<sub>2</sub>. *New Phytologist*, 165(2), pp.351-372.
- ALADIN international team, 1997. The aladin project: Mesoscale modeling seen as a basic tool for weather forecasting and atmospheric research. *WMO Bull.* 46, 317–324.
- Arneth, A., Schurgers, G., Hickler, T. and Miller, P.: Effects of species composition, land surface cover, CO<sub>2</sub> concentration and climate on isoprene emissions from European forests, *Plant Biol.*, 10(1), 150-162, 2008.
- Attema, J., Bakker, A., Beersma, J., Bessembinder, J., Boers, R., Brandsma, T., van den Brink, H., Drijfhout, S., Eskes, H., Haarsma, R., et al., 2014. KNMI 14: Climate change scenarios for the 21st century—a netherlands perspective. Tech. rep., KNMI.
- Bechtold P, Bazile E, Guichard F, Mascart P, Richard E. 2001. A mass-flux convection scheme for regional and global models. *Q. J. R. Meteorol. Soc.* 127(573): 869–886, doi: 10.1002/qj.49712757309
- Beniston M. 2012. Is snow in the Alps receding or disappearing? *Wiley Interdiscip. Rev. Clim. Chang.* 3(4): 349–358, doi: 10.1002/wcc.179.
- Ban N, Schmidli J, Schär C (2014) Evaluation of the convection-resolving regional climate modeling approach in decade-long simulations. *J Geophys Res. Atmos* 119:7889–7907.
- Ban N, Schmidli J, Schär C (2015) Heavy precipitation in a changing climate: Does short-term summer precipitation increase faster? *Geophys Res Lett* 42:2014GL062588.
- Best, M., Beljaars, A., Polcher, J., Viterbo, P., 2004. A proposed structure for coupling tiled surfaces with the planetary boundary layer. *Journal of Hydrometeorology* 5 (6), 1271–1278.
- Blahak, U., 2011: Towards a better representation of high density ice particles in a state-of-the-art two-moment bulk microphysical scheme. *Proc. 15th Int. Conf. Clouds and Precip., Cancun, Mexico. 2008.*
- Bolaños, R., P. Osuna, J. Wolf, J. Monbaliu, A. Sanchez-Arcilla: Development of the POLCOMS-WAM current-wave model, *Ocean Modeling*, 36, 102-115, 2011
- Brasseur, G. P., Gallardo, L., 2016. Climate services: Lessons learned and future prospects. *Earth's Future* 4 (3), 79–89. 14.
- Brisson, E., Demuzere, M., Kwakernaak, B., Van Lipzig, N., 2011. Relations between atmospheric circulation and precipitation in Belgium. *Meteorology and Atmospheric Physics* 111 (1-2), 27–39.
- Brouwers, J., Peeters, B., Van Steertegem, M., van Lipzig, N., Wouters, H., Beullens, J., Demuzere, M., Willems, P., De Ridder, K., Maiheu, B., De Troch, R., Termonia, P., Vansteenkiste, T., Craninx, M., Maetens, W., Defloor, W., Cauwenberghs, K., 2015. MIRA Klimaatrapport 2015, over waargenomen en toekomstige klimaatveranderingen. Flemish Environment Agency - Vlaamse Milieumaatschappij (VMM).

- Brun É, David P, Sudul M, Brunot G. 1992. A numerical model to simulate snow-cover stratigraphy for operational avalanche forecasting. *J. Glaciol.* 38(128): 13–22.
- Bubnova, R., Hello, G., Bénard, P., Geleyn, J.-F., 1995. Integration of the fully elastic equations cast in the hydrostatic pressure terrain-following coordinate in the framework of the ARPEGE/ALADIN NWP system. *Monthly Weather Review* 123 (2), 515–535.
- Catry, B., Geleyn, J.-F., Tudor, M., Bénard, P., Trojakova, A., 2007. Flux-conservative thermodynamic equations in a mass-weighted framework. *Tellus A* 59 (1), 71–79.
- Chan SC, Kendon EJ, Fowler HJ, et al (2014a) Projected increases in summer and winter UK sub-daily precipitation extremes from high-resolution regional climate models. *Environ Res Lett* 9:084019.
- Chan SC, Kendon EJ, Fowler HJ, et al (2014b) The Value of High-Resolution Met Office Regional Climate Models in the Simulation of Multihourly Precipitation Extremes. *J Climate* 27:6155–6174.
- Christensen, O., Gutowski, W., Nikulin, G., Legutke, S., 2012. Cordex archive design, version 3.1, 3 march 2014. Tech. rep., Danish Meteorological Institute. [URL](#).
- Dee, D., Uppala, S., Simmons, A., Berrisford, P., Poli, P., Kobayashi, S., Andrae, U., Balmaseda, M., Balsamo, G., Bauer, P. et al.: The ERA-Interim reanalysis: Configuration and performance of the data assimilation system, *Quarterly Journal of the Royal Meteorological Society*, 137(656), 553–597, 2011.
- Delvaux, C., M. Journée and C. Bertrand, 2015: The FORBIO Climate data set for climate analyses. *Adv. Sci. Res.*, 12: 103-109.
- De Ridder K, Gallée H. 1998. Land surface-induced regional climate change in southern Israel. *J. Appl. Meteorol.* 37: 1470–1485.
- De Ridder, K., Lauwaet, D., Maiheu, B., 2015. Urbclim a fast urban boundary layer climate model. *Urban Climate* 12, 21–48.
- De Wit MJM, Peeters HA, Gastaud PH, Dewil P, Maeghe K, Baumgart J. 2007. Floods in the Meuse basin: event descriptions and an international view on ongoing measures. *Int. J. River Basin Manage.* 5(4): 279–292, doi:10.1080/15715124.2007.9635327.
- Diffenbaugh, N. S., J. S. Pal, R. J. Trapp, and F. Giorgi, 2005: Fine-scale processes regulate the response of extreme events to global climate change. *Proc. Natl. Acad. Sci.*, 102, 15774–15778.
- Dilling, L., and M.C. Lemos, 2011. Creating usable science: opportunities and constraints for climate knowledge use and their implications for science policy. *Global Environmental Change.* 21(2): 680-689.
- Dimitrova, R. et al. Assessment of Planetary Boundary-Layer Schemes in the Weather Research and Forecasting Mesoscale Model Using MATERHORN Field Data. *Boundary-Layer Meteorology* 159, 589–609 (2016).
- Doutreloup, S., Wyard, C., Belleflamme, A., François, L., Fettweis, X., & Erpicum, M. (2017). Évaluation de la capacité du Modèle Atmosphérique Régional (MAR) à simuler la saison des pluies en Afrique Intertropicale. In S., Dahech & S., Charfi (Eds.), *Actes du XXXe colloque de l'Association Internationale de Climatologie : CLIMAT, VILLE ET ENVIRONNEMENT* (pp. 389-395). <http://hdl.handle.net/2268/213232>.
- Dyrddal AV, Saloranta T, Skaugen T, Strandén HB. 2013. Changes in snow depth in Norway during the period 1961-2010. *Hydrol. Res.* 44: 169–179, doi: 10.2166/nh.2012.064.

- Fettweis, X., Franco, B., Tedesco, M., van Angelen, J. H., Lenaerts, J. T. M., van den Broeke, M. R., and Gallée, H.: Estimating the Greenland ice sheet surface mass balance contribution to future sea level rise using the regional atmospheric climate model MAR, *The Cryosphere*, 7, 469-489, 2013.
- Fettweis, X., Wyard, C., Doutreloup, S., Belleflamme, A: Noël 2010 en Belgique : Neige en Flandre et pluie en Haute-Ardenne, *Bulletin de la Société Géographique de Liège* (accepted). *Bulletin de la Société géographique de Liège* 68 (2017).
- Fettweis X, Wyard C, Doutreloup S, Belleflamme A. 2017b. Noël 2010 en Belgique : Neige en Flandre et pluie en Haute-Ardenne, *Bulletin de la Société Géographique de Liège* (accepted). *Bulletin de la Société géographique de Liège* 68.
- Fonteyn, D., 2013. Het federaal klimaatcentrum: Resultaten van het onderzoek naar de mogelijke gebruikersnoden. Tech. rep., Belgian Institute for Space Aeronomy.
- Fosser G, Khodayar S, Berg P (2014) Benefit of convection permitting climate model simulations in the representation of convective precipitation. *Clim Dyn* 44:45–60.
- Fosser G, Khodayar S, Berg P (2017) Climate change in the next 30 years: What can a convection-permitting model tell us that we did not already know? *Clim Dyn* 48:1987–2003.
- Gallée H. 1995. Simulation of the mesocyclonic activity in the Ross Sea, Antarctica. *Mon. Wea. Rev.* 123: 2051–2069. Gallée H, Schayes G. 1994. Development of a three-dimensional meso-primitive equation model: katabatic winds simulation in the area of Terra Nova Bay, Antarctica. *Mon. Weather Rev.* 122: 671–685.
- Gallée H, Guyomarch G, Brun E. 2001. Impact of snow drift on the Antarctic ice sheet surface mass balance: possible sensitivity to snow-surface properties. *Bound.-Layer Meteorol.* 99(1): 1–19, doi:10.1023/A:1018776422809.
- Gallée H, Moufouma-Okia W, Bechtold P, Brasseur O, Dupays I, Marbaix P, Messenger C, Ramel R, Lebel T. 2004. A high-resolution simulation of a West African rainy season using a regional climate model. *J. Geophys. Res.* 109: D05108, doi: 10.1029/2003JD004020.
- Geleyn, J.-F., Catry, B., Bouteloup, Y., Brozková, R., 2008. A statistical approach for sedimentation inside a microphysical precipitation scheme. *Tellus A* 60 (4), 649–662.
- Gerard, L., 2007. An integrated package for subgrid convection, clouds and precipitation compatible with meso-gamma scales. *Quarterly Journal of the Royal Meteorological Society* 133 (624), 711–730.
- Gerard, L., Geleyn, J.-F., 2005. Evolution of a subgrid deep convection parametrization in a limited-area model with increasing resolution. *Quarterly Journal of the Royal Meteorological Society* 131 (610), 2293–2312.
- Giorgetta, M. A., J. H. Jungclaus, C. H. Reick, S. Legutke, J. Bader, M. Böttinger, V. Brovkin, T. Crueger, M. Esch, K. Fieg, K. Glushak, V. Gayler, H. Haak, H.-D. Hollweg, T. Ilyina, S. Kinne, L. Kornblueh, D. Matei, T. Mauritsen, U. Mikolajewicz, W. Mueller, D. Notz, F. Pithan, T. Raddatz, S. Rast, R. Redler, E. Roeckner, H. Schmidt, R. Schnur, J. Segschneider, K. D. Six, M. Stockhause, C. Timmreck, J. Wegner, H. Widmann, K.-H. Wieners, M. Claussen, J. Marotzke, and B. Stevens, “Climate and carbon cycle changes from 1850 to 2100 in MPI-ESM simulations for the coupled model intercomparison project phase 5,” *J. Adv. Model. Earth Syst.*, vol. 5, no. 3, pp. 572–597, 2013.
- Giorgi, F., Jones, C., Asrar, G. R., et al., 2009. Addressing climate information needs at the regional level: the cordex framework. *WMO Bull.* 58 (3), 175.

- Gobin, A., 2010. Modeling climate impacts on crop yields in Belgium. *Climate Research* 44 (1), 55.
- Gobin, A., 2012. Impact of heat and drought stress on arable crop production in Belgium. *Natural Hazards and Earth System Science* 12 (6), 1911–1922.
- Gobin, A., 2017. Weather related risks in Belgian arable agriculture. *Agricultural Systems*. <https://doi.org/10.1016/j.agsy.2017.06.009>.
- Guenther, A. B., Jiang, X., Heald, C. L., Sakulyanontvittaya, T., Duhl, T., Emmons, L. K., and Wang, X.: The Model of Emissions of Gases and Aerosols from Nature version 2.1 (MEGAN2.1): an extended and updated framework for modeling biogenic emissions, *Geosci. Model Dev.*, 5, 1471–1492, 2012.
- Guenther, A., Karl, T., Harley, P., Wiedinmyer, C., Palmer, P. I. and Geron, C.: Estimates of global terrestrial isoprene emissions using MEGAN (Model of Emissions of Gases and Aerosols from Nature), *Atmos. Chem. Phys.*, 6(11), 3181–3210, 2006.
- Günther, H., S. Hasselmann, P.A.E.M. Janssen: The WAM model cycle 4 , 1992
- Hamdi, R., Masson, V., 2008. Inclusion of a drag approach in the town energy balance (teb) scheme: Oine 1d evaluation in a street canyon. *Journal of Applied Meteorology and Climatology* 47 (10), 2627–2644.
- Hamdi, R., Vyver, H., Troch, R., Termonia, P., 2014. Assessment of three dynamical urban climate downscaling methods: Brussels’s future urban heat island under an A1B emission scenario. *International Journal of Climatology* 34 (4), 978–999.
- Heald, C. L., Wilkinson, M. J., Monson, R. K., Alo, C. A., Wang, G. and Guenther, A.: Response of isoprene emission to ambient CO<sub>2</sub> changes and implications for global budgets, *Global Change Biology*, 15(5), 1127–1140, 2009.
- Hewitt, C., Mason, S., Walland, D., 2012. The global framework for climate services. *Nature Climate Change* 2 (12), 831–832.
- Jacob, D., Petersen, J., Eggert, B., Alias, A., Christensen, O. B., Bouwer, L. M., Braun, A., Colette, A., Déqué, M., Georgievski, G., et al., 2014. Euro-cordex: new high-resolution climate change projections for European impact research. *Regional Environmental Change* 14 (2), 563–578.
- Journée, M., Delvaux, C., Bertrand, C., 2015. Precipitation climate maps of Belgium. *Advances in Science and Research* 12 (1), 73–78.
- Kalnay E, Kanamitsu M, Kistler R, Collins W, Deaven D, Gandin L, Iredell M, Saha S, White G, Woollen J, Zhu Y, Leetmaa A, Reynolds B, Chelliah M, Ebisuzaki W, Higgins W, Janowiak J, Mo K, Ropelewski C, Wang J, Jenne R, Joseph D. 1996. The NCEP/NCAR 40-year reanalysis project. *Bull. Am. Meteorol. Soc.* 77: 437–471.
- Katragkou, E., Zanis, P., Kioutsioukis, I., Tegoulas, I., Melas, D., Krüger, B. and Coppola, E.: Future climate change impacts on summer surface ozone from regional climate-air quality simulations over Europe, *J. Geophys. Res.*, 116(D22), 2011.
- Kay AL. 2016. A review of snow in Britain: the historical picture and future projections. *Prog. Phys. Geogr.* : 1–23, doi: 10.1177/0309133316650617.
- Kendon EJ, Roberts NM, Senior CA, Roberts MJ (2012) Realism of Rainfall in a Very High-Resolution Regional Climate Model. *J Climate* 25:5791–5806.
- Kendon EJ, Roberts NM, Fowler HJ, et al (2014) Heavier summer downpours with climate change revealed by weather forecast resolution model. *Nature Clim Change* 4:570–576.

- Kettle, A.J.: Review Article: Storm Britta in 2006: offshore damage and large waves in the North Sea, *Natural Hazards and Earth System Sciences*, 3, 5493-5510, 2015.
- Kotlarski, S., Keuler, K., Christensen, O. B., Colette, A., Déqué, M., Gobiet, A., Goergen, K., Jacob, D., Lüthi, D., van Meijgaard, E., et al., 2014. Regional climate modeling on european scales: a joint standard evaluation of the EURO-CORDEX rcm ensemble. *Geoscientific Model Development*
- Lauwaet, D., Hooyberghs, H., Maiheu, B., Lefebvre, W., Driesen, G., Van Looy, S., De Ridder, K., 2015. Detailed urban heat island projections for cities worldwide: Dynamical downscaling CMIP5 global climate models. *Climate* 3 (2), 391–415.
- Le Moigne, P., Boone, A., Calvet, J., Decharme, B., Faroux, S., Gibelin, A., 2009. Surfex scientific documentation. Note de centre (CNRM/GMME), Météo-France, Toulouse, France.
- Lemonsu, A., Grimmond, C., Masson, V., 2004. Modeling the surface energy balance of the core of an old mediterranean city: Marseille. *Journal of Applied Meteorology* 43 (2), 312–327.
- Lesk, C., Rowhani, P. and Ramankutty, N., 2016. Influence of extreme weather disasters on global crop production. *Nature*, 529(7584), pp.84-87.
- Luyten, P., 2011. Coherens - a coupled hydrodynamical-ecological model for regional and shelf seas: User documentation version 2.0. RBINS MUMM Report, Royal Belgian Institute of Natural Sciences.
- Luyten, P. : A Coupled hydrodynamical-ecological model for regional and shelf seas, User documentation version 2.5.1, 2013
- Masson, V., 2000. A physically-based scheme for the urban energy budget in atmospheric models. *Boundary-layer meteorology* 94 (3), 357–397.
- Masson, V., Champeaux, J.-L., Chauvin, F., Meriguet, C., Lacaze, R., 2003. A global database of land surface parameters at 1-km resolution in meteorological and climate models. *Journal of climate* 16 (9), 1261–1282.
- Masson, V., Grimmond, C., Oke, T. R., 2002. Evaluation of the town energy balance (teb) scheme with direct measurements from dry districts in two cities. *Journal of applied meteorology* 41 (10), 1011–1026.
- Masson, V., Le Moigne, P., Martin, E., Faroux, S., Alias, A., Alkama, R., Belamari, S., Barbu, A., Boone, A., Bouyssel, F., et al., 2013. The surfexv7. 2 land and ocean surface platform for coupled or one simulation of earth surface variables and fluxes. *Geoscientific Model Development* 6, 929–960.
- Meehl, G. A., J. M. Arblaster, and C. Tebaldi, 2005: Understanding future patterns of increased precipitation intensity in climate model simulations. *Geophys. Res. Lett.*, **32**, 1–4.
- Meleux, F., Solmon, F. and Giorgi, F.: Increase in summer European ozone amounts due to climate change, *Atmos. Environ.*, 41(35), 7577–7587, 2007.
- Milbrandt, J. A., and M. K. Yau, 2005: A Multimoment Bulk Microphysics Parameterization. Part I: Analysis of the Role of the Spectral Shape Parameter. *J. Atmos. Sci.*, 62, 3051–3064.
- Monbaliu, J., R. Padilla-Hernandez, J.C. Hargreaves, J.C. Carretero Albiach, W. Luo, M. Sclavo, H. Günther: The spectral wave model, WAM, adapted for applications with high spatial resolution, *Coastal Engineering*, 41, 41-62, 2000
- Müller, J.-F., Stavrakou, T., Wallens, S., De Smedt, I., Van Roozendael, M., Potosnak, M. J., Rinne, J., Munger, B., Goldstein, A. and Guenther, A. B.: Global isoprene emissions estimated

- using MEGAN, ECMWF analyses and a detailed canopy environment model, *Atmos. Chem. Phys.*, 8(5), 1329–1341, 2008.
- Myneni, R.B., Keeling, C.D., Tucker, C.J., Asrar, G. and Nemani, R.R., 1997. Increased plant growth in the northern high latitudes from 1981 to 1991. *Nature*, 386(6626), p.698.
  - Noilhan, J., Planton, S., 1989. A simple parameterization of land surface processes for meteorological models. *Monthly Weather Review* 117 (3), 536–549.
  - Pauquet A, Petit F. 1993. Évolution et fréquence des inondations de l’Ourthe inférieure. *Bulletin de la Société Belge d’Etudes Géographiques*. 62(2): 361–375.
  - Poli P, Hersbach H, Tan D, Dee D, Thépaut J-N, Simmons A, Peubey C, Laloyaux P, Komori T, Berrisford P, Dragani R, Trémolet Y, Holm E, Bonavita M, Isaksen L, Fisher M. 2013. The data assimilation system and initial performance evaluation of the ECMWF pilot reanalysis of the 20th-century assimilating surface observations only (ERA-20C). ERA Report Series 14. (accessed 1 May 2016).
  - Possell, M. and Hewitt, C. N.: Isoprene emissions from plants are mediated by atmospheric CO<sub>2</sub> concentrations, *Global Change Biology*, 17(4), 1595–1610, 2011.
  - Rockel, B., A. Will, and A. Hense, “The regional climate model COSMO-CLM (COSMO-CLM),” *Meteorol. Zeitschrift*, vol. 17, no. 4, pp. 347–348, 2008.
  - Sanchez-Lorenzo, A., Wild, M. and Trentmann, J.: Validation and stability assessment of the monthly mean CM SAF surface solar radiation dataset over Europe against a homogenized surface dataset (1983–2005), *Remote Sens. Environ.*, 134, 355–366, 2013.
  - Segal, Y., and A. Khain, 2006: Dependence of droplet concentration on aerosol conditions in different cloud types: Application to droplet concentration parameterization of aerosol conditions. *J. Geophys. Res. Atmos.*, 111.
  - Seifert, A., and K. D. Beheng, 2006: A two-moment cloud microphysics parameterization for mixed-phase clouds. Part 2: Maritime vs. continental deep convective storms. *Meteorol. Atmos. Phys.*, 92, 67–82.
  - Smiatek, G., Rockel, B. & Schättler, U. Time invariant data preprocessor for the climate version of the COSMO model (COSMO-CLM). *Meteorologische Zeitschrift* 17, 395–405 (2008).
  - Sneyers, R., Vandiepenbeeck, M., Vanlierde, R., 1989. Principal component analysis of Belgian rainfall. *Theoretical and applied Climatology* 39 (4), 199–204.
  - Stavrakou, T., J.-F. Müller, M. Bauwens, I. De Smedt, M. Van Roozendaal, A. Guenther, M. Wild, and X. Xia, Isoprene emissions over Asia 1979-2012 : impact of climate and land use changes, *Atmos. Chem. Phys.*, 14, 4587-4605, 2014.
  - Stocker, T., Qin, D., Plattner, G.-K., Tignor, M., Allen, S. K., Boschung, J., Nauels, A., Xia, Y., Bex, V., Midgley, P. M., 2014. *Climate change 2013: The physical science basis*. Cambridge University Press Cambridge, UK, and New York.
  - Schulz, J.-P., and G. Vogel (2017), An improved representation of the land surface temperature including the effects of vegetation in the COSMO model, in *Geophysical Research Abstracts*, pp. 19, EGU2017–7896, European Geosciences Union General Assembly, Vienna.
  - Taylor, K. E., Stouffer, R. J., Meehl, G. A., 2012. An overview of cmip5 and the experiment design. *Bulletin of the American Meteorological Society* 93 (4), 485.

- Tebaldi, C., K. Hayhoe, J. M. Arblaster, and G. A. Meehl, 2007: Going to the extremes. *Clim. Change*, 82, 233–234.
- Termonia, P., Deckmyn, A., Hamdi, R., 2009. Study of the lateral boundary condition temporal resolution problem and a proposed solution by means of boundary error restarts. *Monthly Weather Review* 137 (10), 3551–3566.
- Termonia, P., Voitus, F., Degrauwe, D., Caluwaerts, S., Hamdi, R., 2012. Application of boyd’s periodization and relaxation method in a spectral atmospheric limited-area model. part i: Implementation and reproducibility tests. *Monthly Weather Review* 140 (10), 3137–3148.
- Termonia, P., Fischer, C., Bazile, E., Bouyssel, F., Brožková, R., Bénard, P., Bochenek, B., Degrauwe, D., Derkova, M., El Khatib, R., Hamdi, R., Mašek, J., Pottier, P., Pristov, N., Seity, Y., Smolíková, P., Spaniel, O., Tudor, M., Wang, Y., Wittmann, C., and Joly, A.: The ALADIN System and its Canonical Model Configurations AROME CY41T1 and ALARO CY40T1, *Geosci. Model Dev. Discuss.*, in review, 2017.
- Uppala, S. et al. (2005). The ERA-40 re-analysis. *Quarterly Journal of the royal meteorological society*, 131 (612), 2961-3012..
- Van de Vyver, H., 2012. Spatial regression models for extreme precipitation in belgium. *Water Resources Research* 48 (9).
- Van Meijgaard, E., 1995. Excessive rainfall over the belgian ardennes in december 1993: evaluation of model predictions. *Meteorological Applications* 2 (1), 39–52.
- Van Vuuren, Detlef P., et al. "A new scenario framework for climate change research: scenario matrix architecture." *Climatic Change* 122.3 (2014): 373-386.
- Van Weverberg, K., E. Goudenhoofdt, U. Blahak, E. Brisson, M. Demuzere, P. Marbaix, and J.-P. van Ypersele, 2014: Comparison of one-moment and two-moment bulk microphysics for high-resolution climate simulations of intense precipitation. *Atmos. Res.*, 147-148, 145–161.
- van Ypersele, J.-P., Marbaix, P., 2004. Impact van de klimaatverandering in België. Greenpeace.
- Vana, F., Bénard, P., Geleyn, J.-F., Simon, A., Seity, Y., 2008. Semi-lagrangian advection scheme with controlled damping: An alternative to nonlinear horizontal diffusion in a numerical weather prediction model. *Quarterly Journal of the Royal Meteorological Society* 134 (631),
- WAMDI Group, The WAM model – A third generation ocean wave prediction model, *Journal of Physical Oceanography*, 18, 1775-1810, 1988.
- Wiedinmyer, C., Tie, X., Guenther, A., Neilson, R. and Granier, C.: Future changes in biogenic isoprene emissions: how might they affect regional and global atmospheric chemistry? *Earth Interactions*, 10(3), 1–19, 2006.
- Wilkinson, M. J., Monson, R. K., Trahan, N., Lee, S., Brown, E., Jackson, R. B., Polley, H. W., Fay, P. A. and Fall, R.: Leaf isoprene emission rate as a function of atmospheric CO<sub>2</sub> concentration, *Global Change Biology*, 15(5), 1189–1200, 2009.
- Witt, A., M. D. Eilts, G. J. Stumpf, J. T. Johnson, E. D. W. Mitchell, and K. W. Thomas, 1998: An Enhanced Hail Detection Algorithm for the WSR-88D. *Weather Forecast.*, 13, 286–303.
- Wu, S., Mickley, L. J., Kaplan, J. and Jacob, D. J.: Impacts of changes in land use and land cover on atmospheric chemistry and air quality over the 21st century, *Atmospheric Chemistry and Physics*, 12(3), 1597–1609, 2012.

- Young, P., Arneth, A., Schurgers, G., Zeng, G. and Pyle, J. A.: The CO<sub>2</sub> inhibition of terrestrial isoprene emission significantly affects future ozone projections, *Atmos. Chem. Phys.*, 9(8), 2793–2803, 2009.
- Zamani, S., Gobin, A., Van de Vyver, H., Gerlo, J., 2016. Atmospheric drought in Belgium – statistical analysis of precipitation deficit. *International Journal of Climatology* 36 (8), 3056–3071.

## ACKNOWLEDGEMENTS

We acknowledge the interactions and support from Martine Vanderstraeten (BELSPO), the CORDEX.be follow-up Committee and discussions with and comments from Bart van den Hurk, Daniela Jacob and Dominique Fonteyn. Claire Colin and Johan Brouwers in particular are thanked for suggesting two case studies and the help with the stakeholder meeting. Sonia Vanderhoeven, Etienne Branquard, Jozefien Hermy and Anneloes Van Noordt are acknowledged for interactions concerning the planning of the case studies. The computational resources and services for the RMI were provided by the VSC (Flemish Supercomputer Center), funded by the Hercules Foundation and the Flemish Government – department EWI. The financial support and the computational resources provided by the Solar-Terrestrial Center of Excellence (STCE) to ROB are acknowledged.

We acknowledge the World Climate Research Programme’s Working Group on Coupled Modeling, which is responsible for CMIP, and we thank the climate modeling groups for producing and making available their model output. For CMIP the U.S. Department of Energy’s Program for Climate Model Diagnosis and Intercomparison provides coordinating support and led development of software infrastructure in partnership with the Global Organization for Earth System Science Portals. We also acknowledge the CLM-community for the developing COSMO-CLM model, and for providing the model code and the EURO-CORDEX boundary conditions. In addition, we are grateful to the World Climate Research Programme (WRCP) for initiating and coordinating the EURO-CORDEX initiative, ECMWF for providing access to the ERA-Interim dataset, the EU-FP6 [project ENSEMBLES](#) and the data providers in the [ECA&D project](#) for making the E-OBS dataset publicly available. We particularly thank Bino Maiheu for coordinating the urban-climate observations for Antwerp, and for providing the data. We also acknowledge Flemish Government through a contract as an FWO (Fund for Scientific Research) post-doctoral position, and from the EU-H2020 programme through the BRIGAD - BRIdges the GAp for Innovations in Disaster resilience project. The computational resources and services used for the downscaling were provided by the Hercules Foundation and the Flemish Government (department Economics, Sciences and Innovation – EWI).

## DATA AVAILABILITY

CORDEX data are centrally archived and publicly available from the international data hub of the Earth System Grid Federation ([ESGF](#)). This includes part of the ALARO-0 data from RMI data. All RCM and H-Res CORDEX.be data is centralized at the RMI and can be provided upon request via email ([cordex@meteo.be](mailto:cordex@meteo.be)). The data of the Local-Impact Model (LIM) simulations are high-resolution past and future time series including. The data for biogenic emissions, which can be downloaded [here](#).

## ANNEXES

### Annex A: The main technical features of the Regional Climate Models

Model name	Important reference	Resolution	Nr. vertical levels	Time step (s)	Important scheme	Focal time series / severity index	Host GCM	Non-hydrostatic
<b>ALARO-0</b>	De Troch et al. (2013); Giot et al. (2016).	RCM: 50 km and 12.5 km; H-Res: 4 km	46	900 (50 km); 300 (12.5 km); 180 (4 km)	Cloud scheme: 3MT	Hourly precipitation	CNRM-CM5	-
<b>COSMO-CLM (UCL) V. 5.0-CLM6</b>	Kotlarski et al. (2014)	H-Res: 2.8 km	40	20	Microphysics scheme	Hail mixing ratio and number concentration, detailed precipitation	MPI-ESM	✓
<b>COSMO-CLM V. 6.0-CLM6 +TERRA_URB V. 2.0</b>	Rockel et al. (2008); Wouters et al., (2016).	RCM: 12.5 km; H-Res: 2.8 km	40	80 (12.5 km); 20 (2.8 km)	Standard physics parameterization of CLIMAQs + urban parameterization	Precipitation, UHI	EC-EARTH	✓
<b>MAR V. 3.6</b>	Wyard et al. (2017)	H-Res: 5 km	30		Snow variables	Snowfall events and snowmelt events inducing floods	NorESM1, MIROC5 and CanESM2	-

**Annex B: The main technical features of the Local-Impact Models**

Name Model	Type of model	Important reference	Spatial resolution	Time series / severity index	Coupling to models
<b>COHERENS</b>	Storm model	Luyten (2011)	1 km	Tides and storm surges	ALARO-0
<b>MEGAN-MOHYCAN</b>	Vegetation emission model	Guenther et al. (2006); Müller et al. (2008)	10 km	Biogenic emissions, local ozone production index	ALARO-0
<b>REGCROP</b>	Crop model	Gobin (2010, 2012)	-	Crop yield, HI, DI, WI	ALARO-0
<b>SURFEX</b>	Urban model	Masson et al. (2013)	1 km	UHI	ALARO-0, COSMO
<b>UrbClim</b>	Urban model	De Ridder et al. (2015)	0.1 km	UHI and UTCI	ALARO-0
<b>WAM</b>	Wave model	Günther et al. (1992)	1 km	Wave heights	ALARO-0

### Annex C: Additional features and of High-resolution climate models for Belgium

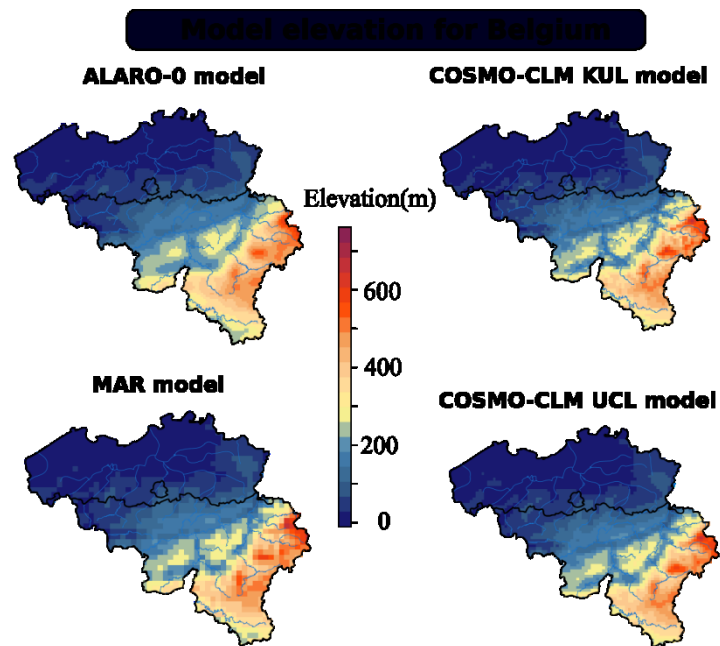


Figure 67: Model elevation for the different H-Res models over Belgium

## Annex D: Abbreviations used in this report

Abbreviation	Description
<b>ALADIN</b>	Aire Limitée Adaptation Dynamique développement INternational
<b>AR5</b>	Fifth Assessment Report of the Intergovernmental Panel on Climate Change
<b>ARPEGE</b>	Action de Recherche Petite Echelle Grande Echelle
<b>BELSP0</b>	Belgian Science Policy
<b>CLM</b>	Community Land Model
<b>CMIP5</b>	Coupled Model Intercomparison Project Phase 5
<b>CNRM</b>	Centre National de Recherches Météorologiques
<b>COHERENS</b>	Coupled Hydrodynamical-Ecological Model for Regional and Shelf Seas
<b>CORDEX</b>	COordinated Regional climate Downscaling EXperiment
<b>COSMO</b>	COnsortium for Small-scale Modeling
<b>DI</b>	Drought Index
<b>ECC</b>	Ensemble Copula Coupling
<b>ECMWF</b>	European Center for Medium-Range Weather Forecasts
<b>ERA-Interim</b>	Global atmospheric reanalysis data from 1979
<b>ESGF</b>	Earth System Grid Federation ( <a href="#">ESGF</a> )
<b>GCM</b>	Global Climate Model
<b>GNSS</b>	Global Navigation Satellite System
<b>HI</b>	Heat Index
<b>H-Res</b>	High Resolution
<b>H-Res runs</b>	Here defined as the high-resolution simulations over a domain over Belgium
<b>IFS</b>	Integrated Forecast System of ECMWF
<b>IPCC</b>	Intergovernmental Panel on Climate Change
<b>ISBA</b>	Interactions between Soil, Biosphere, and Atmosphere
<b>IWV</b>	Integrated Water Vapor
<b>LAM</b>	Limited Area Model
<b>LBC</b>	Lateral Boundary Condition
<b>LIM</b>	Local-Impact Model
<b>MEGAN</b>	Model of Emissions of Gases and Aerosols from Nature
<b>MOHYCAN</b>	MOdel of HYdrocarbon Emissions from the CANop
<b>MOS</b>	Model Output Statistics
<b>MPI</b>	Max Planck Institute
<b>NWP</b>	Numerical Weather Prediction
<b>RCM</b>	Regional Climate Model
<b>RCM runs</b>	Here defined as the 50-km and 12.5-km CORDEX simulations over Europe
<b>RCP</b>	Representative Concentration Pathway
<b>SISVAT</b>	Soil Ice Snow Vegetation Atmosphere Transfer
<b>SURFEX</b>	SURface EXternalisée, surface model from Météo-France
<b>TEB</b>	Town Energy Balance
<b>UHI</b>	Urban Heat Island (effect)
<b>UTCI</b>	Universal Thermal Climate Index
<b>VMM</b>	Vlaamse Milieu Maatschappij or Flemish Institute for Environment
<b>WG</b>	Working Group
<b>WI</b>	Wetness Index
<b>ZTD</b>	Zenith tropospheric Total Delay

## Annex E: COSMO-CLM Hierarchical overview and computational resources

An overview of the different EURO-CORDEX and H-Res simulations of the KU Leuven described in the previous sections is given in Table 6. A substantial amount of computational resources were required for the simulations, which could only be done on a parallel super-computer infrastructure. This was done by means of the VSC TIER1 MUK cluster at the UGent. The 3D output fields require a total storage of 250TB, which are kept available at the KU Leuven. The most essential data are exported to the CORDEX.be archive according to the CORDEX.be output stream specifications, requiring a total storage of 10TB.

Table 6: Overview of the COSMO-CLM model climate simulations by the KU Leuven.

Simulation ID	Domain [res.]	Time-span	Land-use	Boundary conditions
<b>ERA-CLM-EU</b>	EU [0.11°]	1980-2014	COSMO Default	ERA-INTERIM
↳ <b>ERA-CLM-BE2000</b>	BE [0.025°]	1980-2014	Urbanization 2000	ERA-CLM-EU011
↳ <b>ERA-CLM-BE2060</b>	BE [0.025°]	1980-2014	Urbanization 2060	ERA-CLM-EU011
↳ <b>ERA-CLM-BEVEGS</b>	BE [0.025°]	1980-2014	Vegetation scen.	ERA-CLM-EU011
<b>ECECTL-CLM-EU</b>	EU [0.11°]	1980-2014	COSMO Default	ECEARTH RCP8.5
↳ <b>ECECTL-CLM-BE2000</b>	BE [0.025°]	1976-2005	Urbanization 2000	ECECTL-CLM-EU
<b>ECEFUT-CLM-EU</b>	EU [0.11°]	2071-2100	COSMO Default	ECEARTH RCP8.5
↳ <b>ECEFUT-CLM-BE2000</b>	BE [0.025°]	2071-2100	Urbanization 2000	ECEFUT-CLM-EU

**Annex F: Exchange of meteorological data among the different models**

MODEL	Spatial Resolution Domain	Input Variables requested	Cordex Long Name	CORDEX Standard Name	CORDEX abbreviation	Units	CORDEX availability	Temporal resolution requested	Level of variable
<b>MEGAN</b>  + <b>MOHYCAN</b> <b>(BIRA=P7)</b>	EURO-CORDEX  (12.5 km)	Temperature	Near-Surface Air Temperature	air_temperature	tas	K	Tier 2 (3h)	1-hourly	2m
		Dewpoint Temperature	Near-Surface Specific Humidity	specific_humidity	huss	1	Tier 2 (3h)		10m
		U wind	Eastward Near-Surface Wind	eastward_wind	uas	m/s	Tier 2 (6h)		10m
		V wind	Northward Near-Surface Wind	northward_wind	vas	m/s	Tier 2 (6h)		10m
		Downward short-wave radiation	Surface Downwelling Shortwave Radiation	surface_downwelling_shortwave_flux_in_air	rsds	W/m <sup>2</sup>	Tier 2 (3h)		surface
		Pressure	Surface Air Pressure	surface air_pressure	ps	Pa	Tier 2 (3h)		surface

		Total Cloud Cover	Total Cloud Fraction	cloud_area_fraction	clt	%	Tier 2 (3h)	3-hourly	column
		Soil moisture content	Total Soil Moisture Content	soil_moisture_content	mrso	Kg/ m <sup>2</sup>	Tier 2 (6h)	3-hourly	surface
<b>COHERENS + WAM (P8)</b>	EURO-CORDEX (12.5 km)	U wind	Eastward Near-Surface Wind	eastward_wind	uas	m/s	Tier 2 (6h)	3-hourly	10m
		V wind	Northward Near-Surface Wind	northward_wind	vas	m/s	Tier 2 (6h)		
		Pressure	Surface Air Pressure	surface_air_pressure	ps	Pa	Tier 2 (3h)	3-hourly	surface
<b>RMI request (C)</b>	all	U wind	Eastward Near-Surface Wind	eastward_wind	uas	m/s	Tier 2 (6h)	3-hourly	10m,6km if possible 1km,3km
		V wind	Northward Near-Surface Wind	northward_wind	vas	m/s	Tier 2 (6h)		
		CAPE							column

MODEL	Spatial Resolution Domain	Variables	Cordex Long Name	CORDEX Standard Name	CORDEX abbreviation	Units	CORDEX availability	Temporal resolution	Level of variable
<b>URBCLIM (VITO -P6)</b>	H-Res over Belgium (±5 km)	Downward short-wave radiation	Surface Downwelling Shortwave Radiation	surface_downwelling_shortwave_flux_in_air	rsds	W/ m <sup>2</sup>	Tier 2 (3h)	3-hourly	surface
		Downward long-wave radiation	Surface Downwelling Longwave Radiation	surface_downwelling_longwave_flux_in_air	rlds	W/ m <sup>2</sup>	Tier 2 (3h)		
		Surface air pressure	Surface Air Pressure	surface_air_pressure	ps	Pa	Tier 2 (3h)		
		Precipitation	Precipitation	precipitation_flux	pr	Kg/m <sup>2</sup> /s	Tier 2 (3h)		
		Large-scale precipitation				Kg/m <sup>2</sup> /s			
		Convective precipitation	Convective Precipitation	convective_precipitation_flux	prc	Kg/m <sup>2</sup> /s	Tier 2 (3h)		

				x					
		Sea surface temperature	Surface Temperature	surface_temperature	ts	K	Tier 2 (6h)	monthly	soil
		Soil temperature	Surface Temperature	surface_temperature	ts	K	Tier 2 (6h)		
		Soil moisture content	Total Soil Moisture Content	soil_moisture_content	mrso	Kg/m <sup>2</sup>	Tier 2 (6h)		
		Specific humidity		specific_humidity	huss	1		3-hourly	Vertical profiles (0-3km) below 3km potentially only over a few cities
		U-wind		eastward_wind	uas	m/s			
		V-wind		northward_wind	vas	m/s			
		Temperature		air_temperature	ta	K			
<b>SURFEX (RMI - C)</b>	H-Res over Belgium (±5 km)	soil moisture	Total Soil Moisture Content	soil_moisture_content	mrso	Kg/m <sup>2</sup>	Tier 2 (6h)	Initial time (if possible)	surface
		soil temperature	Surface Temperature	surface_temperature	ts	K	Tier 2 (6h)		
		Downward	Surface	surface_down	rsds	W/m <sup>2</sup>	Tier 2 (3h)	1-hourly	

		long-wave radiation	Downwelling Shortwave Radiation	welling_short wave_flux_in_ air					
		Downward short-wave radiation	Surface Downwelling Longwave Radiation	surface_down welling_longw ave_flux_in_ ai r	rlds	W/m <sup>2</sup>	Tier 2 (3h)		
		Snow rate	Snowfall Flux	snowfall_flux	prsn	Kg/m <sup>2</sup> /s	Tier 1 (daily)		
		Precipitation rate	Precipitation	precipitation_f lux	pr	Kg/m <sup>2</sup> /s	Tier 2 (3h)		
		Specific humidity		specific_humi dity	huss	1			50m
		Pressure				Pa			
		U-wind				m/s			
		V-wind				m/s			
		Temperature				K			
<b>REGCROP (P6-VITO)</b>	H-Res over Belgium (±5 km)	Dewpoint Temperature	Near-Surface Specific Humidity	specific_humi dity	huss	K	Tier 2 (6h)	Daily	2m
		Tmax	Daily Maximum Near-Surface Air Temperature	air_temperatu re	tasmax		Tier 1 (daily)		

		Tmin	Daily Minimum Near-Surface Air Temperature	air_temperature	tasmin				
		Downward long-wave radiation	Surface Downwelling Shortwave Radiation	surface_downwelling_shortwave_flux_in_air	rsds	W/m <sup>2</sup>	Tier 2 (3h)		surface
		Downward short-wave radiation	Surface Downwelling Longwave Radiation	surface_downwelling_longwave_flux_in_air	rlds	W/m <sup>2</sup>	Tier 2 (3h)		
		Pressure	Surface Air Pressure	surface_air_pressure	ps	Pa	Tier 2 (3h)		
		Evapotranspiration	Potential Evapotranspiration	water_potential_evaporation_flux	evspsblpot	kg/m <sup>2</sup> /s	Tier 2 (6h)		
		Precipitation	Precipitation	precipitation_flux	pr	kg/m <sup>2</sup> /s	Tier 2 (3h)		
		U wind	Eastward Near-Surface Wind	eastward_wind	uas	m/s	Tier 2 (6h)		2m
		V wind	Northward Near-Surface Wind	northward_wind	vas	m/s	Tier 2 (6h)		
<b>GNSS</b>	H-Res over	Temperature	Near-Surface Air	air_temperature	tas	K	Tier 2 (6h)	1-hourly	2m

<b>(ROB=P9)</b>	Belgium (±5 km)		Temperature	re				
		integrated water vapor						column
		integrated temperature (to be defined)						
		Pressure	Surface Air Pressure	surface_air_pressure	ps	Pa	Tier 2 (3h)	surface

## Annex G: Meeting minutes